

CRANFIELD UNIVERSITY

Sandra Wilson

Design and Development of a Polymer Patch Clamping Device

School of Applied Science
Department of Materials

PhD Dissertation
Academic Year: 2010

Supervisor: Dr Paul Kirby (Cranfield)
Prof. Volker Saile (KIT)

CRANFIELD UNIVERSITY

Sandra Wilson

Design and Development of a Polymer Patch Clamping Device

Academic Year 2010

School of Applied Sciences

Department of Materials

Supervisor: Dr. Paul Kirby

Prof. Volker Saile

©2010 Cranfield University. All rights reserved. No part of this publication may be reproduced without the written permission of the copyright owner.

ABSTRACT

Patch clamping is considered the gold standard in measuring the bioelectrical activity of a cell. It is used to detect and measure ion transport through ion channels located throughout a cell membrane. Ion movement is crucial to cell viability and cell-to-cell communication. Pharmaceutical companies increasingly target ion channels because of their significance in disease and to help design better targeted drugs. However, the traditional method of patch clamping is cumbersome and is being replaced by planar high throughput screening (HTS) systems. These systems are reaching their limits due to materials and cost of processing; cell handling methods and small varieties of applicable cell types are also issues to be addressed.

In this work, the core components of a new kind of planar patch clamping device have been designed and developed, after analysis of currently available HTS systems. This design approaches patch clamping using polymers to overcome some of the limitations in current systems, specifically cell handling and positioning, by using a simple modification technique to provide distinct attractive areas for cell binding. This uniquely allows the culture of both single cells and cell networks to increase the range of cell types that can be measured and circumvents challenges from using suction to pull cells onto measurement holes. The components of the design are a 10 x 10 array of small holes drilled in a polymer then aligned modifications for precise cell placement are added and a planar electrode array for individual addressing of each cell. A study of methods to produce a leak-tight seal required between microfluidic chambers was done. Cell adhesion parameters for the modification techniques were established. The principle viability of this approach was confirmed using the modification technique to culture cells over holes and measure their resistance using a rig developed for this work.

Keywords: bioMEMs, patch clamping, microhole drilling, polymer surface modification

ACKNOWLEDGEMENTS

This work has been carried out between the Materials Department, Cranfield University and the Institute for Microstructure Technology at the Karlsruhe Institute of Technology (formerly Forschungszentrum Karlsruhe). My deepest gratitude goes to my supervisors Dr. Paul Kirby and Professor Volker Saile for their support, guidance and the freedom to take this work where it needed to go.

I would also like to thank the people who supported this work, their engagement, resources and kindness are inspiring.

Cranfield University: Heather Almond, Sue Impey, Jeremy Ramsden and Severine Saint-Martin

University of Hertfordshire: Areles Molleman

KIT-IBG: Alexander Welle, Eric Gottwald, Tim Scharnweber, Stefan Giselbrecht, Martina Reinhardt, Maria Marin, David Thiele, Anke Dech.

KIT-IHM: Lars Wegner

KIT-IMF1: Wilhelm Pfleging, Maik Torge, Heino Besser, Markus Beiser and Adriano de Oliveira

KIT-IMT: the colleagues with whom I have worked the last 10 years, with special thank you's to Markus Guttman, Joachim Schulz, Juergen Mohr, Mathias Hecke, Andreas Guber and Alexandra Moritz and her team.

I would like to thank my family and friends who have supported me through all these years, you all contributed to this in ways you probably were not aware of.

TABLE OF CONTENTS

ABSTRACT	i
ACKNOWLEDGEMENTS.....	iii
LIST OF FIGURES.....	vii
LIST OF TABLES	xi
1 Glossary	xii
1 Key contributions in the thesis.....	xv
1.1 Structure of the thesis	xvi
2 Introduction.....	19
2.1 The cell	21
2.2 The cell membrane	23
2.2.1 Transport across the cell membrane	27
2.2.2 Electrostatic structure of the cell membrane – electrical double layer	29
2.2.3 The isoelectric point	31
2.2.4 The electrical properties of the cell membrane.....	31
2.2.5 The action potential	33
2.3 Historical development of the patch clamping technique	35
2.4 Traditional patch clamping	36
2.4.1 Making a patch clamping measurement.....	36
2.4.2 Physical challenges with traditional patch clamping	43
3 Patch clamping – High Throughput Screening (HTS) systems.....	46
3.1 Planar patch clamping	46
3.2 Patch clamping systems in the research / early stage business	53
3.3 Series Resistance Calculations	57
3.4 Limitations in High Throughput Screening	61
3.5 Addressing the Identified Limitations – Design Analysis	63
3.5.1 Materials.....	63
3.5.2 Cell placement using suction.....	64
3.5.3 Cell sample preparation and handling	65
3.5.4 Microfluidics and micro-electrodes	66
4 Aim	67
4.1 Design approach.....	70
5 Biocompatible polymer materials for patch clamping	75
5.1 Selected biocompatible polymer materials.....	77
5.1.1 SU-8.....	77
5.1.2 Polystyrene	79
5.1.3 Polycarbonate	80
5.2 Surface analysis of polymer materials	81
5.2.1 Contact angle measurement	81
5.2.2 Contact Angle Experiments – Dynamic Method	85
5.2.3 X-ray Photon Spectroscopy (XPS) measurement	87
5.2.4 X-Ray Spectroscopy Experiments.....	91
5.3 Cell Adhesion and Competitive Protein Adsorption	92
5.4 Methods of surface modification for cell adhesion	93
5.4.1 Laser and Lamp modification below 200 nm	94

5.4.2 The isoelectric point, Vroman effect and selective protein adsorption	95
5.5 Cell culture method	96
5.6 .1 Micro-injection moulding and overmoulding	98
5.7 Injection Moulding Experiments	100
5.8 Laser drilling and laser surface modification	102
5.8.1 Laser hole ablation	103
5.8.2 UV laser surface modification	105
5.9 Microlithography	106
5.9.1 UV Lithography of holes	107
5.10 Physical Vapour Deposition (PVD)	108
5.10.1 Electrode deposition experiments	110
5.11 Resistance measurement set up	112
5.12 Considerations for single part design and material bonding of two part design	113
6 Results and discussion	117
6.1 Hole drilling	117
6.2 Biocompatible polymer selection	121
6.3 Single or two part design analysis	126
6.3.1 Solvent bonding	127
6.3.2 Direct injection moulding	129
6.4 Surface Modification	133
6.4.1 Defining laser modification parameters using cells	139
6.4.2 Defining lamp modification parameters using cells	142
6.5 Patterned / selective cell culture	145
6.6 Integration of cell culture on modified surfaces over holes	149
6.7 Electrode fabrication	151
6.8 Resistance Measurement	155
7 Conclusions and Outlook	162
8 List of Publications	165
9 References	168
Appendix A	174

LIST OF FIGURES

Figure 1-1 Structure of the thesis.....	xvi
Figure 2-1 the ideal membrane, a lipid bilayer of phospholipids	24
Figure 2-1 Schematic representation of a potassium ion channel in a closed and open configuration	27
Figure 2-2: Schematic of a transporter, specifically an Na ⁺ - K ⁺ ATPase exchanger	29
Figure 2-3 Schematic illustration of an electrical double layer.(Glaser, 2009).	30
Figure 2-4 : Electronic model of the plasma membrane of an intact cell (Molleman, 2003)	32
Figure 2-5 An electrical circuit as a model illustrating the Na ⁺ - K ⁺ diffusion potential of a cell as a result of a sodium and potassium battery (Glaser, 2009).	33
Figure 2-6: Traditional patch clamping setup (left), right, illustration of the patch pipette/ electrode in cell attached mode	38
Figure 2-7 The equivalent circuit for the cell-attached configuration	38
Figure 2-8: Patch clamp recordings (left) for acetylcholine receptors (right, shown as a sectional view) (F.A. Ashcroft, 2006).....	41
Figure 2-9 The equivalent circuit for a patch clamp measurement in the whole cell configuration	43
Figure 2-10: Glass pipette approaching a neural cell under a microscope (Duprat, April 2000)	44
Figure 3-1: Schematic example of a planar patch clamping system	49
Figure 3-2: Cytocentrics GmbH patch clamping chip {{{}	50
Figure 3-3: Nanion borosilicate glass chip (Nanion, 2010a).....	50
Figure 3-4: Flyion and a 'flip the chip pipette' arrangement	51
Figure 3-5: Sophion bioscience QPatch chip schematic (Sophion bioscience, 2009)	52
Figure 3-6 Top and enlarged views of PDMS integrated multiple patch clamp array with lateral cell trapping junctions	53
Figure 3-7: The fluxion lateral patch clamping approach: (a) schematic diagram of cell trapping by applying negative pressure to capillaries, (b) SEM of three recording sites from the main microfluidic channel and (c) dark field optical microscope image of cells trapped at three recording sites images. Images taken from www.fluxion.com	55
Figure 3-8: Model of a CNRC silicon/silicon nitride/silicon oxide chip	56
Figure 3-9: geometry of conical pore	57
Figure 3-10 Calculation of the sidewall angles for series resistance	59
Figure 4-1 Design and fabrication considerations for a patch clamping chip	71
Figure 4-2: Section of proposed patch clamping system design, left array for neuronal type cells; right cross-sectional representational view through a hole with electrodes and isolated microfluidics to each hole	72

Figure 4-3: Schematic drawing of a high-throughput chip well structure for cell inoculation.....	73
Figure 4-4: Inverted well structure becomes microfluidic chamber permitting surface modification for single or neuronal cells	74
Figure 5-1: Chemical structure of SU-8 with functional side chains	78
Figure 5-2: Contact angle measurements, SU-8 exposed to standard lithography UV lamp (305-436nm)	78
Figure 5-3: Advancing and receding contact angle results for SU-8 exposed to 185nm UV lamp	79
Figure 5-4: Chemical structure of polystyrene (formed from many styrene monomers, left).....	80
Figure 5-5: PC12-GFP cells on UV modified (185nm) polystyrene petridish.....	80
Figure 5-6: Chemical structure of polycarbonate	81
Figure 5-7: Illustration of different degrees of wetting: High wetting on the left gives a small contact angle whereas on the right there is little wetting and a large contact angle.	82
Figure 5-8: Contact angle measurement and wetting	83
Figure 5-9: Data Physics OCA goniometer	84
Figure 5-10: Dynamic contact angle measurement (above), ellipse fitting method, (below).....	86
Figure 5-11: Simplified schematic of an X-ray Photon Spectroscopy (XPS) unit (left), an actual XPS unit (right).....	87
Figure 5-12: Schematic representation of a single photoelectron emission by X-ray for XPS measurement	88
Figure 13 : Binding energy - example of an XPS result screenshot (INRS, Canada (Paynter,)).....	89
Figure 5-14: An example of polystyrene exposed to an oxygen plasma analyzed by XPS.....	90
Figure 5-15: Battenfeld 50 micro-injection moulding system.....	100
Figure 5-16 Injection moulding machine set up for overmoulding foil to microfluidic structures.....	101
Figure 5-17 Test injection mould layout, red areas are through holes used for leak testing.....	102
Figure 5-18: ATLEX 185nm laser set up.....	104
Figure 5-19: Exitech laser PS2000	105
Figure 5-20: Schematic of laser surface modification, ambient air as process gas.	106
Figure 5-21: Schematic of microlithography processing	107
Figure 5-22: The dependence of vapour pressure on melting temperature for selected materials.....	110
Figure 5-23: Edwards thermal evaporator, chamber exterior and interior (Cranfield)	111
Figure 5-24: Sputter masks – test electrode design.....	111
Figure 5-25: Patch clamping system used for measurement	113

Figure 5-26: Section of a cell chip showing a drilled hole for patch clamping	114
Figure 5-27: Inverted cell chip well structure as a microfluidic chamber permitting surface modification for single or neuronal cells	115
Figure 5-28: Solvent bonding unit chamber	116
Figure 6-1 Layout of this work	117
Figure 6-2 248nm UV laser holes in polycarbonate	119
Figure 6-3 PC foil, 2J/cm ² 25ns duration: 300 pulses (left), 250 pulses (right) ...	119
Figure 6-4 3J/cm ² 250 pulses (left) 1J/cm ² 1500 pulses (right)	120
Figure 6-5 Cross-section of a hole drilled in 50µm thick norflex polystyrene foil, 0.5J/cm ² laser fluence (image also shows uncleaved neighbouring holes) .	121
Figure 6-6: Advancing contact angle measurements for a range of polymers	123
Figure 6-7: Milled cell chip	126
Figure 6-8: A sectional view of a milled and drilled well showing surface roughness effects	127
Figure 6-9: From left to right, 5 sec, 10 sec and 17 seconds gas phase acetone solvent bonding on polystyrene	128
Figure 6-10: Photographs (1,2) plus raw and adjusted ImageJ® image analysis (3,4)	131
Figure 6-11: Contact angle measurements advancing and receding for norflex® polystyrene	137
Figure 6-12: oxygen concentration compared to total exposure dose (E _{tot}) for laser and lamp surface modification	139
Figure 6-13: Stained cells on exposed petri dish material (polystyrene)	140
Figure 6-14: Laser modified petridish, 5mJ/cm ² energy, number of pulses and cell adhesion	140
Figure 6-15: Cell adhesion as a function of laser pulse number and laser fluence	141
Figure 6-16: L929 cells on norflex® polystyrene , 48 hours after inoculation, diameter of circle 1mm.....	142
Figure 6-17: L929 cells on Goodfellow polystyrene foils, 48 hours after inoculation (magnification as in figure above)	142
Figure 6-18: Cell adhesion for UV lamp exposure in terms of oxygen content (%) and exposure time	144
Figure 6-19: XPS data summary, C-H binding over UV exposure time norflex® PS foil	145
Figure 6-20 Collagen control petridish, culture day 7, showing greater than 85% neurite growth of PC-12 GFP cells (200x)	146
Figure 6-21 PC12 GFP cells, cultured on a lamp modified petridish, 9 days line/space pattern 10µm/100µm	146
Figure 6-22 L929 cells cultured 5 days onto UV patterned norflex® foil	147
Figure 6-23 PC-12 GFP cells after 7 days of culture, left a modified circle with no modified tracks sits isolated, right, modification with tracks shows the development of a neural network 10x10, spacing of tracks is 435µm.....	148

Figure 6-24 Fluorescence micrographs: left, labelled albumin, right, labelled laminin on laser patterned norflex foils. High brightness indicates a high concentration of adherent proteins (squares 435x435 μm^2)	149
Figure 6-25: PC12 GFP misaligned surface modification to holes, and cell culture	150
Figure 6-26: PC12-GFP cells cultured over holes.....	151
Figure 6-27: Electrodes (green) on the lower side of a microfluidic chamber.	152
Figure 6-28: Steel VD masks with a test electrode design	152
Figure 6-29: Chloration of silver after two minutes in a diluted bleach solution...	153
Figure 6-30 100nm deposited silver electrode after chloration.....	154
Figure 6-31 400nm silver after electrolytic chloration, left, a contact pad, right an electrode path	154
Figure 6-32 Single hole and alignment marks drilled in 50 μm thick polystyrene, left laser entrance side (9 μm) and right, laser exit side (4 μm)	155
Figure 6-33: on left, PDMS measurement rig top view, right, rig with foil during measurement.....	156
Figure 6-34: IV curve results for PS foil drilled with one hole (dia. top = 4-5 μm , bot. 12 μm)	157
Figure 6-35: IV curve results for PS foil drilled with one hole (dia. top 2 μm , bot. 8-9 μm hole)	157
Figure 6-36: Patch clamp resistance measurements over hole diameter in Norflex© polystyrene – red crosses denote calculated values from Section 3.3	159
Figure 6-37: PMMA measurement rig (rig version 2) with measurement electrode inserted into a rubber stopper and clamps to ensure no leak around the foil	160
Figure 6-38: Cross-sectional schematic view of the measurement rig setup	160

LIST OF TABLES

Table 1: Biological components relative sizes.....	22
Table 2: The concentration distribution of typical ions found in mammalian cells .	25
Table 3: Planar patch clamping systems on the market (Comley, 2003)	48
Table 4 Influence of pore dimensions and area on series resistance	60
Table 5 Electrical properties of materials suitable for patch clamping ^a	76
Table 6: Survey and classification of PVD deposition techniques (Kern and Schuegraf, 1994)	109
Table 7: Apotome microscope analysis of purchased polystyrene foil materials.	125
Table 8: Injection moulding results BASF PS granulate onto 50µm Norflex foil..	130
Table 9: Influence of laser exposure on surface roughness of polystyrene	135

Glossary

agonist - a chemical substance capable of activating a receptor to induce a full or partial pharmacological response.

axon - the part of a cell which conducts impulses (electrical signals) away from the body of the cell to the synapse of another cell

ATP to ADP - the hydrolysis of adenosine **tri**-phosphate to adenosine **di**-phosphate releasing energy used to drive other chemical processes within the cell, such as moving ions against their concentration gradient in transporter pumps

cell attached patch - pipette forms a seal with the membrane. Used in single channel recording, easy to obtain. Exact patch potential unknown

Central Nervous System (CNS) – brain and spinal cord including both sensory and motor cells

cultured cells - tissues or cells which grow by asexual division, grown for experimentation

dendrite - short projections on the neuron that receive signals from other neurons. Neurotransmitters bind to receptors located on the surface of dendrites, causing changes within the nerve cell.

gene expression - conversion of the information encoded in a gene first into messenger RNA and then to a protein

ion channel expression - clarity of signals produced from ion channels opening and closing, good expression is a signal which is clear and well defined

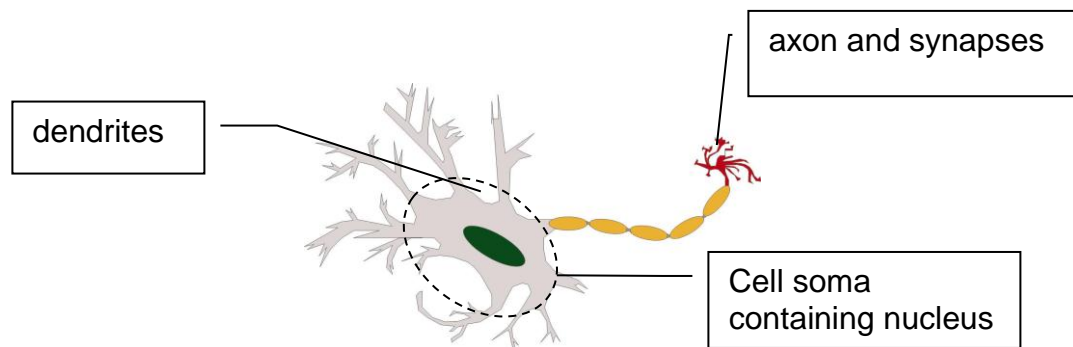
inside out patch - used in single channel recording, a patch of membrane is pulled into a pipette away from the cell and briefly pulled out of the bath so that an attached vesicle is broken and the cytosolic side of the cell is facing the bath. Used for studying cytosolic factors on ion channels. A difficult patch to obtain due to the extra vesicle

removal step. Pipette electrolyte should mimic the extracellular solution. Bath solution, representing the intracellular solution, must be changed after every measurement.

ligand gated channels - see receptor operated channels

neurites - axon and dendritic growth from a cell

neuron - nerve cells, fundamental units of the nervous system that allow it to conduct signals by taking advantage of the electrical charge across its cell membrane.



outside out patch - used in single channel recording, a patch of membrane is pulled into a pipette and the pipette pulled away until the membrane patch breaks away from the cell. Due to the properties of the phospholipid bilayer, the patch folds back on itself forms a cover over the pipette opening; the extracellular factors on ion channels can be studied. Electrolyte solution in this case mimics the intracellular solution

prion - a small proteinaceous particle similar to a virus but with no genetic component, thought to be an infectious agent in bovine spongiform encephalopathy and Creutzfeld-Jakob disease.

Peripheral Nervous System (PNS) – somatic nervous system (voluntary skeletal muscle movements) and autonomic nervous system (involuntary movements of heart, greater intestinal tract, blood vessels and some glands)

primary cell - a cell taken directly from a living animal, which is not immortalised and does not reproduce

primary screening first screening of potential drug compounds (100,000) by measuring their response to cells to identify target hits (compound produces response on intended target)

receptor operated channels (ROC) – open or close depending on the binding of an extracellular factor, such as a hormone or neurotransmitter

second messenger operated channels (SMOC) - channels which open or close in response to an intracellular factor, such as Ca^{++} ions or activated G protein subunits

secondary screening - after primary screening, reduced number of potential hit compounds (2700) are tested on cells at reduced concentrations to identify lead compounds (top 20 hits) for medicinal chemistry eventually leading to clinical testing

synapse - a highly specialized junction between two neurons, or between a neuron and an effector cell (e.g., muscle or gland cell), at which electrical and/or chemical signals are passed from one cell to another.

trypsin - trypsin predominately cleaves peptide chains at the carboxyl side of the lysine or arginine amino chains. It is used to separate clusters of cells into individual cells

voltage dependant channels, voltage operated channels (VOC) – ion channel proteins which are voltage sensitive, i.e. charged residues within the protein which shift position in response to potential difference changes in the membrane

whole cell patch - small patch of membrane pulled into pipette, electrolyte solution slowly enters the cytosolic side of the cell and washes out the intracellular solution. Most common configuration used in high throughput screening for quick assertion of ion channel populations. May lose cytosolic factor information

1 Key contributions in the thesis

The contributions of this research consist of laser drilled holes of 1-10 μ m diameter produced in a 50 μ m polymer foil with a modified surface around the patch hole used for cell guidance. These holes, being the smallest feature and therefore the limiting factor in terms of electrical conductivity in the system, were measured with a resistance in the same range as automated patch clamp systems on the market (<5 MOhm). The use of a surface modification to attract cells to the measurement holes is unique to all patch clamping methods to date and it is relevant because it enables cells to grow over measurement holes days in advance of measurement rather than using suction to pull cells over holes directly before measurement. Surface modifications using a UV laser and lamp were characterized using contact angle measurement, XPS and cell culture studies and controlled cell growth was shown. The advantages of a specific patterned surface modification means it is possible to measure not only single cells but potentially also measure networks of cells, "cell clusters", for the first time. It was demonstrated that cells settle and grow preferentially as networks or single cells, onto the modified surfaces over the holes, and the feasibility of this approach was measured electrically by a significant increase in cell-over hole resistance compared to a hole without a cell (increase from 675 kOhm to 86 MOhm). A commercially available patch clamping system begins to measure at 100MOhms (Molecular Devices Corporation, population patch clamp in the cell attached configuration). The system microfluidics were simply modeled and planar silver-silver chloride electrodes were deposited using physical vapour deposition techniques and evaluated for up to ten days (maximum cell culture time).

1.1 Structure of the thesis

The thesis write-up has been arranged as shown in figure 1-1:

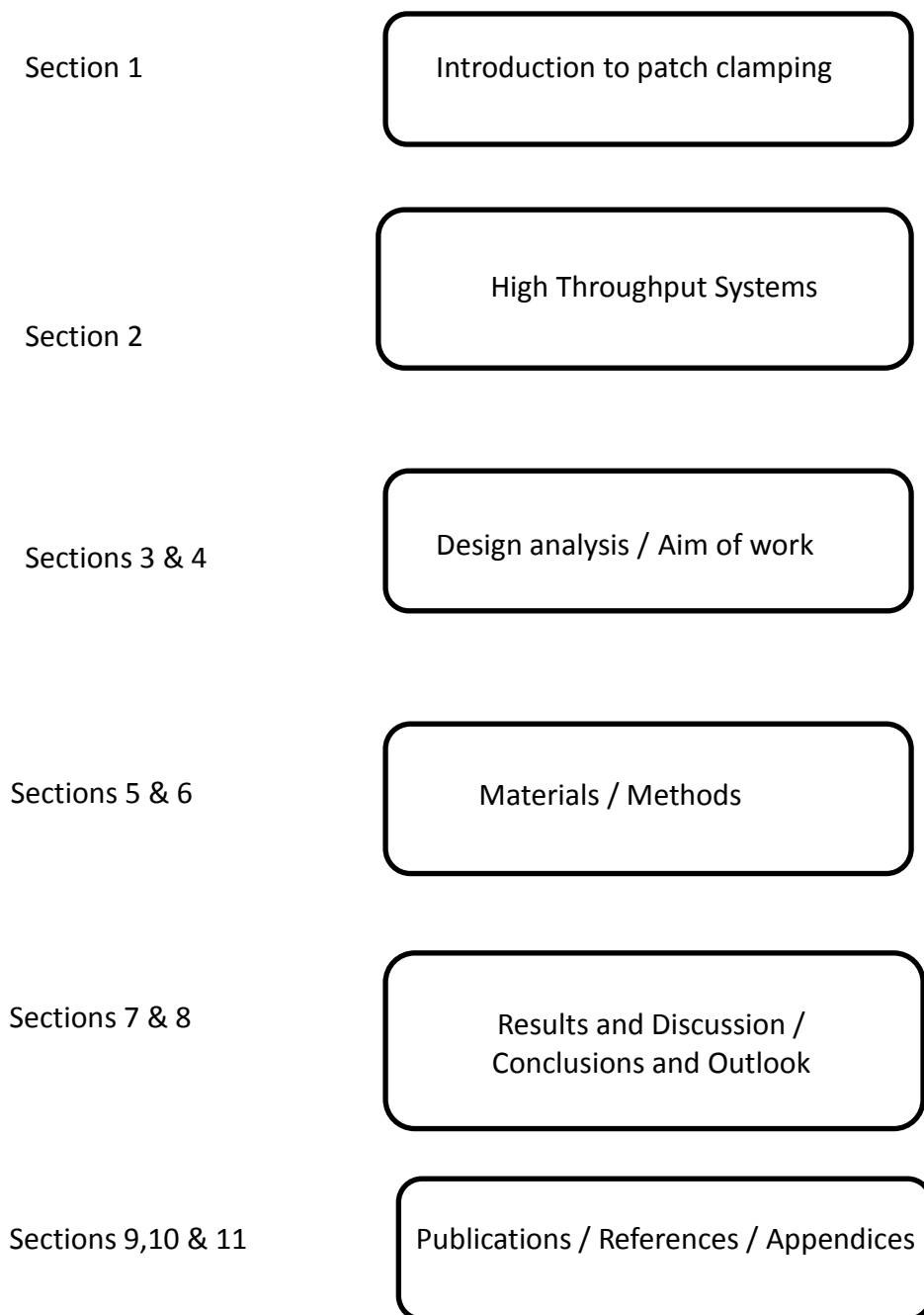


Figure 1-1 Structure of the thesis

Section 1 is an introduction to basic biology and the theoretical background of patch clamping and the basic measurement method. Section 2 introduces commercially available high throughput screening (HTS) systems, assesses their capabilities, how throughput issues have been addressed successfully and their current limitations which were used in a design analysis in section 3. The aims of this work follow in. Biocompatible materials selection is discussed in Section 5, and fabrication and characterization methods used in this work are introduced in Section 6. Sections 7 and 8 contain results, discussion, conclusions and outlook. Sections 9 through 11 refer to publications from this work, references and the appendices.

2 Introduction

Complex biological life consists of a large multitude of single cells that co-inhabit and survive only due to an exchange of information and corresponding processing of that information. This is carried out principally via chemical or electrical signals between cells. To measure and understand the exchange between cells, an interface is needed between the biological system and a sensing and measurement system made of inanimate materials. Due to its scale, microsystems technology is perfectly suited to the production of structures required for this interface in the appropriate materials. Microsystems devices include acquiring chemical signals such as sensors used to measure cell activity by their oxygen usage and release of carbon dioxide (Pancrazio et al., 1998). Microsystems also lend themselves to acquiring electrical signals, such as the electrical activity of neurons as already measured in medical devices such as by ECG (ElectroCardioGram). In this type of measurement, electrodes are placed directly onto the body surface to measure and investigate electrically active tissues rather than individual cells. For more detailed understanding of cellular processes the electrical activity of single cells or small groups of cells below the tissue level is of extreme importance.

Currently there is a division in terms of research activity below the level of the tissue, between the methods used to measure from single cells to small numbers of up to ten cells, and cell measurements above 1000 cells. This division is due mainly to the difference in the level of informational detail required for the application area and the ability of technology to meet the required demands. Above 1000 cells, bulk and average cell properties can be analyzed using methods such as calcium fluorescence or other binding assays and electrophoresis, for example in DNA fingerprint analysis where differentiation between samples is required but not necessarily a deeper understanding of physiological function. When dealing with single cells, or groups of up to ten cells, handling techniques are much more stringent and require either cell separation techniques such as laser cutting and capture, chemical means, or the use of very precise micromanipulators to accurately

select a specific cell for excision. The interest here is in gaining precise knowledge of cell function for better understanding of physiology and also to analyze and understand, for example, the effects of drugs on cell function. It is of course, more time consuming and requires more expertise to obtain measurements of such detail on single cells and is therefore more expensive.

In terms of microsystems development then, it can be said that researchers working with 1000+ cells are developing methods to increase the sensitivity of their measurements; and researchers working with single cells are looking at means to increase throughput and lower the cost of measurement per data point.

With this in mind, the range between 10 cells and 1000 cells is a void in terms of measurement technology, and this lack of information in the so-called 'cell cluster' range is important for researchers looking at the physiological implications of cell-to-cell communication, chemistry and kinetics on the micro and nano scale which are different to the macro or tissue scale. A cell measurement system capable of working in this range would be of interest not only to drug screening and pharmacology, but also for fundamental research into for example, nerve cell interactions.

Patch clamping is considered the gold standard in cell analysis as it gives highly sensitive information about the bioelectric (ion channel) activity of a cell membrane. It is historically a method used to measure single cells individually or of many single cells in parallel. It is used in fundamental research to assess the ability of the brain to learn (cell plasticity), to better understand cell to cell communication, and has impacted the understanding of the role of ion channels in diseases such as Alzheimer's, epilepsy and pain management. It also has a multi-million dollar application in the clinical screening of drugs (Neubert, 2004) as it was discovered that some drugs can affect ion channels even if these drugs are designed for totally unrelated targets, causing serious health hazards such as cardiac arrhythmia or ventricular fibrillation. These discoveries resulted in the establishment of new guidelines in 2004 imposing new tests to screen drugs on known ion channels to rule out potential side effects before clinical

trials are performed (Neubert, 2004). In comparison with other assay techniques such as fluorescence and binding assays, patch clamping provides the highest sensitivity and information content, good selectivity, flexibility and physiologically relevant measurements making it the method of choice for screening the physiological effects of drugs (Neubert, 2004; Comley, 2003). However, traditional patch clamping has one major disadvantage, it has very low throughput and high labour costs – an experienced electrophysiologist may, on a good day, be able to make up to 10 measurements. In order to understand the importance of patch clamping, a brief introduction to the biological background follows.

2.1 The cell

Cells are fundamental to existence; the human body contains more than 200 different types, varying in size, shape and function all coordinating with each other so that the body functions as a cohesive unit. Table 1 gives an indication of the magnitude of cells and some of their constituent parts.

It can be seen that the average mammalian cell (eukaryotic cell) has a diameter between 10 and 30 μm , the average egg cell is larger than 100 μm .

The history of the electrical measurement of cell activity is relatively recent. Membrane potentials were first measured by Hodgkin and Huxley in 1948 (Hodgkin and Huxley, 1952) using crude electrodes on the squid giant axon which has a diameter of 1mm making it comparatively large. Graham and Gerard (Graham and Gerard, 1946) were able to produce much finer electrodes (2-5 μm) and were able to measure the resting potential in muscle cells (which belong to the eukaryotic animal cell group); the procedure involved puncturing the cell membrane, and is known as intracellular measurement. Intracellular measurement was also expanded to measure nerve cell processes, the synaptic potential. The voltage clamp technique was developed by Cole in 1949 (Cole, 1949).

Between 1949 and 1981, continuing work was focused on developing voltage clamping and intracellular recording. It was in 1976 that Erwin Neher and Bert Sakmann (Neher and Sakmann, 1976) for the first time used microelectrodes and voltage clamping together with large bore pipettes which did not penetrate the cell, but rather formed a tight seal with it. The development of patch clamping won them the Nobel Prize in 1991. Patch clamping has steadily developed, and is used in basic research, secondary screening and safety screening of drugs (Xu et al., 2004).

Table 1: Biological components relative sizes

Cell Type	Cell Size (µm)
DNA alpha helix	0.002
Globular protein	0.004
Cell membrane thickness	0.010
Large virus	0.100
Prokaryotes	1-10
Human nerve cell processes	1
E-Coli bacteria	2
Human blood cell	9
Eukaryotic animal	10-30
Eukaryotic plant	10-100
Human Egg	100+
Large Amoeba	to 800
Squid giant axon diameter	1000

Significant demand for increased throughput patch clamping has resulted in development of more automated high throughput systems (HTS). Current HTS patch clamping equipment often uses egg-type cells (oocytes) which have diameters above 100µm and express their ion channel functions clearly. Also of interest to patch clamping investigations are cells belonging to and in the size range of, the eukaryotic grouping, which are cells with a distinct nucleus. Animal cells, including tissue cells, muscles, and nervous system and bone cells belong to this group. With diameters between 10 – 30µm, they are substantially smaller than egg cells, and inherently more difficult to patch clamp. Cell membranes, which are discussed in the following section, have a relatively constant thickness of 10nm.

2.2 The cell membrane

All living cells are enveloped by a plasma membrane which acts as a barrier between the cytoplasm (cell interior - intracellular) and the outside (extracellular) environment. The membrane mainly consists of phospholipids which contain lipophilic (hydrophobic) and hydrophilic (polarised) residues. Phospholipids arrange themselves spontaneously into structures where the lipophilic residues face each other and the polar heads face away from each other (figure 1, (Molleman, 2003)) thus making an effective barrier to charged molecules. The electrostatic structure of the cell membrane is discussed in more detail in section 2.2.2.

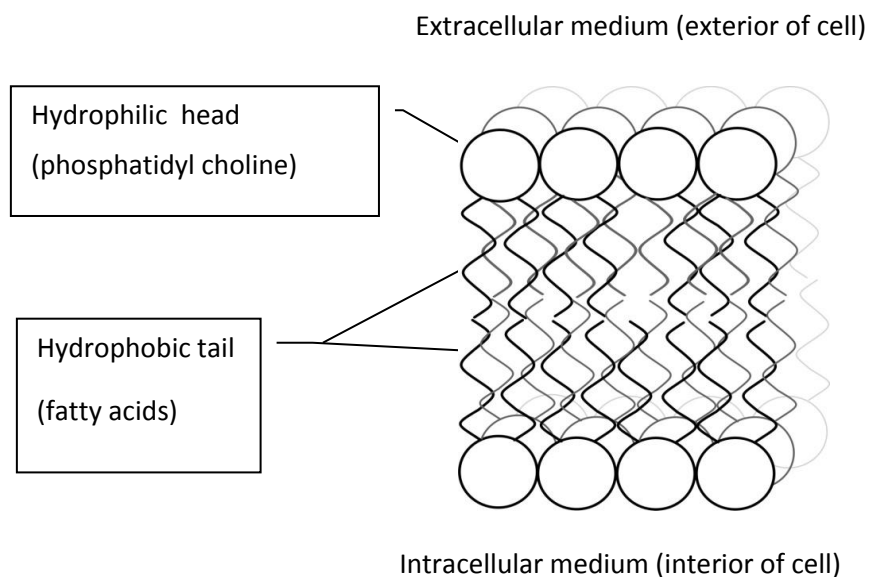


Figure 2-1 the ideal membrane, a lipid bilayer of phospholipids

The membrane is not a perfect bilayer structure, as important functional proteins are embedded and protrude from the cell membrane, which are important for maintaining an electrochemical gradient to maintain cell viability and generate energy.

These membrane proteins are involved in controlling the flow of ions and signalling chemicals through the membrane. This control is crucial to the viability and function of the cell, as concentration gradient diffusion would be too slow to protect a cell from sudden changes in ion concentration inside or outside the membrane. This is where the proteins in the membrane become relevant. They form channels, which act to move ions along or against their concentration gradient in a controlled manner from one side of the membrane to the other. These channels are collectively known as ion channels. It quickly becomes evident that their mechanisms are varied and complex, for example; some are selective to only one type of ion, such as K^+ . Some are voltage gated, meaning they open and close at a specific voltage, some depend on an exterior (extracellular) factor such as a hormone or neurotransmitter binding, some are dependent on an interior (intracellular) factor such as Ca^{++} , and many are combinations of the above.

To give an idea of the osmotic control that the cell membrane has to achieve, Table 2 (Molleman, 2003) shows the intra- and extracellular concentrations of the most prominent ions in a typical mammalian cell.

Table 2: The concentration distribution of typical ions found in mammalian cells

Ion	Intracellular Range (mM)	Extracellular Range (mM)
Na ⁺	5 – 20	130 – 160
K ⁺	130 – 160	4 – 8
Ca ⁺⁺	0.05 – 0.1	1.2 – 4
Mg ⁺⁺	10 – 20	1 – 5
Cl ⁻	1 – 60	100 – 140
HCO ₃ ⁻	1 – 3	20 – 30

Notable differences can be seen in the intracellular and extracellular concentrations of Na⁺ and K⁺ on which many physiological processes depend. The largest concentration gradient is that of Ca⁺⁺. Calcium ion movement is important for many functions including contractions of the heart during the heartbeat (Benitah et al., 2002). The difference in ion concentration between the intracellular and the extracellular mediums across the membrane introduces a concentration gradient $\frac{[ion_o]}{[ion_i]}$ where particles naturally begin to diffuse from a higher to lower concentration, releasing energy ΔG , according to the Nernst equation:

$$\Delta G = -RT \ln \frac{[ion_o]}{[ion_i]}$$

where ΔG = Gibbs energy released by the diffusion process (J/mol)

R = Universal gas constant (8.31 J mol⁻¹ K⁻¹)

T = Temperature (K)

$[ion_o]$ and $[ion_i]$ are the extracellular and intracellular ion concentrations in solution under investigation.

This suggests that if the membrane is permeable to potassium ions, then potassium will leave the higher concentration intracellular side of the membrane and diffuse to the extracellular side. This in turn leaves the intracellular side of the membrane becoming increasingly electronegative E , which eventually will attract the potassium ions back to intracellular side. This release of energy due to changes in net charge ΔG , can be quantified as:

$$\Delta G = -EzF$$

where E = potential across the membrane (Volts)

z = oxidation state of ion under investigation

F = the Faraday constant ($9.65 \times 10^4 \text{ Cmol}^{-1}$)

An equilibrium state occurs where diffusion $\frac{[ion_o]}{[ion_i]}$ and charge $\frac{RT}{zF}$ balance and there is no net movement of ions, this is the equilibrium (resting) potential E , for a specific ion and can be quantified by:

$$E = \frac{RT}{zF} \ln \frac{[ion_o]}{[ion_i]}$$

For potassium ions, this resting potential can be measured across the membrane at around -90mV. As there are other ions in varying concentrations for different cell types, they will pull the equilibrium membrane potential towards their resting potentials with the result that typical membrane resting potential values measure between -50mV to -80mV.

This value is a good indicator of the dominant types of ion channel present in a membrane and gives the electrophysiologist a starting point from which to base his measurement scans.

2.2.1 Transport across the cell membrane

Ion transportation through the cell membrane is facilitated by specialised proteins which fall into the following groups:

Ion channels form aqueous pores between the intracellular and extracellular mediums. These are mostly hydrophilic amino acid residues which when open allow the flow of ions along their concentration gradients. The opening and closing of ion channels is known as 'gating' and there are various types of gating including voltage dependant, ligand (binding) dependant and second messenger operated. These terms are explained in the glossary. Figure 2-1 is a schematic representation of a potassium ion channel, when the pore is closed there is a concentration gradient of potassium from the intercellular (bottom of figure) to the extracellular (top of figure). When the ion channel is activated, it opens and ions flow along the concentration gradient to a more balanced state.

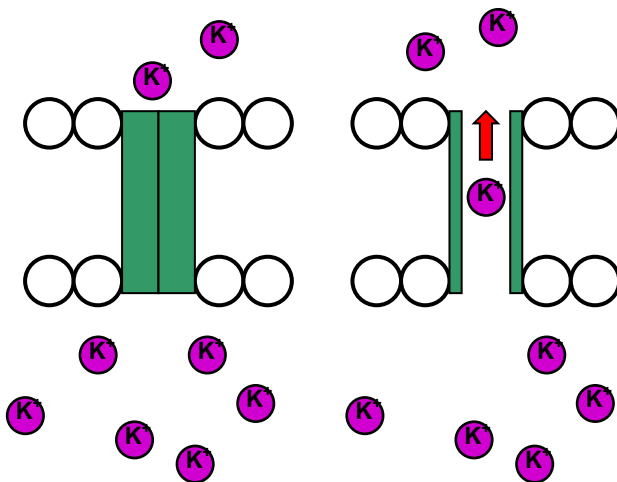


Figure 2-1 Schematic representation of a potassium ion channel in a closed and open configuration

Transporters move ions across a membrane without forming a pore. Instead the protein configuration of the channel undergoes a conformational change to move ions. Transporters are considered active as they require some form of energy to activate. They are subdivided into pumps which operate either as co-transporters or exchangers. Exchangers move molecules against their concentration gradient as shown in figure 3, an $\text{Na}^+ - \text{K}^+$ ATPase exchanger, where the potassium concentration is higher outside the cell (top of figure) than inside the cell, and vice-versa for sodium. The energy for the exchanger to move ions against their concentration gradient is supplied by the hydrolysis of ATP to ADP on the intracellular side of the membrane (not shown). In Figure 2-2, sodium ions bind to high affinity sites inside the channel, which stimulates a conformational change in the channel that exposes the sodium binding sites to the outside of the cell and reduces their affinity for sodium; the bound sodium is released into the extracellular fluids. At the same time, high affinity potassium binding sites are exposed on the cell surface. The binding of extracellular potassium to these sites then stimulates hydrolysis of the phosphate group bound to the pump and triggers the second conformational change which exposes the potassium binding sites to the cytosol of the cell and lowers their binding affinity so that potassium is released inside the cell.

Rather than using energy derived from ATP to ADP, co-transporters use concentration gradients as an energy source to move ions against their concentration gradients. An example would be the flow of sodium ions along its concentration gradient (intracellular to extracellular) which provides enough energy to move dietary glucose at a rate of two sodium ions per one glucose molecule, thereby increasing the glucose concentration inside the cell.

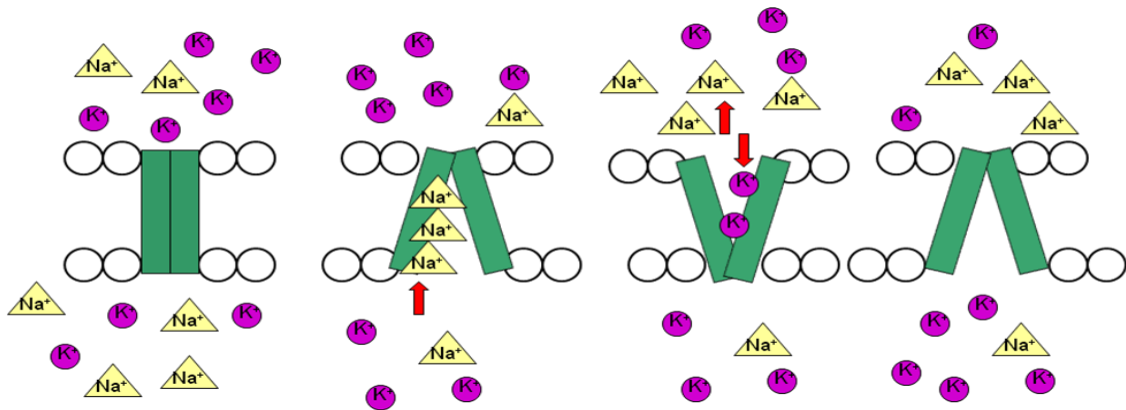


Figure 2-2: Schematic of a transporter, specifically an Na⁺ - K⁺ ATPase exchanger

The membrane becomes more complicated in that there are ion channels which are selective to only one kind of ion, as well as ion channels which are selective, voltage gated and ligand gated (meaning a ligand binds to an extracellular point of the ion channel). The membrane itself behaves as a capacitor (an insulator between two conductive salt solutions in this case).

2.2.2 Electrostatic structure of the cell membrane – electrical double layer

The cell membrane forms an electrical double layer; a surface with a fixed charge induces an electrical field in its vicinity which modifies local ionic conditions in the surrounding solution. In a simple case a double layer happens with the fixed charges on one side, and electrostatically attracted counter-ions on the opposite side. This leads to the formation of a diffuse double layer whose electrical potential declines exponentially with distance from the charged surface as shown in Figure 2-3. The top area of the figure shows the fixed charges and counter ions near a surface. The figure below is the function of the electrical potential according to the Stern model: ψ_0 is the surface potential, ψ_H is the potential at the end of the Helmholtz layer, x_H is the thickness of the Helmholtz layer and $1/k$ is the Debye-Huckel length as a measure of the effective thickness of the diffuse double layer. A Helmholtz layer is formed only when the concentration of mobile ions in solution is high, a great portion of ions

are repelled away from positions near the fixed charges due to thermal movement thus forming the diffuse double layer shown by an exponentially decreasing electrical potential as distance from the surface increases.

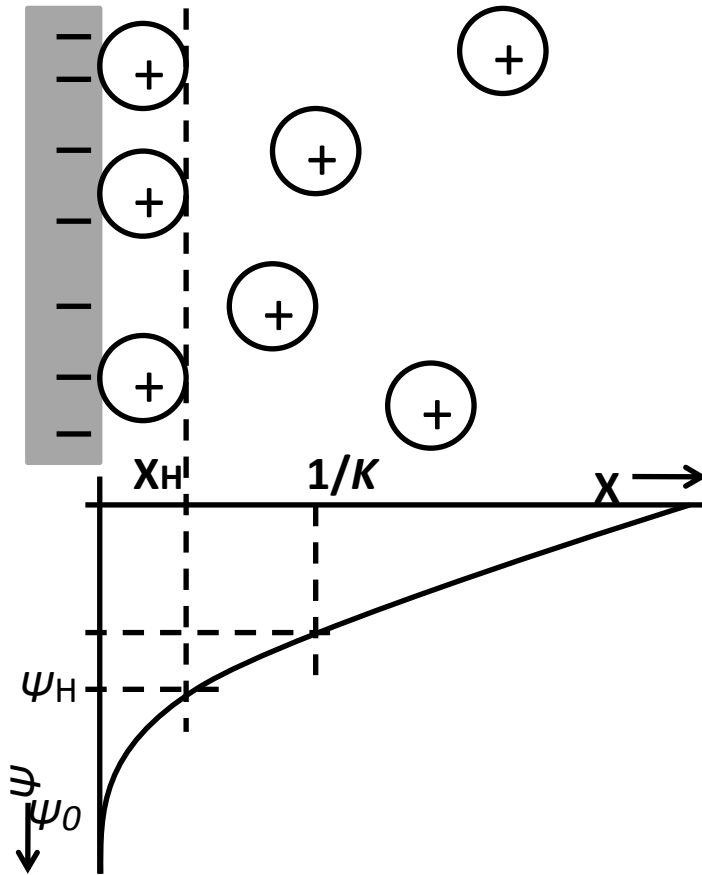


Figure 2-3 Schematic illustration of an electrical double layer.(Glaser, 2009).

The distribution of the double layer is based on the Poisson-Boltzmann equation which allows the calculation of the concentration of ions at given potentials and distance from a central ion, and the Debye-Huckel radius determines the thickness of the ionic cloud and depends on the ionic strength of the solution, where ions are considered to have point charges. The higher the ionic concentration of the solution, the smaller the thickness of the cloud.

2.2.3 The isoelectric point

The equilibrium double layer (known as the relaxed double layer) has a slipping plane which separates fluids that are mobile from those remaining attached to the surface as explained in the previous section (Debye-Huckel length). The electrical potential at this plane is known as the zeta potential. This value is used to estimate the degree of double layer charge. The chemical composition of a sample where the zeta potential is zero, the point of zero charge, is also known as the isoelectric point (pI). It is usually determined by the pH value of the solution since protons and hydroxyl ions are the charge determining ions for most surfaces. The pI (zeta potential of zero) is important as it is a measure of the solubility of molecules at a given pH value and is particularly useful when dealing with amphoteric molecules (with both acidic and basic functional groups) such as proteins. Amino acids, which make up proteins, may be positive, negative, neutral or polar and give a protein its charge. At a pH below pI proteins have a net positive charge due to the presence of more hydrogen atoms (NH₃); above the pH of pI they will have a net negative charge due to hydroxides which remove hydrogen from an amino acid leaving it negatively charged. The isoelectric point is a significant factor in cell adhesion as adhesion mechanisms are driven by transmembrane proteins, selectins, integrins and cadherins, which will have a greater or lesser affinity for a surface at a given charge. This premise is important later in this work as proteins can be used to assist in the definition of distinct areas of cell repulsion and attraction using materials with a surface charge and proteins with different isoelectric points. It is notable that integrins, cadherins and selectins have isoelectric points in the range between 5.2 (cadherins) to 6.2 (selectins) which suggests that cell adhesion will be better on a surface with more hydrogen acceptors available (COO⁻), meaning more hydrophilic surfaces.

2.2.4 The electrical properties of the cell membrane

The structural properties of a cell membrane were discussed in Section 2.1 where the amphiphilic nature of the lipid bilayer was introduced. For biophysical

considerations, the electrical properties of the biological membrane are important. In contrast to the external medium and the cell plasma, the cell membrane has a high electrical resistance and a low dielectric constant. It therefore can be considered as an extremely thin hydrophobic electrically isolating surface between two aqueous phases (intracellular and extracellular liquids) behaving as a capacitor with a certain capacity (C_m), and resistance (R_m). (Figure 2-4) which polarizes.

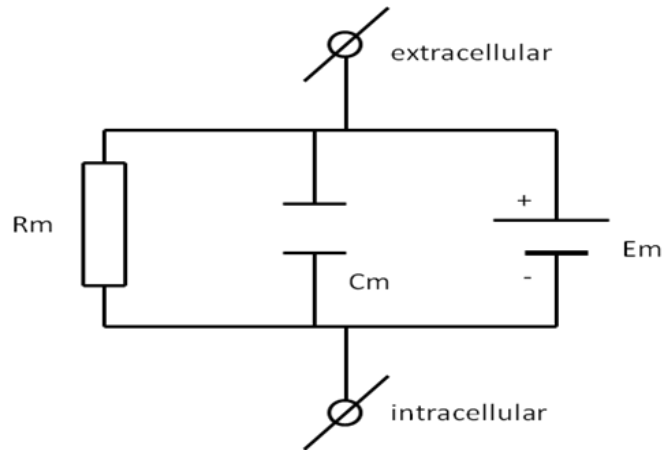


Figure 2-4 : Electronic model of the plasma membrane of an intact cell
(Molleman, 2003)

The specific capacity (C_{sp}) can be calculated from the membrane thickness (Δx) and the dielectric constant (ϵ)

$$C_{sp} = \frac{\epsilon_0 \epsilon}{\Delta x}$$

The specific capacity of the membrane is relatively constant because the dielectric constant (ϵ) and the membrane thickness (Δx) do not vary significantly. For a normal cell membrane this is approx. 10 mF.m^2 (measurements are performed in a plate capacitor setup to measure AC conductance, or by application of electrical fields (Gabriel et al., 1996)(Gimsa and Wachner, 1999)).

2.2.5 The action potential

The action potential of nerve cells is an example of the feedback loop between an electric field and ionic permeability. While action potentials occur mainly in neuronal type cells, they are also present in other cell types. The electrochemical gradient of a cell membrane was discussed briefly in section 2.2 and introduced the idea of using the gradient to trigger various levels of membrane potential simply by differences in ion permeability. The action potentials of various cells can be explained with the aid of Figure 2-5.

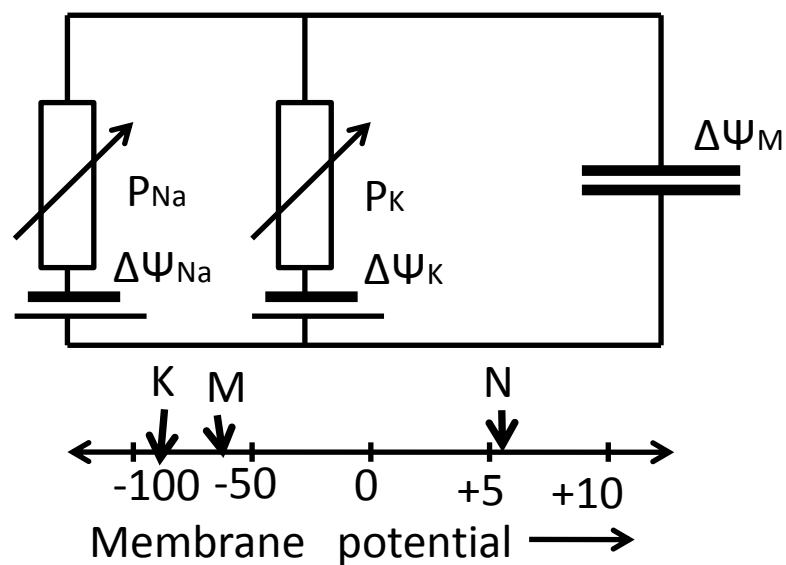


Figure 2-5 An electrical circuit as a model illustrating the $Na^+ - K^-$ diffusion potential of a cell as a result of a sodium and potassium battery (Glaser, 2009).

The electrochemical gradients of potassium and sodium which are generated using metabolic energy can be considered as capacitors with opposite polarities. The permeability characteristics of ions are expressed here as the variable resistors P_{Na} and P_K or potentiometers through which the accumulators are discharged. If the resistance is low then a large discharge current flows and if the accumulator is not recharged continuously it would be quickly empty. The effective membrane potential in this figure is the voltage difference across the membrane capacitor, $\Delta\psi_M$. If P_{Na} and P_K have about the same value then $\Delta\psi_M$ is small, if they are large then a membrane potential will be established. The

lower section of Figure 2-5 shows the membrane potentials limited by the Nernst potentials for potassium and sodium, so between approx. -95 and +65 mV. The actual membrane potential in vivo is found to be -90mV (M in the diagram)(Glaser, 2009).

The surface charge density as a function of transmembrane potential can be calculated from the charge transfer across the membrane capacitor ($\Delta\Psi_M$ in Figure 2-5) which is required to adjust the potential differences. This value is extremely small; it amounts to approximately 10^{-8} charge equivalents per square metre taken from the equation for specific capacity in Section 2.2.2.

In essence this means that an ion pump driven by metabolic energy accumulates electrochemical energy by generating a concentration gradient of sodium and potassium which can be converted into electrical energy and used to control membrane permeability. This enables a wide range of control of the electrical field in the cell membrane without any sizeable input of energy. This permeability can be induced by the cell itself or by external influences (such as during patch clamping measurements).

In terms of nerve cells, the non-excited nerve has very low sodium permeability, its resting potential is then determined mainly from the diffusion potential of potassium which is negative. After excitation the membrane permeability for ions increases rapidly, and the sodium permeability increases more rapidly than that of potassium. For a short time the diffusion potential of sodium becomes dominant, and with the opposite polarity to potassium, it creates the current peak seen in action potentials.

An action potential is transmitted when a local action potential triggers the neighbouring proteins in the membrane. The impulse can only go in one direction due to the time it takes a protein to become excitable after it has been already excited (milliseconds).

Similarly, in a voltage clamp set up (almost always used in high throughput screening (HTS) systems) a stepwise change in applied potential will always

come into effect at the cell membrane with some delay and loss because of the membrane's capacitive properties, and the series resistance of the setup controlling the membrane potential. Series resistance and the setup are explained in the following section, after a short introduction to the traditional patch clamping technique.

2.3 Historical development of the patch clamping technique

For almost 60 years, direct membrane potential measurements on single cells has been possible by intracellular signal measurement where a small sharp tipped glass pipette is pushed through a cell membrane. (Hodgkin and Huxley, 1952). Development of the patch clamping technique in 1976 by Neher and Sakmann (Neher and Sakmann, 1976) significantly increased the potential and time resolution of cell signalling and allowed the measurement of individual ion channels over a cell membrane by using a glass pipette arrangement with a larger bore tip (up to 10 μ m) to isolate a patch of the cell membrane for measurement (Neher and Sakmann, 1976) (Hamill et al., 1981). While patch clamping measurements give the most detailed and physiological detail about cell ion channel activity, the technique is cumbersome and has very low throughput. The demand for data and the sheer size of the potential market for drug screening applications alone (>\$100 million a year) (Neubert, 2004) has helped drive the development of High Throughput Systems (HTS). The future prospects for an automated patch clamping system are exceptional; with no current system available to sensitively measure either high volumes (>100 cell measurements simultaneously) of single cells, or to precisely measure cell-to-cell interactions such as in neural networks, or palpitating heart cells, there is a wide area of application for which an automated patch clamping system could be effective, specifically when dealing with 'ensembles' or clusters of cells. Some of the HTS systems available on the market will be introduced in Section 2 after an introduction to the classical patch clamping technique and background

2.4 Traditional patch clamping

The patch clamping technique itself is relatively recent, having only been developed in 1976. In 1991, Erwin Neher and Bert Sakmann were awarded the Nobel Prize (medicine and physiology) for the development of the technique. It has quickly become recognised as the gold standard of electrophysiological measurements due to its high sensitivity and the ability to obtain precise, detailed information about ion transport through the cell membrane. In brief, measurements are made by pulling a small patch of a cell membrane into a glass pipette containing a conductive salt solution and a silver/silver chloride electrode. There are several ways in which the membrane patch can be manipulated, but commonly the patch itself is sucked into the pipette until it breaks – giving the electrophysiologist access to the cytosol of the cell (whole cell recording). This permits the electrophysiologist to artificially open and close ion channels in a manner similar to the cells own internal mechanisms when, for example, a voltage is applied. The second pipette/electrode filled with the same solution as the first electrode, serves as a reference electrode, and it is placed in the solution on the extracellular side of the cell.

A classical patch clamping set-up is shown below in Figure 2-6. The typical configuration has an inverted microscope and two micromanipulators for precise x, y and z placement of two glass pipettes each containing a silver chloride electrode. An exploded sketched view is shown of a pipette with electrode in Figure 2-6, right. The electrodes are connected to pre-amplifiers (head stage) and then amplifiers in a rack outside of the Faraday cage; the cage is used to prevent interference from electrical noise. The amplifiers are connected to a computer with control software (PatchXpress®, from HEKA, Lambrecht, Germany, for example).

2.4.1 Making a patch clamping measurement

Before measurement, cells are typically prepared by culturing on a collagen film on a glass microscope slide (over a few days), or primary cells are taken from

the animal on the day of measurement and are perfused (given nutrition) during measurement to keep them viable for the duration of measurement.

The measurement setup includes two electrodes, an amplifier, a microscope and a computer with relevant software for acquiring and processing data.

To perform a measurement, a glass capillary pipette with an Ag/AgCl electrode (Figure 2-6, right) is used to pull a patch of the cell membrane into a glass pipette to electrically isolate it from the rest of the cell membrane. Borosilicate or quartz glass pipettes are drawn and fire polished daily from capillary tubes to a tip opening of between 1 to 4 μm in diameter, depending on the cell type and type of patch clamp measurement to be made. Two pipettes are used during patch clamping; one is used for measurement while the other is placed in the bathing solution and becomes the reference electrodes.

The pipettes are then filled, one with intracellular solution (the solution broadly resembles the ionic composition and pH of the cytoplasm, (high $[\text{K}^+]$), then the activated Ag/AgCl electrode is placed into it as shown in Figure 2-6. The other electrode is filled with the extracellular (or bathing) solution.

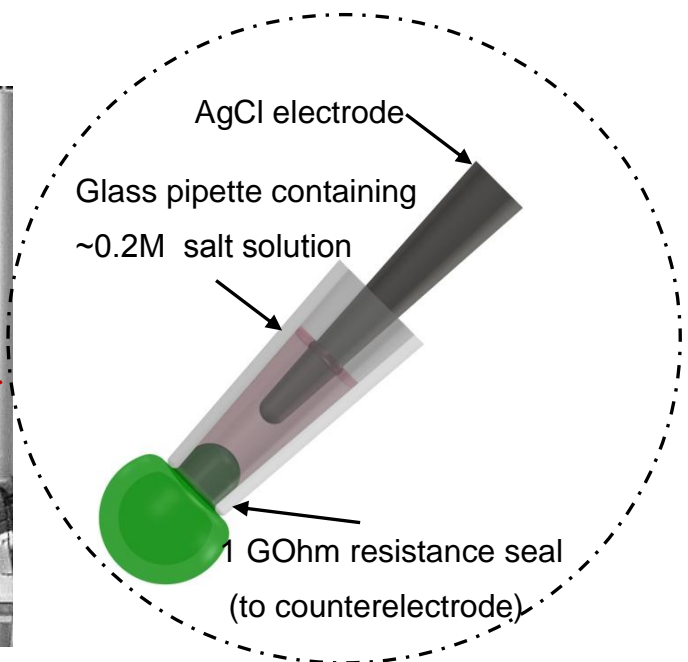
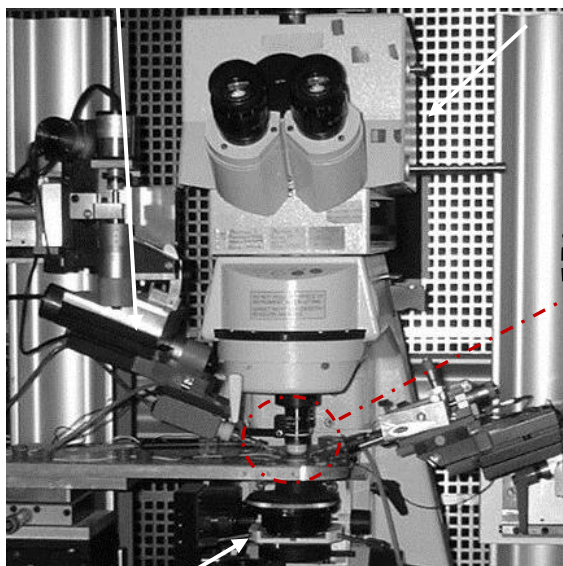


Figure 2-6: Traditional patch clamping setup (left), right, illustration of the patch pipette/ electrode in cell attached mode

The pipette/electrode is gently lowered into the cell culture media until the selected cell is reached. The electrophysiologist then gently sucks on a tube/valve connected to the pipette (pressure <10 mmHg) to pull a patch of the cell membrane into the pipette opening. This is known as the 'cell attached' configuration and is shown as an equivalent electrical circuit in Figure 2-7.

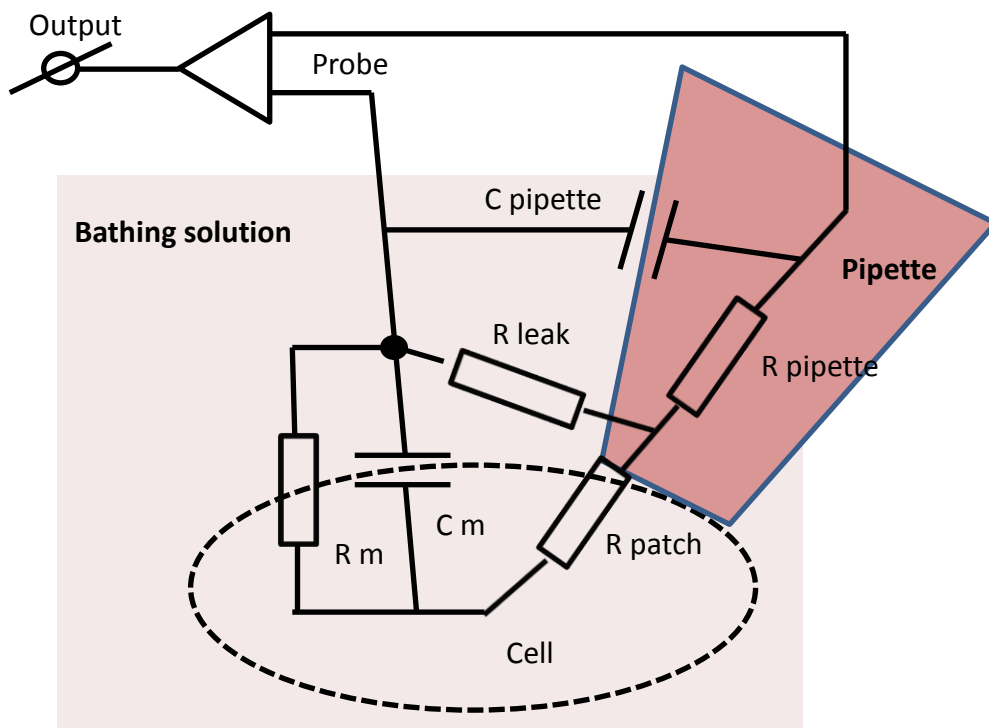


Figure 2-7 The equivalent circuit for the cell-attached configuration (adapted from Molleman)

In this circuit, the pipette and cell membrane are resistors in series, R_{pipette} and R_{patch} . As the pipette is filled with conductive solution it is considered a low resistance compared to the patch area, R_{patch} . As the highest resistance in a series circuit determines the current flow, if R_{patch} is high compared to the resistance of the rest of the cell membrane, R_m and the pipette resistance,

R_{pipette} , then the circuit actually monitors current flow through the patch and any ion channels in it.

However, measurements can be short-circuited if resistance of the parallel resistor, R_{leak} is too low. In practice, R_{leak} signifies the quality of the seal between the pipette tip and the membrane. A good seal means that R_{leak} will be high, and current flow to ground sources (the bath, the reference electrode) is minimized.

The capacitances in the circuit are the pipette capacitance, C_{pipette} , and the capacitance of the patch of membrane. The membrane capacitance, C_m , is not so important in this configuration as the whole cell membrane resistance, R_m , is usually much smaller than R_{patch} so that C_m is effectively 'not seen'. However, the pipette capacitance C_{pipette} must be compensated for, even though its value is small, as capacitive artefacts must be considered when recording channels over a fast time scale with high magnification such as in single channel recording. Capacitive effects also have to be considered in planar patch clamping systems which often use materials with different dielectric and capacitive properties (see Section 5.1).

The cell attached configuration is easy to obtain and the cytosol of the cell remains intact as the membrane is not perforated, however there is no easy way to manipulate the media on either side of the membrane and the exact membrane potential cannot be measured directly. For high quality data recording the membrane voltage is typically controlled.

There are four types of patch clamping in addition to the cell attached configuration. Outside-out excised patch, Inside-out excised patch, whole cell and perforated patch.

Outside-out and inside-out are configurations for single channel measurement where the patch of membrane is completely removed (excised) from the cell. "Outside" and "inside" refer to the extracellular and intracellular side of the membrane; "out" refers to the bath. The outside-out patch is obtained by pulling

the patch pipette away from the cell in a whole cell configuration (shown in Figure 2-9). The membrane eventually breaks and the phospholipids in the membrane fold back on themselves into a patch covering the pipette tip. In this case the pipette solution should be the intracellular side of the membrane. This configuration is used to study the extracellular influences on the channels as the bath composition can be changed easily during recording.

The inside out patch is based pulling a patch of membrane away from a cell attached configuration which leaves a vesicle attached to the pipette tip. The vesicle can be destroyed by exposure to air (i.e. remove the pipette briefly from the bath) which leaves a patch with the cytosolic side facing the bath. Inside out patches are useful for studying the cytosolic factors on channels. In this case the bath is filled with intracellular solution.

In perforated patch clamping, the cell is placed in the cell attached configuration and suction applied until a gigaseal forms. Rather than breaking a patch of membrane, antifungals such as amphotericin B, are applied after a set time through the pipette to make holes in the membrane which enables access to the cytosol without washing out the cytosolic factors. This configuration allows a macro current recording from all ion channels in the cell membrane and the extracellular side can be superfused, but it is difficult to obtain and timing of drug introduction is very important. (Molleman, 2003)

The whole cell configuration is based on the cell attached configuration, with an additional suction pulse or electrical 'zap' used to actually rupture the membrane patch to give direct electrical access to the cytosol. The pipette solution closely mimics the intracellular solution. As the measurement electrode is on the cytosolic side of the membrane and the reference electrode in the bathing solution on the extracellular side of the membrane, the membrane potential can be directly controlled. This configuration is probably the most often used of all of the configurations as it is a fast method of obtaining information about ion channel populations, the cytosolic environment is controlled and the extracellular side can be superfused (with test drug compounds for example).

The disadvantage is that some cytosolic factors may be washed out by the intracellular solution in the pipette, inadvertently changing measurements. If this is an important consideration, the perforated patch configuration can be used. As measuring the whole cell is so important, and is the configuration most often used, the equivalent circuit will be discussed in more detail.

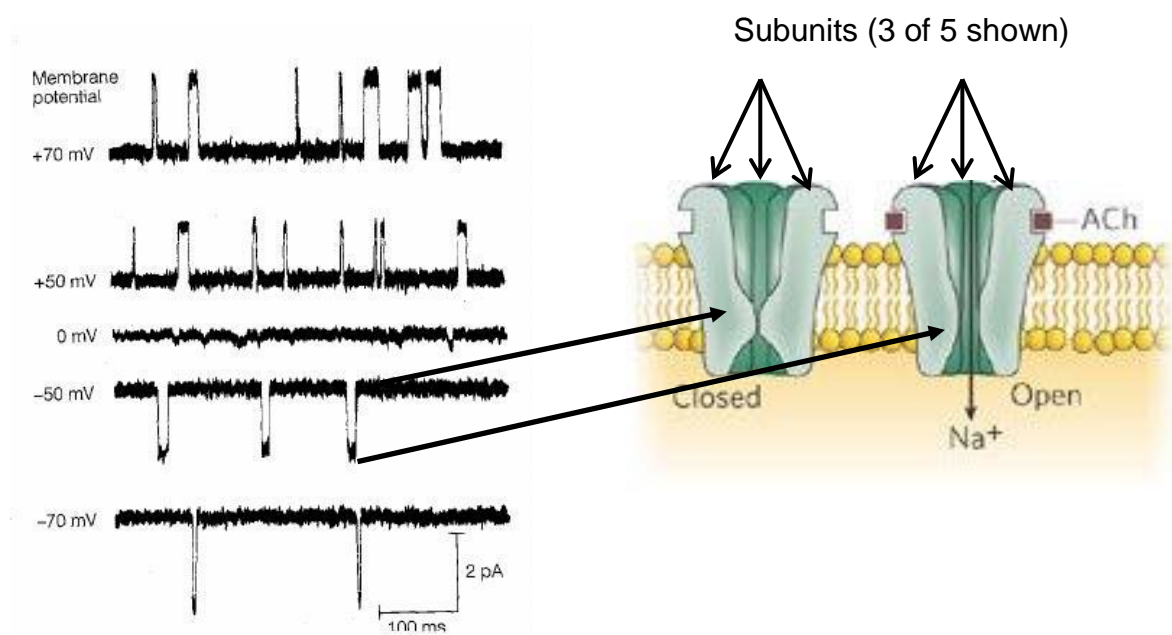


Figure 2-8: Patch clamp recordings (left) for acetylcholine receptors (right, shown as a sectional view) (F.A. Ashcroft, 2006)

Figure 2-8 left, is an example voltage clamp measurement showing the response to acetylcholine (ACh) ligands binding externally and opening an ion channel allowing sodium ions to flow into the cell measured as a 2 picoampere current flow. Not shown here, but also occurring, is that calcium and potassium flow along their concentration gradients when this ion channel is open. Nicotinic acetylcholine receptors are found at neuro-muscular junctions in the body and mediate transmission between neurons and muscles. The physical structure of this ion channel is formed by a pentamer of protein subunits - Figure 2-8, right shows three of the five subunits. The channel is shown in its closed and open configuration (open showing the extracellular ACh binding sites in their closed and opened configuration and the graph on the left shows the corresponding

current (approx 2 picoamperes) at -50mV, this signifies Na^+ ions passing through the membrane. In terms of drug discovery, this information is important to know the effects of a drug on the activation of the ion channel.

The whole cell configuration is achieved after the cell attached configuration has been achieved. In the whole cell situation the membrane is not disturbed so R_{patch} remains high. However in the whole cell configuration the membrane patch is ruptured and R_{patch} becomes very low and is renamed the access resistance R_{access} . In electronic terms the series resistance for a whole cell recording consists of the pipette resistance R_{pipette} , the access resistance, R_{access} and the membrane resistance R_m . As in the cell attached configuration the only parallel resistor is the leak resistance R_{leak} , which should be as high as possible to minimize short circuiting to ground and increased noise.

Membrane capacitance is a particularly important factor in whole cell recording as the entire cell membrane capacitance contributes and not just the patch capacitance. A spherical cell membrane capacitance is related to the diameter of the cell, so $C_m = \pi d/100$, a $20\mu\text{m}$ cell will have a capacitance of 12pF or larger if the membrane has folds, meaning that it will require longer recharge times (repolarization).

If the pipette, or in the case of this work, an aperture, has a geometry which creates a high series resistance (R_{access} and R_{pipette}), then a voltage drop occurs across the membrane and the intended clamping voltage intended for the membrane will not be delivered. Electronics can compensate for this by injecting a voltage of a specific factor measured after the pipette resistance and membrane capacitance have been measured, but it introduces feedback delays into measurement and if the cell membrane is unstable over measurement duration, measurements can become inaccurate.

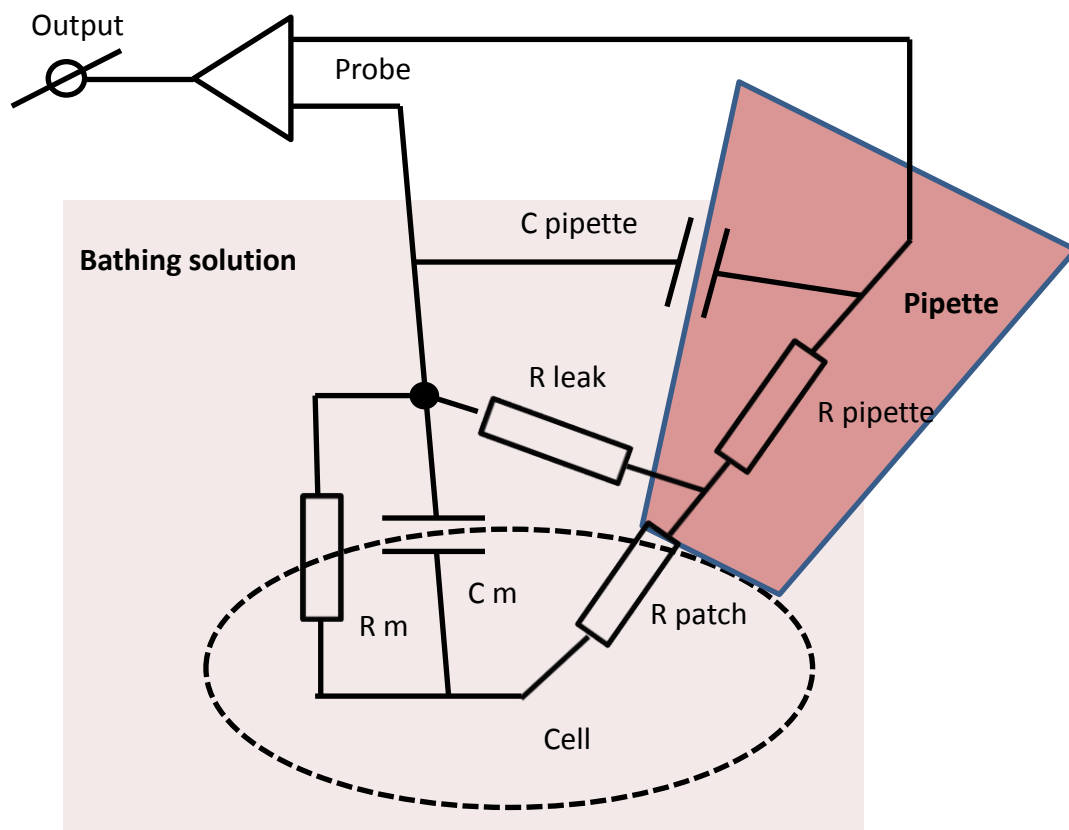


Figure 2-9 The equivalent circuit for a patch clamp measurement in the whole cell configuration (adapted from Molleman)

In practical terms this means that the pipette resistance (which is dictated by the tip diameter and pipette tip shape) should be as low as possible, and its capacitance (dictated by material selection) is also as low as possible to reduce RC noise. The shape and the materials selected for planar patch clamping designs are of critical importance and are discussed in more detail beginning in Section 3.4.

2.4.2 Physical challenges with traditional patch clamping

Physically making patch clamping measurements requires experience to obtain any relevant result. The first requirement for patch clamping is the ability to move a transparent small glass pipette tip under a microscope to a cell without piercing it or breaking the pipette tip. Depth perception is extremely challenging

under a microscope. Figure 2-10 is an image of a micropipette approaching a neuronal cell. It is difficult to have the transparent glass pipette in focus at the same time as the cell, and experience is required to ascertain distance to the cell so that the pipette does not break, or the cell is pierced.

Once the pipette has reached the cell membrane, suction is applied to pull up a patch of the membrane into the pipette, thereby electrically sealing it from the remaining cell. This is a fine movement and care must be taken not to pierce the cell causing immediate cell death. After the pipette has touched the cell membrane it cannot be easily repositioned as the membrane is sticky and may be damaged.

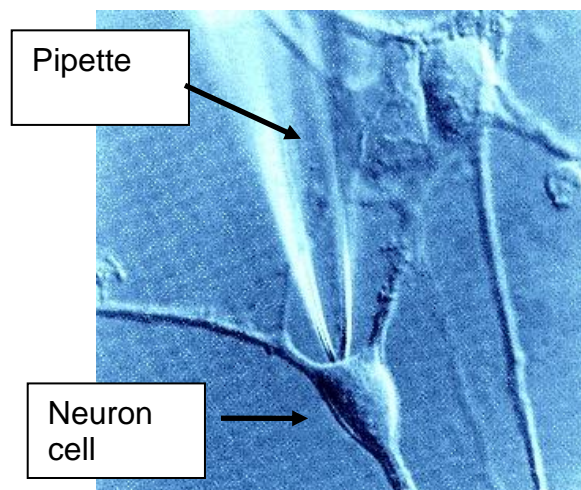


Figure 2-10: Glass pipette approaching a neural cell under a microscope (Duprat, April 2000)

Other common problems are that the membrane patch must seal completely onto the pipette tip – cells must be preselected for their healthiness (requires experience) and a more round-shape cell is more suitable for obtaining a patch. If a seal is not achieved, or an insufficient/incomplete seal - then the pipette tip is generally replaced as a part of the membrane typically sticks to the pipette walls partially blocking it. The pipette opening may also be blocked by floating debris as it is moved through the culture media towards the cell. Pipette tips are also easily broken, these of course must be replaced, and the cell may die during measurement and another must be selected and a fresh pipette charged.

Measurement results for patch clamping require a well-controlled electrical environment in terms of noise. Excessive electrical noise, losses and vibrations need to be prevented by using Faraday cages, well-grounded equipment on a floating vibration reducing table. Ventilation and wiring in the room must also be carefully handled and shielded from the measurement area.

Traditional patch clamping uses silver wire as electrodes, these electrodes are chlorated and passivate over time. Electrode passivation exhibits as drift during measurement and the electrodes should be rechlorated.

Once a high resistance seal has been obtained and is stable, the cell can be measured until recordings become unstable signalling cell death.

In summary, an ideal patch clamping system would remove the need for a pipette, precise micromanipulators and a microscope. In addition, the option of measuring single cells and cell networks in parallel would be a major improvement towards HTS patch clamping.

3 Patch clamping – High Throughput Screening (HTS) systems

Over the last decade, much research has taken place in the development of marketable high throughput screening (HTS) patch clamping systems. Interest in these systems is primarily targeted towards pharmacology screening, but there are also interests in basic and applied research activities, for example for measuring artificially produced bi-lipid layers with implanted ion channels to better understand channel function. With the exceptions of Celectricon (Celectricon, 2008) and Flyion (Flyion, 2007) who use pipettes in a clever manner, most HTS system developers have moved to a planar substrate design which completely removes the need for a fragile glass pipette, certainly the weakest part of patch clamping measurement.

By removing the pipette, no micro-manipulators are required and a microscope is also not necessarily required. Systems that have been developed and are being marketed and sold, use a planar substrate with holes to replace the pipette and either use suction from below or pressure from above, to draw cells to the hole area to form a seal for measurement. This has dramatically improved throughput from 10 cells per day to hundreds of cells per day. However challenges remain, some of which are addressed in this work.

3.1 Planar patch clamping

A major advance in higher throughput patch clamping has been removing the glass pipette from the system and a few companies have successfully developed such systems which are based on a planar substrate with small diameter holes perforating through it. The holes are integrated into a well or chip format either as single holes as an array of holes. These systems remain based on the traditional materials of glass or silicon, with only two systems using novel materials such as polymers. The limitation of using these materials is that they remain comparatively expensive due their low fracture toughness and difficulties in machining them. A longer term move away from these

materials is of focus to companies manufacturing and using patch clamping systems. The systems on the market also use suction as a means of moving cells from a solution down to the planar holes for measurement. This is inherently a risky endeavour as there are no guarantees that the cell entirely covers the hole (particularly if the cell is non-spherical) and causes low throughput per chip – adding expense. There is also the possibility that debris covers the hole instead of a cell. Below is a summary of main manufacturers and the cost of their system, the cells measured and a price per data point (Table 3). The advantages offered by HTS are clear. Higher throughput means more potential hits per day (ion channel responses to drug compounds), faster drug screening and that the cumulative effects of drugs on cells can be monitored, this is not possible using the traditional technique. The advantages and limitations of five HTS systems on the market shown in Table 3 are discussed after a short overview of how planar patch clamping functions compared to the traditional method.

In planar patch clamping, the pipette is replaced by a substrate (Figure 3-1), with a micro-machined hole of between 1 and 5 micrometers. The substrate (typically glass or silicon) is embedded into a well type structure. Cells are suspended in a solution in the well above the measurement hole. The reference electrode is placed into the well solution. The measurement electrode is placed in the microfluidic channel which is initially filled with a salt solution with a concentration similar to the cytoplasm solution of the cell to be measured. Suction is applied to the microfluidic channel below the measurement hole to draw and pull a cell over the hole forming a 'seal' (an effective increase in resistance measured between both electrodes). Once a seal has been established, a patch clamping measurement can be performed the same as the traditional method (see Section 1.3.1).

Table 3: Planar patch clamping systems on the market (Comley, 2003)

Manufacturer /device	Materials	Max. measurements/ run + throughput	Cost (\$/dp)	Cell Types
Cytocentrics CCS GmbH	Quartz chip	20 40,000 dp /day	<3.2	N/A
Flyion GmbH FlyScreen 8500	Glass pipette embedded in plastic jacket	2 channels 300-1,000 dp/day	<1.6	CHO, Jurkat HEK
Molecular Devices IonWorks HT PatchXpress 7000A	Glass /plastic chip	12 channel 3,000 dp/day 16 channels 2,000 dp/day	<2.0 <3.8	CHO Jurkat Neuro 2A
Nanion Technologies NPC 1 (port-a-Patch) NPC 16s (sequential) NPC 16p (parallel)	Glass chip	1 or 16 channels NPC 1 – 50 dp/day NPC – 200 dp/day NPC 16p – 2kdp/day	<2.5 for NPC 16	CHO Jurkat HEK 293
Sophion Bioscience Qpatch 16 Qpatch 64	Silicon chip	Qpatch 16 – 16 channels 1.2k dp/day Qpatch 64 – 64 channels 7kdp/day	<2.5	CHO Herg

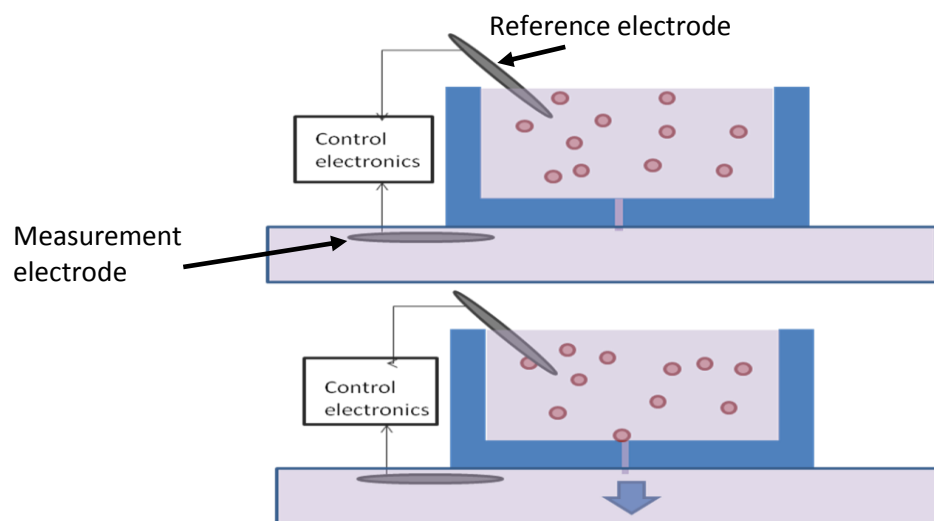


Figure 3-1: Schematic example of a planar patch clamping system

The following section is an overview of the elements, functionality and limitations of patch clamping systems currently on the market.

Cytocentrics GmbH (Cytocentrics, 2008) developed the 'Cytopatch' system for drug screening purposes. The chips are made of quartz glass and their website states that the chip hole resistance is less than 5 M Ω in physiological saline (Cytocentrics, 2008). Cells are fed into a well-type arrangement above holes which are 4 μ m in diameter (Stett et al., 2003; Knott et al., 2002). Suction is applied to the cytocentering channel until a cell is pulled onto the hole area, forming a gigaseal. The Cytopatch channel (Figure 3-2) is backfilled with a KCl solution and the cell is ready for measurement. This automated system can perform up to 20 parallel measurements on single cells, with a rate of 3 patches per site per hour, and a seal success rate of over 50%. Cells measured using the system are CHO (Chinese Hamster Ovary, diameters up to 200 μ m), Jurkat round shaped leukemia cells with a diameter of approx. 20 μ m and Neuro 2A heterogeneous round brain cells. These cells are commonly found in patch clamping measurements as they are large (>10 μ m) round, are stable in culture and have stable signal expression.



Figure 3-2: CytoCentrics GmbH patch clamping chip {}

Nanion GmbH (Nanion, 2010b) developed the Port-a-Patch system to be self-contained. It can perform up to 16 parallel patch measurements as well as for ion channel research purposes, artificially produced lipid bilayers. The system is based on borosilicate glass, the 1-2μm holes are ion-track etched (Fertig et al.,) as seen in Figure 3-3 and have an aperture resistance of 2-3MΩ in physiological saline (Kirchner et al., 2005). Cells here are also fed into a well above the hole, and a vacuum is applied until a cell is pulled onto the hole and a seal is formed. Recently, Nanion introduced a perfusion system into the self-contained unit so that cells can be kept viable for longer measurement periods. Throughput is 30-50 data points per day, with a whole cell recording rate of 30-50%. Cells measured by the system are Jurkat and RBL leukemia cells and HEK 293 kidney embryo cells, round cells with diameters a minimum of 20μm. CHO cells have also been measured. The selling point of this system is that it is highly portable, requiring only a laptop and the device which is smaller than a shoebox.

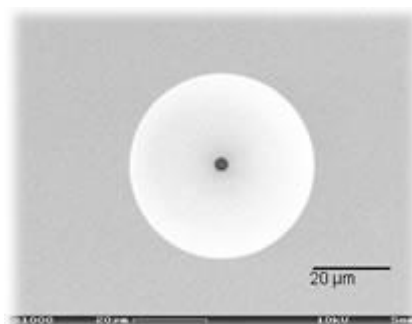


Figure 3-3: Nanion borosilicate glass chip (Nanion, 2010a)

Flyion GmbH (Flyion, 2007) developed 'Flip-Tip' technology from a glass pipette with a plastic sheath for improved robustness. A few cells are delivered in solution to the inside of the inner pipette, and gravity fed into the opening where gentle suction forms a 1-5 GOhm seal for whole cell clamping. Compounds for screening are then delivered to the outer pipette area chip tip (see Figure 3-4). The company states that the flyscreen system can measure 500 cells per day and states that measurements have been performed on CHO, Jurkat, and HEK cells.

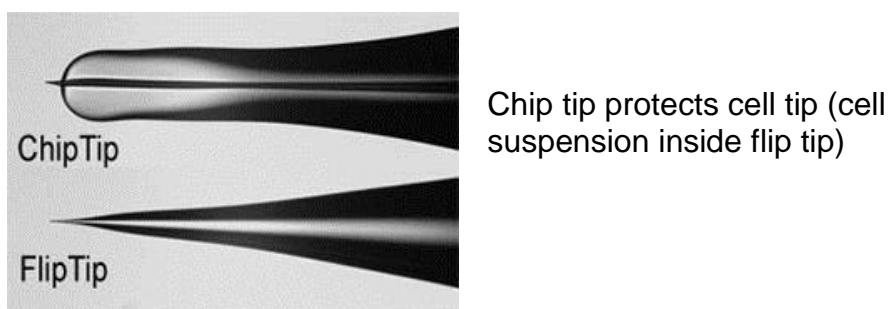


Figure 3-4: Flyion and a 'flip the chip pipette' arrangement

Sophion Bioscience (Sophion bioscience, 2009) has developed a silicon / glass based chip which fits into the Q-Patch system. The chips for measurement are produced by ThinXXS GmbH (Thin XXS, 2009) and have a measured aperture resistance of $2.04 \pm 0.02 \text{ M}\Omega$ in physiological solution ($n=274$) (Kutchinsky et al., 2004). Suspension cells are pre-centrifuged, then re-suspended in the measurement solution and then delivered to the well-plate (Figure 3-5, label 7) which can measure 64 patch sites in parallel. Cells are pulled using vacuum onto the hole in silicon (see Figure 3-5, label 1). For drug testing, drug compounds of varying concentrations are sequentially added after flushes between concentration changes, to the channel above the cell (7) to test its effects on the ion channel activity with cumulative drug additions. The channel below the cell contains measurement solution (which mimics the salt concentrations inside the cell). Cell types that have been measured include CHO expressing hERG channels (human ether-a-go-go, heart channels). The

success of cell sealing varies dependent on cell type and preparation but is on average about 60%.

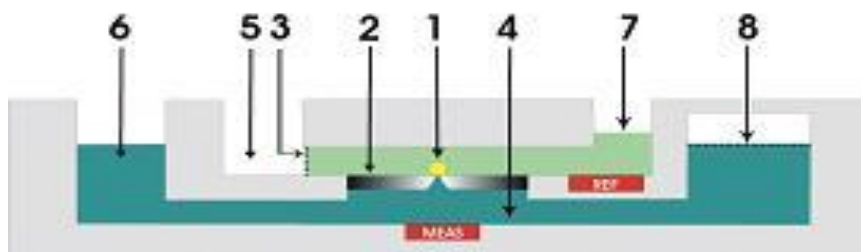


Figure 3-5: Sophion bioscience QPatch chip schematic (Sophion bioscience, 2009)

Molecular Devices (Molecular Devices, 2009) has the Ion Works and PatchXpress systems on the market. Ion works uses the idea of population patch clamping, where a well plate contains 64 measurement holes to patch 64 cells simultaneously and gives an average response of all cells in a well. This system measures up to 2000 data points per day making it useful for secondary screening (see glossary) of drugs. This approach begins to measure with a resistance of 100MOhms and is one of the systems on the market using a polymer chip. This polyimide foil chip has the lowest starting point resistance of all the HTS systems on the market and is a baseline value to assess this work against.

The PatchXpress system can measure ion channel activity of up to 16 cells in parallel and uses a *Sealchip* produced by Aviva Biosciences. The chip materials are not given but it is stated that the chip is comprised of a transparent substrate on a plastic cartridge. The substrate has been chemically modified to interact maximally with the cell membrane for fast gigaOhm seal creation (<10 seconds). Depending on cell type, this system can measure from 100 – 600 cells per day.

3.2 Patch clamping systems in the research / early stage business

While systems currently on the market were at one time research projects in a university environment, it is worth mentioning a few early stage companies and advanced research groups working with novel materials.

Founded in 2005, the company Fluxion bioscience spun out of a planar patch clamping system developed by the Luke Lee bioengineering group at the University of California (Berkeley){{16 Seo,J. 2004;}}. The design is based on a clever use of a lateral hole geometry known as a 'mouse hole' produced in PDMS (Polydimethylsiloxane). The approach uses silicon which is surface machined with 3.5 μ m high guides, onto which 50 μ m SU8 is patterned for wider cell delivery channels. PDMS is then poured into the prepared SU8/Si mould and a completed planar patch clamp chip as shown in Figure 3-6 below is formed. The unique design of this system allows cells to be patched horizontally, maximizing the efficiency of a planar design with channels.

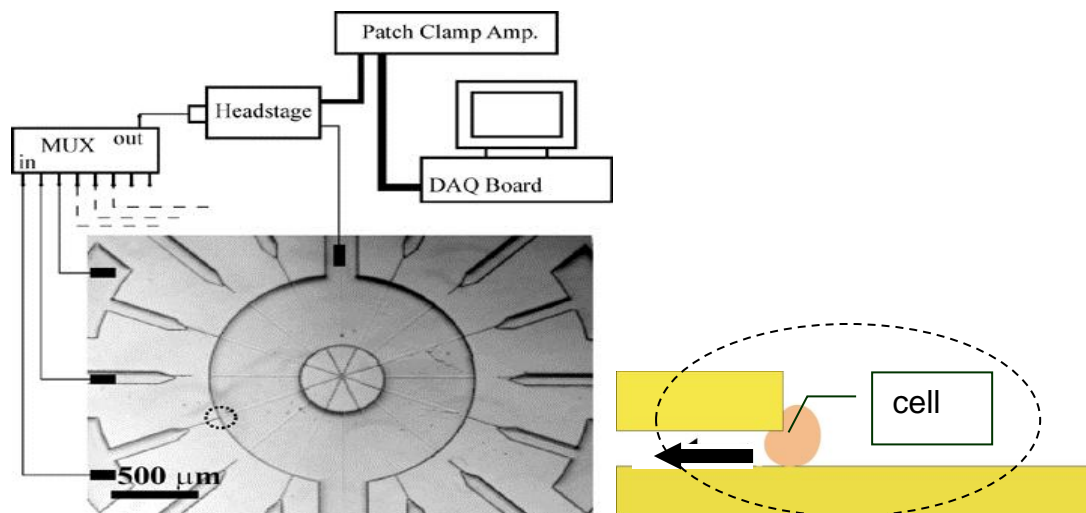


Figure 3-6 Top and enlarged views of PDMS integrated multiple patch clamp array with lateral cell trapping junctions

The dotted area is a cell patch area; there are 14 such multiplexed channel areas in this design shown above. However, the distances between channels can be reduced to some tens of micrometres apart, significantly increasing the number of measurements possible. The fluidic connections required for patching are manually punched at the outside of the PDMS moulded structure. Cells are placed in the round well area and those found within 100-200 μ m of the cell patch area are pulled into the cell patching area by applying a 2psi negative pressure to the patch channel. After cell trapping, negative pressure is removed and the cell forms a seal with the rim of the patch channel, which due to forming has a 'tunnel arch entrance' shape from moulding. This system allows for 14 patch measurements to be performed simultaneously, and HeLa round cancer cells of about 15 μ m diameter have been measured. The central hub wheel area serves as the perfusion inlet point, the group state that allowing culture medium to flow into the central well, reduces noise from perfusion drip. The layout of this system is original and effective for small cells, and the well type design maximizes cell use. The limiting factor in the design is the space required when each cell requires its own vacuum/ electrolyte inlet (labelled MUX in Figure 3-7).

The fluxion chip uses the same PDMS material, but has a different configuration, the mouse holes are placed along the sidewall of a microfluidic channel in an original array of 12 holes (in the meantime increased to 16 holes) with a spacing of 20 μ m, using a as shown in Figure 3-7 {{16 Seo,J. 2004;}}, {{92 Ionescu-Zanetti, C. 2005;}} The advantages of the chip is that it is low cost, and the clever design allows for the addition of many compounds simultaneously to different wells in the layout, so parallel compounds can be measured simultaneously. The use of PDMS also permits the formation of a gigaseal, although the mechanism for this is not well understood.

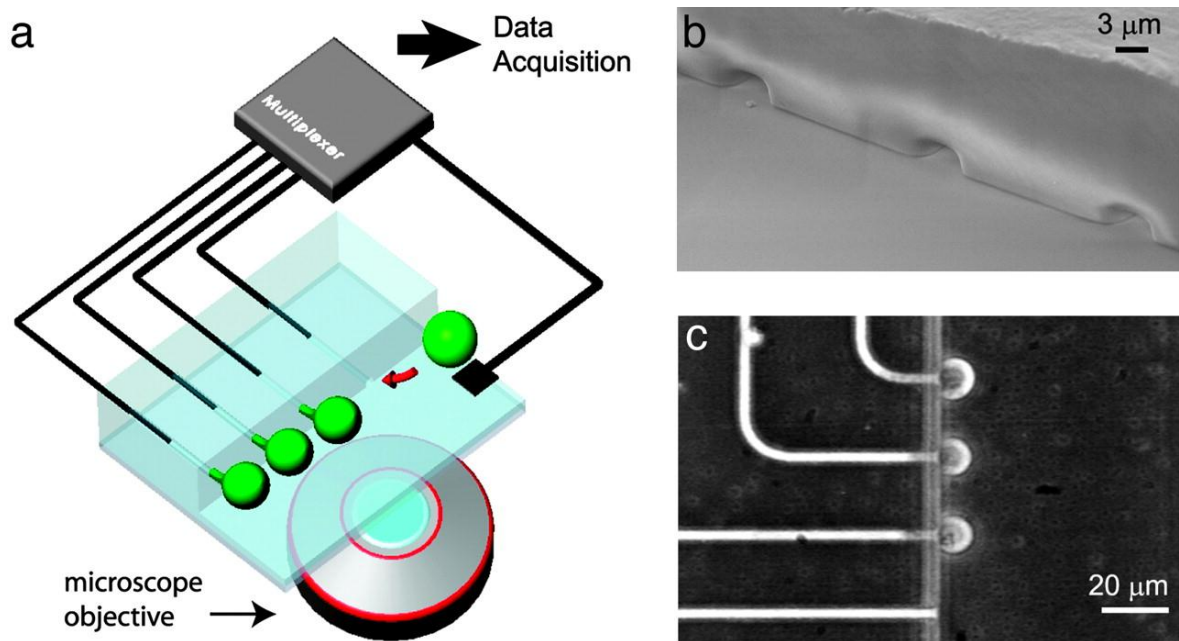


Figure 3-7: The fluxion lateral patch clamping approach: (a) schematic diagram of cell trapping by applying negative pressure to capillaries, (b) SEM of three recording sites from the main microfluidic channel and (c) dark field optical microscope image of cells trapped at three recording sites images. Images taken from www.fluxion.com

Patch clamp array on a microfluidic platform. (a) Cell trapping is achieved by applying negative pressure to recording capillaries, which open into a main chamber containing cells in suspension. Attached cells deform, protruding into the capillaries. Patch clamp recordings are obtained by placing AgCl electrodes in each of the capillaries, as well as in the main chamber. Signals are fed through a multiplexing circuit and into the data acquisition system. (Multiplexer setup and microscope objective are not to scale.) The device is bonded to a glass cover slip for optical monitoring. (b) Scanning electron micrograph of three recording capillary orifices as seen from the main chamber. The capillary dimensions are $4 \times 3 \mu\text{m}$, with a site-to-site distance of $20 \mu\text{m}$. (c) Dark field optical microscope image of cells trapped at three capillary orifices. Trapping was achieved by applying negative pressure to the recording capillaries. The device consists of 12 capillaries arrayed 6 along each side of the main chamber fluidic channel, along a $120\text{-}\mu\text{m}$ distance.

A Canadian group (The Mealing group at the Canadian Research Council in Ottawa, Canada) are pursuing a silicon oxide, silicon nitride on silicon wafer based approach to patch clamping (Figure 3-8). These chips are intended for measuring cultured neuron cells to better understand the synaptic activity of neuronal networks. The chips are glued into a PMMA chamber then coated with Poly-L-lysine for cell adhesion. The top of the chamber is used for cell culture, while the bottom chamber access is used during measurement. Snail neurons are applied to the cell culture side and cultured for two hours before measurement.

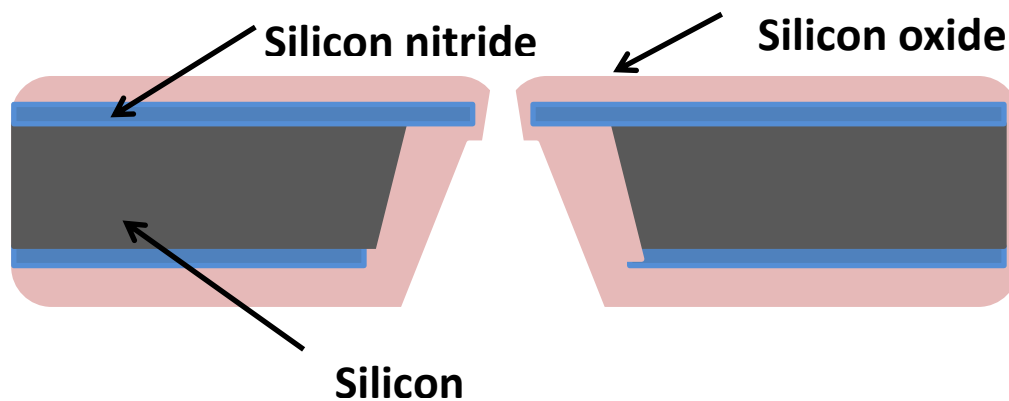


Figure 3-8: Model of a CNRC silicon/silicon nitride/silicon oxide chip

A chip resistance through hole diameters measured on a diameters between 1.3-1.8 μ m in a PBS (phosphate buffered saline) solution with a resistivity of 55 Ω .cm at 1.5 to 3M Ω , respectively (Py et al., 2010) The group states that an average whole cell capacitance of 34.2 \pm 3.13 pF (n=5) was measured and that the capacitance of the chip could not be directly measured as the cells formed spontaneous whole cell configuration without the addition of suction. This spontaneous formation of whole cell is considered as being precipitated by the high concentration of potassium (50mM) in the subterranean channel below the chip.

Whole cell recording was done in both a voltage clamp and current clamp configuration on the snail neuron (LPeD1) where robust action potentials were measured between two cells. Work is ongoing by the group to reduce bubble

formation and for longer term studies where the whole cell configuration is more controlled.

3.3 Series Resistance Calculations

The Mealing group (see p.56) developed a formula to calculate the series resistance of a conical hole or pore (Py et al., 2010) filled with a conductive solution which has been used here to assess the importance of hole shape and thickness of material which corresponds to the length of the hole.

The proposed formula

$$R_m = \int_0^l \frac{\rho}{A(z)} dz$$

Where z is the distance along the axis of the aperture- The integral can be done by measuring the entrance and exit holes to estimate the area A , as a function of z . A solution resistivity (ρ) of 55 Ω .cm was assumed for calculations.

To solve for $A(z)$:

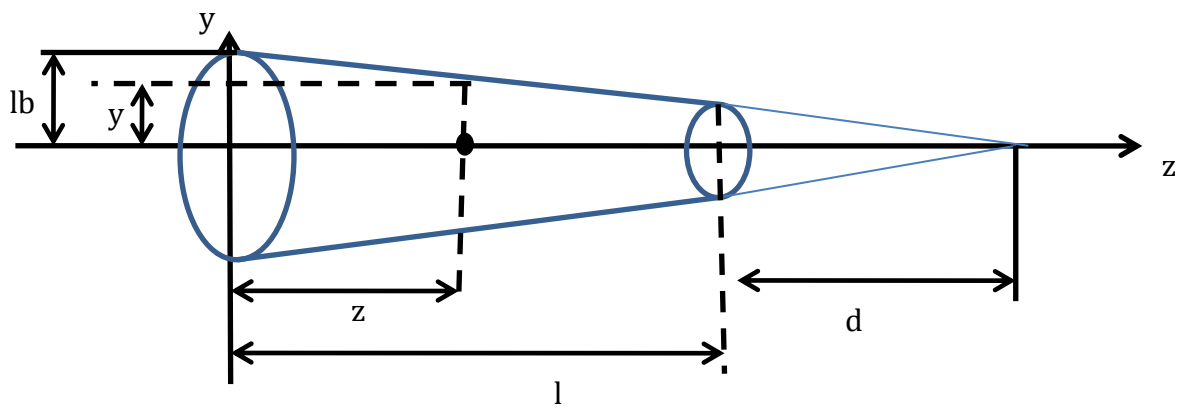


Figure 3-9: geometry of conical pore

$$l + d : l + d - z = lb : y$$

$$\frac{l + d}{l + d - z} = \frac{lb}{y}$$

$$y = \frac{lb}{l+d} \cdot (l+d-z)$$

where: $0 < z < l$

Area at z,y: $A(z) = \pi y^2(z)$

$$A(z) = \left(\frac{lb}{l+d} \right)^2 \cdot \pi (l+d-z)^2$$

Where $\left(\frac{lb}{l+d} \right)^2 = \text{a constant } B$, then

$$R_m = \int_0^l \frac{\rho}{B (l+d-z)^2} dz$$

$$R_m = \frac{\rho}{B} \int_0^l \frac{dz}{(l+d-z)^2}$$

Where $t = l + d - z$, then $\frac{dt}{dz} = -1 \Rightarrow dt = -dz$

$$\int_{l+d}^d \frac{dt}{t^2} = \int_d^{d+l} \frac{dt}{t^2}$$

so:

$$R_m = \frac{\rho}{B} \cdot \left[\frac{1}{d} - \frac{1}{d+l} \right]$$

Example calculation:

A foil material of 50 μm thickness ($l = 50$), has a conically shaped laser drilled via (assumption is that the sidewall gradient remains constant along the entire length, l) with a laser beam entrance diameter of 4 μm ($lb = 2$) and exit diameter of 1.8 μm ($ld = 0.9$)

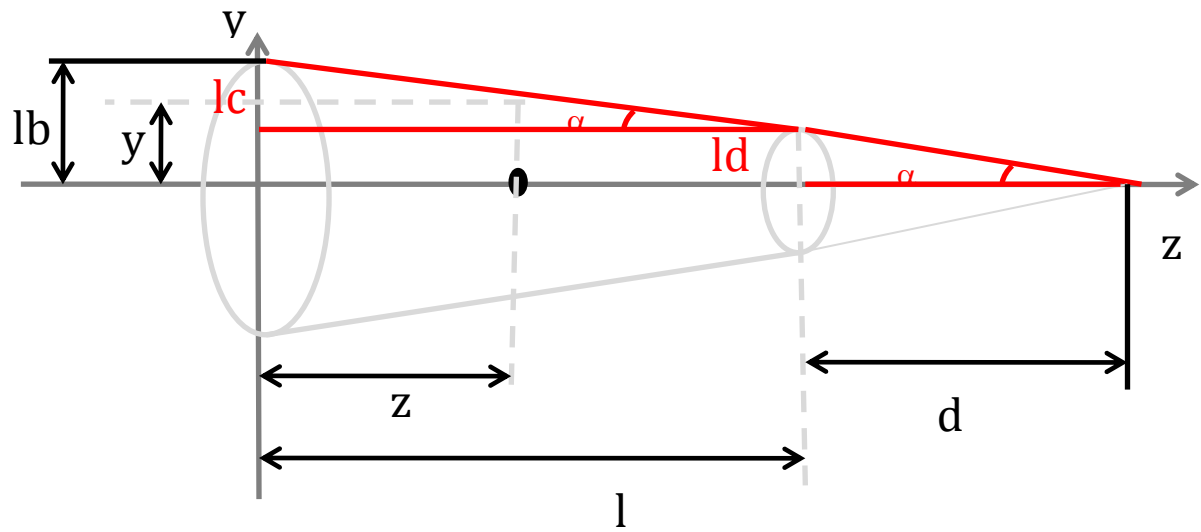


Figure 3-10 Calculation of the sidewall angles for series resistance

Calculate angle to obtain length d:

$$lc = lb - ld \quad \tan \alpha = \frac{lb - ld}{l}$$

$$\text{Angle } \theta = 1.26^\circ$$

$$d = \left[\frac{\tan \alpha}{ld} \right]^{-1} = 40.9 \mu\text{m}$$

$$B = \left(\frac{lb}{l+d} \right)^2 \cdot \pi = \left(\frac{2}{50+40.9} \right)^2 \cdot \pi = 1.52 \times 10^{-3} \mu\text{m}$$

Plugging values into formula:

$$R_m = \frac{\rho}{B} \cdot \left[\frac{1}{d} - \frac{1}{d+l} \right]$$

$$\text{Then } R_m = 4.70 \text{ M}\Omega$$

Table 4 Influence of pore dimensions and area on series resistance

Foil thickness (l) (μm)	Entrance diameter (μm)	Exit diameter (μm)	Angle (θ)	R _m
50	4	1.8	1.26	4.7M Ω
50	12	4	4.57	733k Ω
30	12	4	7.75	62.88 k Ω
50	100	4	45	7k Ω

All calculations use a solution resistivity of 55 $\Omega\cdot\text{cm}$

From these calculations, it can be seen that smaller dimensioned holes (less area) significantly increase the resistance, as expected, smaller pore areas (entrance diameter 4 μm , exit diameter 1.8 μm) have a much higher resistance (4.70M Ω) compared to a 12 μm exit and entrance diameter (733k Ω) for the same material thickness. Changes in the hole area caused by varying foil thickness also contributes to resistance changes (changing the effective access area); a 20 μm reduction in thickness causes resistance to drop by a factor of 10 from 733k Ω to 62k Ω for the same entrance and exit diameters. The sidewall angle also causes a change in liquid access area, an extreme example of the influence of sidewall angle is also calculated for a 45 degree angle, the greater the angle, the larger the reduction in effective access resistance. Ideally, a wide sidewall angle and very thin foil and the largest possible hole would create the lowest resistance situation for measurement. In practice, however, compromises must be made so that the cell does not pass through the hole. A large sidewall angle and thinner foil also lower the series resistance value; however there are limitations as a large sidewall angle acts effectively like a thinner film which will be subject to flexure which may be large enough that a cell can squeeze through. Foil flexure may also result in increased

measurement noise and handling difficulties during fabrication. For this reason a range of hole diameters and sidewall angles will be pursued in this work using different fabrication methods.

3.4 Limitations in High Throughput Screening

Almost all of the companies with High Throughput Screening (HTS) systems presently on the market achieve significant throughput in secondary drug screening (see glossary) by removing the need for a pipette (with the exception of Flyion who uses a pipette in a novel way), micro-manipulators and microscope. Marketed systems which use planar substrates containing micro-holes have significantly increased measurement throughput. An example is the system produced by Sophion Bioscience which is capable of measuring up to 64 single cells in parallel. However, despite this progress some significant challenges and limitations must be overcome if the future throughput demands of the pharmaceutical industry are to be met through reduction of cost per data point.

Both glass and silicon patch clamp chips are expensive. Fabrication costs with these materials are high and since the chips can only be used once the consumable costs are seen as the top limiting factor in the use of HTS in primary screening (see glossary). So prices still must be reduced significantly to under \$1 per data point for the uptake of HTS systems by drug companies (Comley, 2003). The population patch clamp Ion Works Barracuda is unique in its approach of sacrificing sensitivity for average response of a population of cells – this is useful for initial drug compound screening. The ion works barracuda plates use an array of holes which are laser drilled into a polyimide foil which is attached to a modified 384 well plate. Polyimide is a cheaper alternative material which enables higher throughput but does not allow for a highest quality seal, and pore formers (amphotericin) must be used to create a whole cell configuration for measurement.

PDMS is in use in the Fluxion system, which makes it a low cost chip capable of measuring a gigaseal, however there are challenges as the material is

extremely hydrophobic and must be pre-treated immediately prior to use (the fluxion system has a built-in oxygen plasma system to assist with this). PDMS also absorbs water over time causing swelling of the polymer, and more significantly for drug screening, low concentrations of hydrophobic drug compounds cannot be measured using this system as they adsorb onto and absorb into the channel sidewalls en route to the cell (Regehr et al., 2009). This means that the actual volume and concentration of compound delivered to the cells is unknown and non-reproducible. PDMS has also been found to have migrated to cell membranes (Regehr et al., 2009) PDMS is also quite difficult to manufacture (handle) in large volume production settings.

Cell sample preparation is still a slow and arduous process. In most cases before measurements can be undertaken, cells are trypsinated to chemically separate them. Trypsination weakens the cell membrane which increases the chance of cell rupture during placement by suction. Before injection into the measurement wells the cells must remain in suspension without re-clustering. This immediately precludes many cell types which cannot be suspended including heart, many primary and nerve cells. The latter cells are physiologically very relevant to ion channel research and drug screening and the fact that they cannot be measured in existing HTS systems is without a doubt a limitation.

Typically in HTS systems, suction is used to pull a cell from the suspension onto a hole for measurement. This is a method that is inconsistent and imprecise as there are no guarantees that a cell rather than a piece of debris will land over the hole, or indeed if a cell is pulled towards the hole, that it covers it completely to enable measurement. Depending on cell type, successful high resistance seal rates vary between 30 – 80%

The shape of cells themselves becomes a factor in seal rate success. Cells must be more or less round and be large enough ($>10\mu\text{m}$) for good seal quality.

However, most cells are not round; heart cells for example are long and fibrous and epithelial cells have a long spindle shape.

Only single cells can be measured and no networked cell systems, similar to above, the behaviour of cells in clusters is different to single cells. For neuronal networks, action potential measurements can only be performed when cells are physically connected. In traditional patch clamping measurement of neuronal cells if more than one cell is to be measured, the cells must be carefully selected to be physically close due to the limited viewing field of the microscope, and opposingly there must be enough space to guide pipettes to the cells of interest. These constraints mean a maximum of two cells can be measured at any one time, not really a cell network situation.

In the next section, some of the identified limitations are addressed.

3.5 Addressing the Identified Limitations – Design Analysis

A design concept arises from a synthesis and analysis of design requirements. In this study, the synthesis includes considerations of how to address limitations in current HTS patch clamping systems as well as consideration of future requirements. A high throughput, high resolution patch clamping system must comprise of a hole for measurement, two electrodes, one for measurement, one providing a reference, and a method of delivering and exchanging solutions, compounds of interest and flushing media between compounds, to the cells.

3.5.1 Materials

Materials used in patch clamping must be biocompatible with low dielectric constants, low dielectric loss (Mayer et al., 2003) to obtain the Gigaohm seal resistance (often simply called a “gigaseal”). In this case the ion currents will not be swamped by other leakage currents. Materials must be formable to a high surface finish (low roughness, less than 0.05 μ m). It must be possible to form holes of diameters between 1 and 5 μ m in a reproducible manner similar to that of a glass pipette, with a shape which can be filled with measurement fluids where resistance measured is not extremely high (<5 MOhm). It is preferable

that materials chosen be optically translucent so that a combination of other complimentary techniques, such as calcium fluorescence may be incorporated into the design at a later date. Traditional materials used in patch clamping are borosilicate glass, or for higher quality patch clamping measurements, quartz glass, both of which are difficult to form and therefore more expensive to produce.

Polymers are suitable alternative materials due to their high dielectric constants and low dielectric losses; thermoplastics are of specific interest due to their ease of forming by laser cutting, injection moulding, and hot embossing. Light sensitive polymer resist materials such as SU-8 which may be formed using traditional semiconductor technology processes, may also be appropriate. The second factor which must be considered with regards to process and design requirements is cell placement.

Three polymer types were selected for this work and are discussed in detail in Section 5.1.

3.5.2 Cell placement using suction

The limitations of using suction for cell placement were listed in Section 3.4. One of the novel ideas of the design put forward in this thesis is to use surface modification techniques to modify polymer surfaces to make the area around the measurement hole cell attractive. As the isoelectric point is important to cell adhesion (proteins), particularly hydrogen acceptors (COO⁻), specifically modifying a polymer surface to create these hydrophilic areas around a drilled hole should positively influence cell attraction, placement and adhesion. The rationale for this approach is to culture cells and allow them grow over and partially into the holes forming a “self seal” thus removing the need for suction for cell placement. Placing additional tracks on the surface between the holes enables cells which physically connect to each other (such as neuronal cells) to use the attractive tracks as guides for growth, enabling the formation of controlled neuronal networks, each cell can be made individually addressable

by placing single electrodes under each measurement hole. This is a new method of creating networks for patch clamping measurements and it should allow the measurement of neuronal cells in manner which is physiologically extremely relevant. A large part of this work has been in producing, optimizing and analyzing surface modifications and is covered in Sections 5 and 6 where the background on surfaces and cell adhesion is also explained.

3.5.3 Cell sample preparation and handling

One of the limitations of current HTS systems detailed in Section 2.2 is that cells must be kept in suspension without agglomerating or settling onto the well surfaces. This typically requires almost immediate pre-treatment of cells prior to measurement and is typically done by trypsination (see glossary and Appendix A for procedure) which weakens cell membranes so they can separate. Cells are mechanically re-suspended using pipettes and stirred before being placed into the measurement wells above the hole, where suction is applied below the hole to pull a cell to it. Suction is an aggressive way of moving cells to a hole, and can cause weakened cells to rupture before correct placement over the hole. In the approach pursued here, the surface areas around the hole are modified to be cell attractive, so cells, after injection, voluntarily migrate to these areas (within some minutes) and are left to grow over and slightly into the hole, positioning themselves and culturing over a period of days. This has several advantages, neuronal cells can grow to physically contact each other, a pre-screening can be done in advance so improperly situated cells can be removed from a test protocol - sparing expensive compounds, and cells are rested and potentially give more physiologically relevant measurements. As cells culture over days, consideration must be given with regards to cell nutrition and removing spent medium.

As each cell must be individually addressable, each measurement electrode must also be electrically insulated from its neighbouring electrode. This requires a separate microfluidics arrangement for each electrode and cell with sufficient capacity for cell nutrition and also for measurement.

3.5.4 Microfluidics and micro-electrodes

The previous section highlighted that cell nutrition must be provided to each cell in a manner such that the designed microfluidic system also electrically isolates each measurement electrode individually. Silver electrodes must be of sufficient dimensions to be chlorated for stability. The design must also allow the freedom to culture single cells or cell networks. The microfluidics system must deliver nutrition to a cell at an approximate rate of 400-700 $\mu\text{L}/\text{hour}$ as taken from a bioreactor used in the same lab (Altmann et al., 2008; Gottwald et al., 2008). For measurement purposes cell exchange must be much faster – the maximum estimated rate is an exchange at the cell interface of 10 $\mu\text{L}/\text{second}$ for ligand gated cells (Wilson, 2009).

While some microfluidics modelling work has been done, it requires more detailed analysis of diffusion rates for drug compounds to become relevant and so is not covered in this work. Some electrode characterization work was performed and this is included.

4 Aim

The future of HTS patch clamping systems not only requires lower cost chips and application to an increased range of cell types, but also to a more physiologically relevant measurement of cells for drug screening and better understanding cell to cell communication in fundamental research. The goal of this work has been to evaluate novel materials and processes for reducing cost while improving cell handling and preparation and to increase the range of cells that can be made available to patch clamping technology, with this in mind the major focus of this work became the following:

A polymer device should be fabricated which makes it possible to measure the ion currents through a cell membrane. To achieve this, the following activities were undertaken:

- a membrane with an array of microstructured holes for fixing and measuring cells was produced
- structured surface modification for precise placement of cells over holes
- bringing an electrode system which allows signal acquisition over an entire hole array, the electrodes to be individually addressable
- measuring a Mega- to GigaOhm resistance, to allow measurement of currents in the nano to pico-ampere range
- setting up a biological system (cells on structures)

Polymers are materials well-suited for this application because they can be selected for bio-compatibility, ease of forming and handling, cost-effectiveness and easily modified surface properties.

Manufacturing a membrane: a planar design approach has been used and laser drilling as well as traditional semi-conductor lithography processing have been used to fabricate arrays of small holes with diameters ranging from 1 to

10µm as a feasibility study. However, the lower range of diameters (<3µm) only are suitable for cell measurement.

Surface modification: to prevent the challenges arising from suction in HTS systems to date, surface modification techniques have been used to provide specific cell attractive areas around the measurement holes to attract cells to situate above the holes. This has a few distinct advantages; cells compete for attractive regions over holes making it more likely to have cell coverage and, rather than culturing in a flask up until shortly before measurement, cells are taken from the flask up to ten days before measurement and are cultured over the measurement holes where they not only cover but grow into the holes forming a “self seal”.

Techniques for the modification of polymer surfaces to make them attractive or repellent to cells for specific cell placement and the ability to produce small micrometre sized holes in the polymer material were evaluated with robust and simple processing being an important criterion. Design and materials selection of the microsystem were based around the selected surface modification technique.

In terms of isolation of single cells on a surface, the average mammalian cell sitting on a surface has a cytoplasm diameter (the ‘body’ of the cell) of between 10 and 25µm. A neuronal cell also has neurites which are long thin growths used to send electrical impulses between cells to enable communication, the largest of these are a few micrometers in diameter. The method used to produce the surface modification then must be capable of this kind of resolution. Suitable methods are Dip Pen Nanolithography, UV-lithography processes and UV laser processes.

UV lithography is a high throughput method used traditionally to produce silicon chips. It is a mainstream manufacturing technique that is extremely efficient and cost effective. UV lithography uses a quartz glass mask with a thin patterned chrome layer used to reflect the UV light and create the pattern on a light sensitive photoresist material below it. The same technique can be used to

modify a patterned area of a suitable polymer material, and also to make holes in materials of sufficiently small diameter for patch clamping measurements, assuming that there are polymer photoresist materials available which are biocompatible and can be suitably modified to have cell attractive regions.

UV lasers are initially high cost equipment, however, once set up; they can be used to rapidly and cost-effectively create both surface modifications and drilled holes.

Dip Pen Nanolithography (DPN) involves the use of a treated atomic force microscope (AFM) tip which is dipped into a protein 'ink' and creates Langmuir-Blodgett films of one or multiple layers onto a surface. It has only recently become viable in terms of high-parallelism using multiple tips simultaneously, so was not pursued in this work.

In this work, a UV lamp (185nm wavelength) and a UV laser (193nm wavelength) were evaluated for their effectiveness for modifying polymer surfaces for cell adhesion. At wavelengths below 200nm and the application of sufficient energy, UV photons break carbon-carbon bonds without thermal influences seen in polymers at even 248nm. Upon exposure to oxygen, carboxyl groups are formed which can be used for protein attachment (see Section 2.2. isoelectric point).

The surface modification methods used must be characterized to include cell adhesion parameters, and also confirm that cells will grow over holes. The holes are drilled at the same wavelength as the surface modification to provide a very similar cell attractive surface. It was unknown at the start of this work whether a cell would prefer to migrate to the modification area and grow around the hole, or if it would cover the hole, and if so, whether sufficiently enough to permit measurement of a high resistance (>100 MOhm).

Electrode arrays: platinum and silver/silver chloride arrays were evaporated onto polymer foils and resistance measured in conductive solutions (KCl) up to 10 days.

Measuring resistance: a test rig was developed for clamping foils without a leak path, the impedance of the test rig and setup was measured as a baseline and then with foils, and finally with cells on foils.

In the design consideration must also be given to microfluidics layout to include cell perfusion, a supply of nutrition and removal of waste products, for up to ten days at a suitable rate, as well as for compound exchange at faster rates during measurement, this work is not a part of this thesis. The following section details the design approach and fabrication methods considered in this work.

4.1 Design approach

The design and fabrication approaches used in this work cover materials selection, including the suitability of polymer materials for their electrical properties (good dielectric properties), hole fabrication by laser and UV lithography, biocompatibility and the ability of surfaces to be modified for cell attraction.

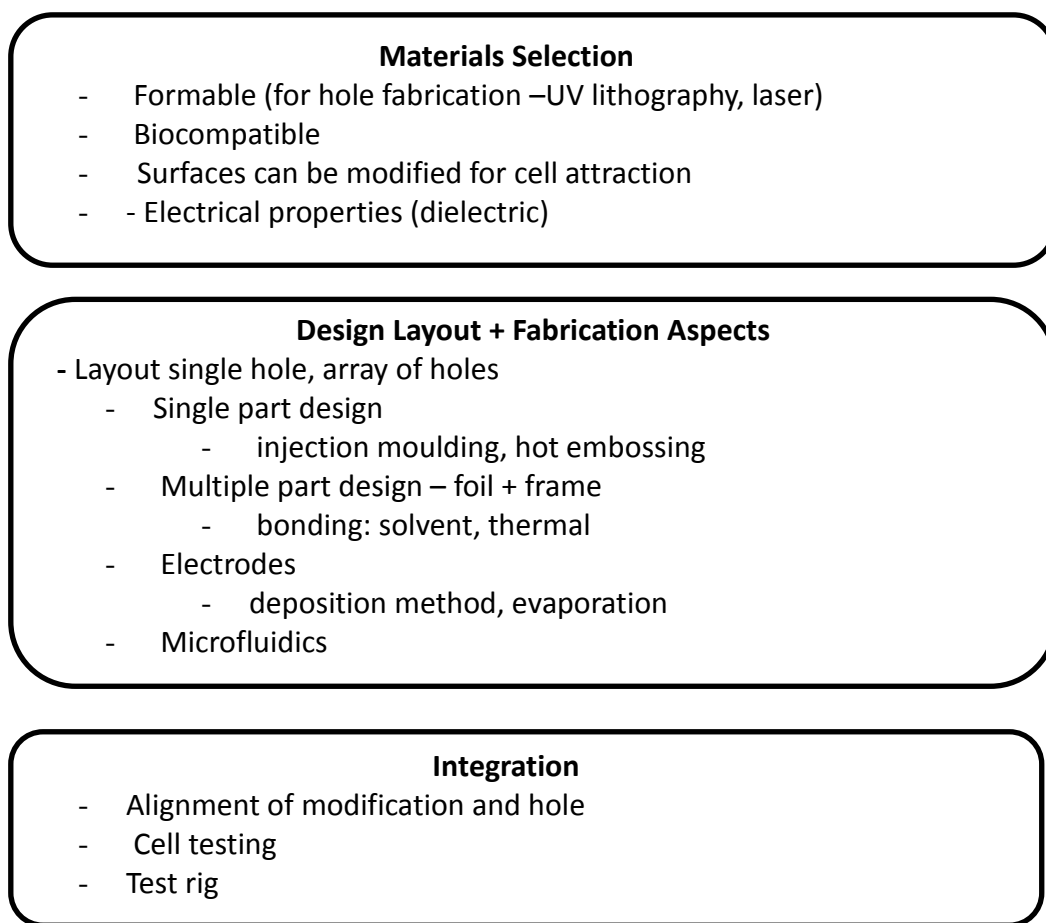


Figure 4-1 Design and fabrication considerations for a patch clamping chip

In terms of design, a layout for the attraction of single cells and an array of 10x10 cells was produced, the cell array can be provided with very narrow surface modified ‘tracks’ to enable the preferential growth of neuronal type networks. Patterned cell spacing must be sufficient to allow physical space for the microfluidics, but must not exceed for the cells 1100µm which is the maximum distance to observe chemical kinetics between cells (Birault et al., 2009). Microfluidics design must provide flow for cell perfusion up to a maximum 10 days while cells are growing (400-700µL/h), this value is taken from the cell chip and bioreactor setup at IBG (KIT – Institute for Biological Interfaces), with good distribution above and below the cell, and a exchange rate for compound measurement (10µL/s for ligand gated compounds)(Wilson,

2009). Perfusion and measurement are carried out at 37°C with the addition of 5% CO₂ for optimum cell health.

Provision must be made for placement of Ag/AgCl microelectrodes, one common reference electrode immersed in the bathing solution and a measurement electrode placed underneath each individual measurement hole for single addressing of each cell. Each measurement electrode has its own microfluidic chamber. It must be technically feasible to form leak-tight chambers below the measurement holes, as any leaks between chambers between measurement electrodes will cause signal cross-talk. Figure 4-2 shows a rendition of one potential design for a network of neuronal cells.

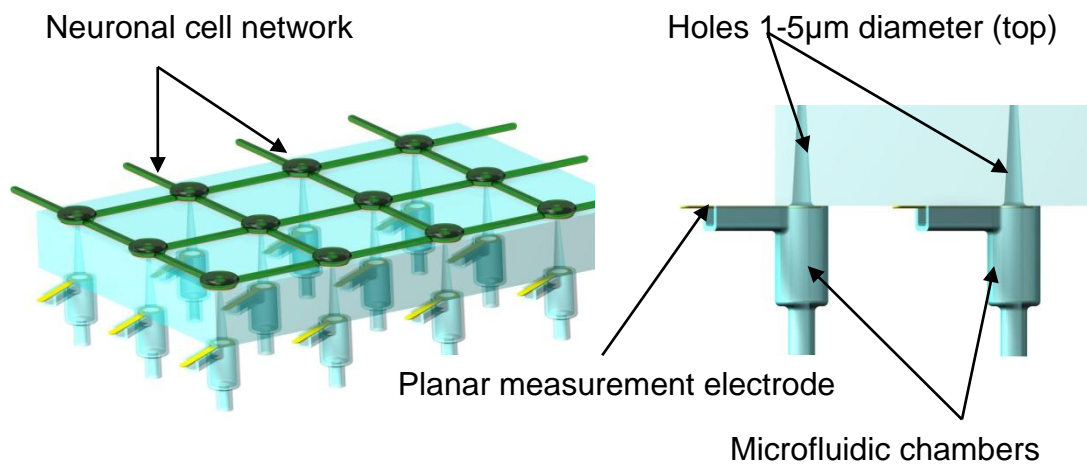


Figure 4-2: Section of proposed patch clamping system design, left array for neuronal type cells; right cross-sectional representational view through a hole with electrodes and isolated microfluidics to each hole

It is a planar system, replacing the pipette with an array of holes shown in Figure 4-2 left as an orthogonal view of a section of a network of cells (green) on top of an array of holes drilled into a polymer substrate (aqua). Measurement electrodes can be seen deposited (protruding openly for display purposes only) on the bottom side of the foil. Under the electrodes, the microfluidic system for non-pressured flow for cell nutrition purposes and measurement media exchange. It is important that no pressure be built up in the system that would

blow the cell away from or dislodge it, from the hole, but that liquids can be exchanged quickly so that drug compounds are delivered quickly to the cells. On the right is a cross-sectional view of the system. The hole diameters are intended to be between 1-5 μm . Hole diameters must be small enough that cells do not pass through them but large enough that a patch of membrane can be isolated for measurement.

Leak tightness between individual measurement chambers is crucial to the success of the system, as electrical cross-talk should be prevented. For this reason, a single part and multiple part design have been considered. A single part 'chip' could be produced either by injection moulding or by hot embossing. A multiple part design would have a foil drilled with a patch hole integrated into a frame by solvent bonding or thermal bonding.

Figure 4-3 below shows an adapted cell chip schematic which is injection moulded and the single part approach first adopted for this work. The well is a bioreactor chip used for cell culture at the Institute for Biological Interfaces at KIT (www.fzk.de/ibg). A single hole drilled in the bottom of each well could be used for cell measurement, however such a design would only be suitable for measuring single cells due to the sidewalls and does not provide any increased functionality compared to systems already on the market.

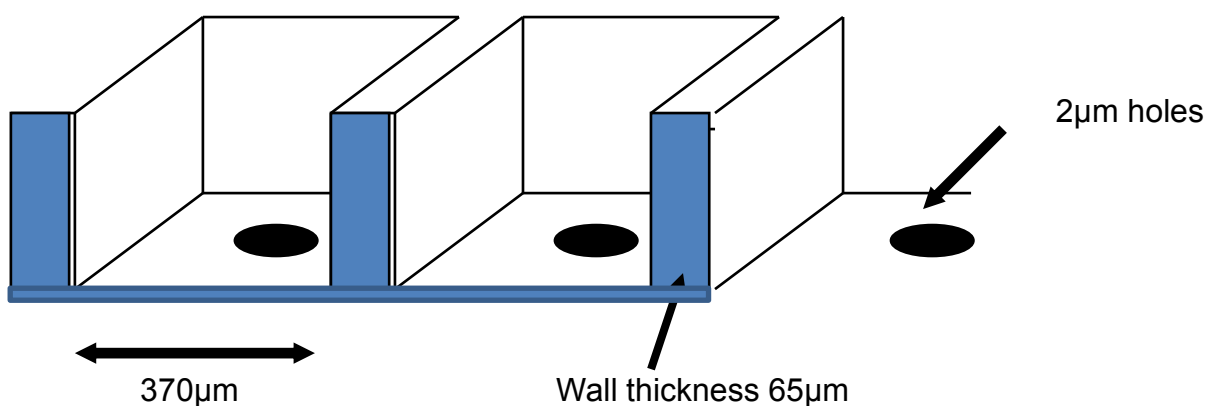


Figure 4-3: Schematic drawing of a high-throughput chip well structure for cell inoculation

However, by flipping the cell chip over and using the 'top' side as the cell inoculation side, the surface can be patterned in a planar way to accommodate for cell types that require physical connection to communicate, and microfluidics can be integrated into the bottom side as shown in Figure 4-4.

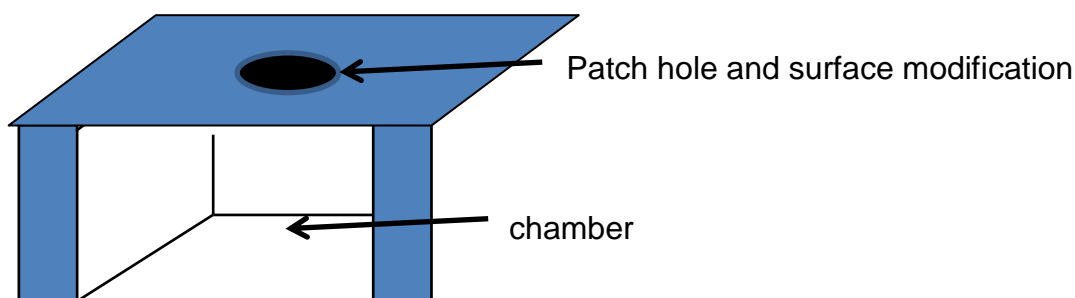


Figure 4-4: Inverted well structure becomes microfluidic chamber permitting surface modification for single or neuronal cells

This microfluidic well element can be produced either as a single part design with holes and surface modification produced afterwards, and using a wire type Ag/AgCl electrode, or using a two part design where a foil material is provided with a hole, modified and a planar Ag/AgCl electrode deposited onto the bottom side of the foil which is then bonded to a microfluidic chip. In a two part system, foil bonding must be sufficient to prevent any liquid leaks between chambers as this will cause loss of addressability to single cells and signal loss. The following section provides background information on the materials considered for this work. Some previous work of relevance is also summarized briefly.

5 Biocompatible polymer materials for patch clamping

Glass is the material of choice for patch clamping (Comley, 2003; Xu et al., 2004; Stett et al., 2003; Knott et al., 2002; Fertig et al., 2002). Such dominance is due partly to the excellent dielectric properties of quartz and borosilicate glasses as shown in Table 4. The use of quartz over decades means that there is a huge knowledge base of patch clamp measurements performed with this material has been built up resulting in considerable resistance to the introduction of new material unless the advantages are clear. Despite this, cost-effective future mass production and increasing the range of cell types for patch clamping means polymers become a very attractive alternative with their low production costs, forming flexibility and the wide range of properties and surface modification options available. The following section briefly describes three materials selected for their biocompatibility and ease of processing used in this work.

As previously described in Section 2.2.2, the cell membrane is an insulator between two conducting solutions. To permit measurement of ion channels, the materials used in patch clamping must also have good dielectric properties. For the highest quality readings, traditionally quartz glass is used which has a dielectric constant between 3.8 and 5 at 1MHz and a dielectric loss of 0.0002 @ 100MHz (www.rfcafe.com). As can be seen from Table 4, there is a wide range of polymeric materials available for use which have dielectric properties close to, if not lower than quartz glass. Dielectric values are important as they contribute to the series resistance (R_s) of the measurement as discussed in the description of whole cell recording in Sections 2.2 and 2.4.

Table 5 Electrical properties of materials suitable for patch clamping^a

Material	Dielectric Constant at 1Mhz (21°C)	Dielectric Strength (kVmm⁻¹)	Dielectric Loss [#] (tan delta, absolute value)
SU-8 2-3000*	5.0-5.2	⁺ 44	Data not available
Quartz	3.8-5.0	25-40	[#] 0.0002@100MHz [#] 0.00006@3GHz
Silicon dioxide (thin film)	3.8	25-40	0.01-0.03@3GHz
Polyamide Nylon 6	3.6	25	0.2@1kHz
Polyimide	3.4	22	0.0018@1MHz
Polycarbonate	2.9	15-67	0.01 @1MHz
PMMA	2.6	25	0.014@1MHz
Polystyrene	2.4-3.1	20	[#] 0.0001 @ 100 MHz [#] 0.00033 @ 3 GHz
Polypropylene	2.2-2.6	30-40	0.0003-0.0005@1MHz

Values taken from ^a Goodfellow, * microresist, ⁺(Melai et al., 2009) [#]www.rfcafe.com

The dielectric loss values are important as they give an indication of a signal loss due to polarization of the material, which becomes more significant when measuring smaller, faster ionic currents (i.e. picoampere range and less than a few milliseconds). The dielectric loss values given in Table 5 show that polymers have a low dielectric loss in general and that polystyrene is a particularly good candidate. However, it should be noted that the values are ranges which are heavily dependent on the method of material preparation and of any proprietary additives used in manufacture – this requires further study. In the whole cell configuration, which is used in high throughput screening, it is

possible to compensate for R_s by using a method developed by Sherman in the late 1990's. In order to achieve recording of fast ionic currents, any bandwidth limitations are overcome by using a state estimator to calculate the membrane potential which is then used as part of a feedback loop to voltage clamp implementation, in essence a factor increase is used in the voltage clamp setup which compensates for R_s . This method has been validated and successfully implemented since the turn of the millennium (Sherman et al., 1999)

5.1 Selected biocompatible polymer materials

This section briefly describes the polymers chosen for this work, their properties, suitability and processing. Some materials have been tested prior to this work, and the results of this are also briefly discussed.

5.1.1 SU-8

SU-8 is a biocompatible (Voskeican et al., 2003)(Cho et al., 2008) epoxy based UV sensitive photoresist, based on an arrangement of 8 epoxy (bisphenol A Novolak glycidic ether) groups with photosensitive triaryl-sulphonium salts in a propylene carbonate solution, diluted in either PGMEA (polyglycol methyl ethyl acetate) or GBL (gamma butyl-L acetone). SU-8 has 8 epoxy groups with 16 functional side chains shown in figure 15 which are available for crosslinking. SU-8 can be processed using standard UV lithography processes.

During exposure to UV light, Lewis acids (HSbF_6) are formed acting as a catalyst assisting the functional side chains to crosslink. The amount and diffusion of Lewis acid produced determines the degree of crosslinking. Lewis acid produced depends on the amount of its precursors available and the viscosity of the solution, which controls the diffusion process as the resist is heated to above its glass transition temperature (T_g) between 50 – 65°C during a post exposure bake. The time, temperature and heating rate of this bake also affects the degree of crosslinking as it influences diffusion.

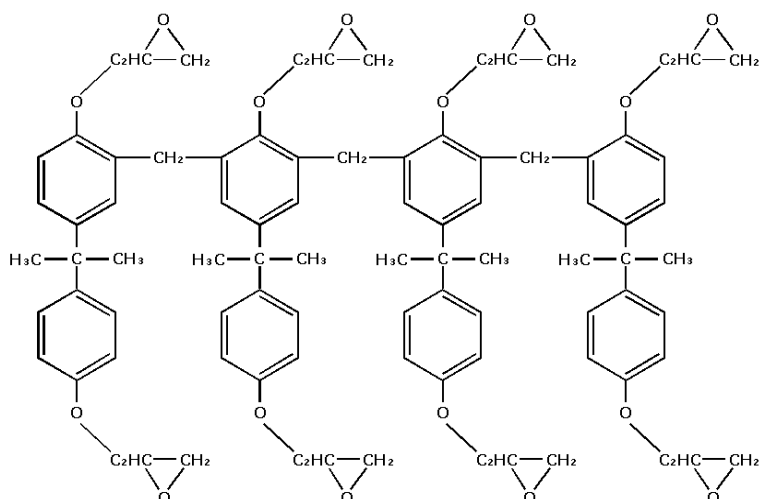


Figure 5-1: Chemical structure of SU-8 with functional side chains

The key consideration in using SU-8 for this work is the ability to produce small holes (1 – 5 μm) using standard lithography. Previous work showed that SU-8 processed using standard UV lithography techniques maintains a constant contact angle as shown in Figure 5-2, but the surface can be modified using a UV lamp with a wavelength of 185nm to become hydrophilic indicating a chemical modification on the surface as shown in Figure 5-3. This may make it suitable for cell adhesion (Wilson, 2005).

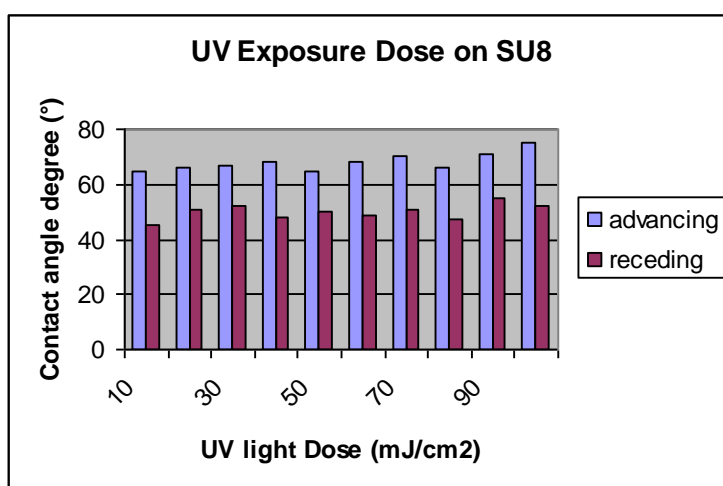


Figure 5-2: Contact angle measurements, SU-8 exposed to standard lithography UV lamp (305-436nm)

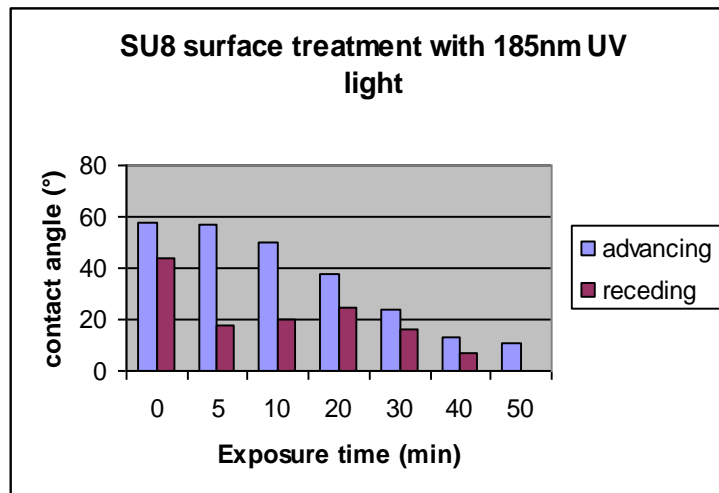


Figure 5-3: Advancing and receding contact angle results for SU-8 exposed to 185nm UV lamp

The fundamental biocompatibility of SU-8 was also tested in this work by coating a layer of SU-8 with collagen and placing cells onto the surface where they cultured up to ten days. Viable cells could be seen up to ten days showing the principle biocompatibility of this material.

5.1.2 Polystyrene

Polystyrene is a transparent, thermally insulating and relatively brittle aromatic thermoplastic that is economical and has good processing properties. It comes in a variety of forms such as extruded foils, expanded foams, extruded expanded foam and is easily injection moulded into arbitrary shapes. The chemical structure of polystyrene consists of repeated chains of the styrene monomer whose phenyl (benzene) groups are bonded together at every second carbon molecule (see Figure 5-4). The random arrangement of phenyl groups in manufactured polystyrene prevents crystallinity; polystyrene has an amorphous structure. It can be recycled, it is not biodegradable. An important use for polystyrene apart from such things as cd cases, plastic cutlery and so on, is in medical and biological applications - petri dishes, test tubes, well plates and food packaging are made of polystyrene. It also shows very good surface modification properties for cell adhesion using UV light (Wilson, 2005; Welle

and Gottwald, 2002; Welle et al., 2005) as shown in figure 19, where cultured PC-12 GFP, an adrenal tumour cell type which differentiates as a neuron-type cell when a nerve growth factor (NGF) is added. This cell line has been treated with a Green Fluorescent Protein, hence the GFP at the end of the cell name. The modified areas in Figure 5-5 form the hexagonal pattern, and the cells grow preferentially along the modified areas.

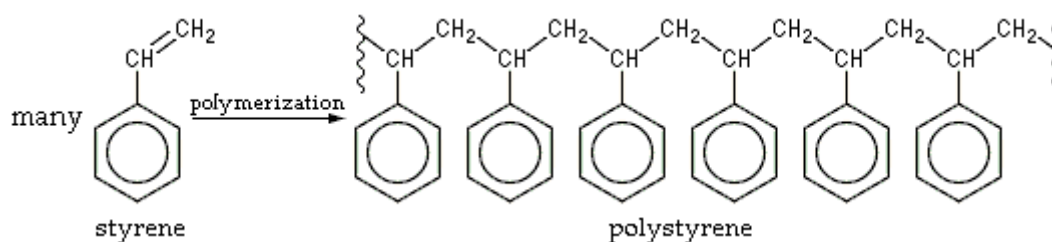


Figure 5-4: Chemical structure of polystyrene (formed from many styrene monomers, left)

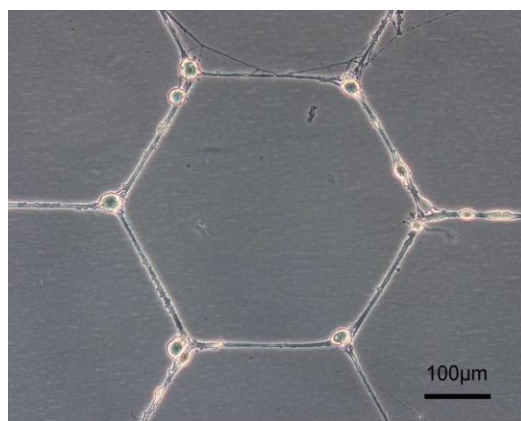


Figure 5-5: PC12-GFP cells on UV modified (185nm) polystyrene petridish

5.1.3 Polycarbonate

Polycarbonate is a multipurpose thermoplastic composed of bisphenol-A units connected with carbonate (di-ester carbonate) links in the backbone chain (polycarbonate Figure). It has high transparency, high strength, high heat resistance (good for sterilisation), good dimensional stability which permits

shape retention in a range of conditions, good electrical insulation properties, it is biologically inert, recyclable, has excellent processability, and is cost effective. The key consideration in the decision to use polycarbonate is its surface modification by 185nm UV light where it forms carboxyl groups (Welle and Gottwald, 2002; Welle et al., 2005; Welle, 2003a), although this work showed that preferential adhesion was not as well defined as for polystyrene.

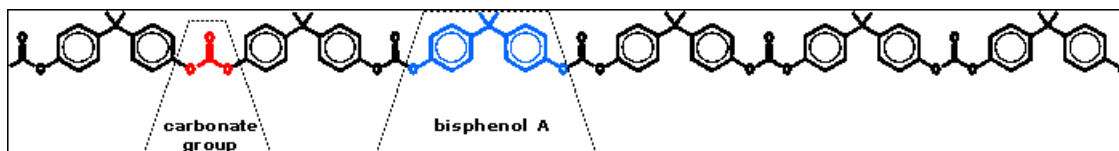


Figure 5-6: Chemical structure of polycarbonate

In order to properly assess the characteristics of these materials some surface analysis techniques have been used which are introduced in the next section.

5.2 Surface analysis of polymer materials

To characterise whether a polymer has been changed by a surface modification technique, contact angle measurements were initially performed. Contact angle measurements give information about the wettability of a surface and can be used to indicate changes in surface chemistry. A surface change from a more hydrophobic surface to a more hydrophilic one gives an indication of physical and chemical change on the polymer surface, however it does not give information about *what* the surface changes are. X-ray photon spectroscopy (XPS) gives more detailed information about how the surface has been modified chemically, and both of these methods have been used in this work to evaluate the surfaces of modified polymers selected in the previous section. The basic theory of both contact angle and XPS are covered in this section.

5.2.1 Contact angle measurement

Contact angle measurement (CA) is a simple-to-adopt method for surface analysis related to surface energy and tension. Contact angle measurement describes the shape of a liquid droplet resting on a solid surface. When drawing

a tangent line from the droplet to the solid surface, the contact angle is the angle between the tangent line and the solid surface. If a liquid of known properties is used, the resulting interfacial tension can be used to identify the nature of the solid surface.

CA measurement is based on the shape of a droplet of liquid on a material's surface. The droplet shape is based on the balance of the interfacial liquid (γ_L), vapour (γ_G), and solid (γ_S) surfaces as shown in Figure 5-7.

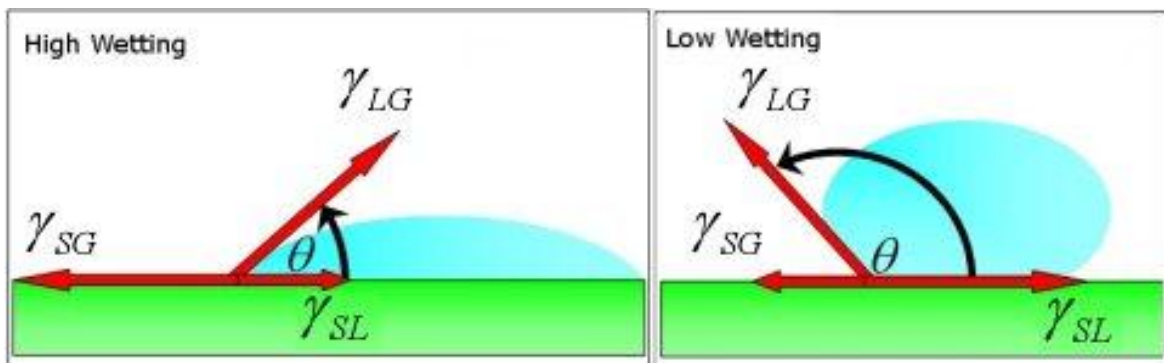


Figure 5-7: Illustration of different degrees of wetting: High wetting on the left gives a small contact angle whereas on the right there is little wetting and a large contact angle.

When a droplet of higher surface tension liquid is placed on a solid substrate of low surface energy, the liquid surface tension causes the droplet to form its lowest energy shape, a sphere - measured as a high contact angle or low surface wetting as shown in Figure 5-7 right. Wetting or low contact angle occurs when the liquid surface tension is low and the solid substrate surface is similar or higher

The Young equation expresses the cosine of the angle as:

$$\gamma_{LG} \cos \theta = \gamma_{SG} - \gamma_{SL}$$

where

γ_{LG} = surface tension between the liquid and gas

γ_{SG} = surface tension between the solid and gas, and

γ_{SL} = surface tension between the solid and liquid

If surface tension between the liquid and the air (γ_{LG}), is higher, the contact angle approaches 90 degrees. In this state, and shown in Figure 5-8, the droplet has the form of half a sphere so that the area between air and liquid is minimal. To achieve a state of a perfectly spherical drop ($\theta=180^\circ$, a state with no wetting at all) a greater surface tension between the surface and liquid is needed than between the surface and the air ($\gamma_{SL} > \gamma_{SG}$), and in addition the constraint that $\gamma_{SL} - \gamma_{SG} = \gamma_{LG}$. Note that in the opposite case of complete wetting ($\theta=0^\circ$), when $\gamma_{SG} - \gamma_{SL} = \gamma_{LG}$ and also γ_{SG} is greater than γ_{SL} , the liquid spreads uniformly over the surface and creates a monomolecular layer. This shows the great importance of the relative magnitude of the various surface tensions involved.

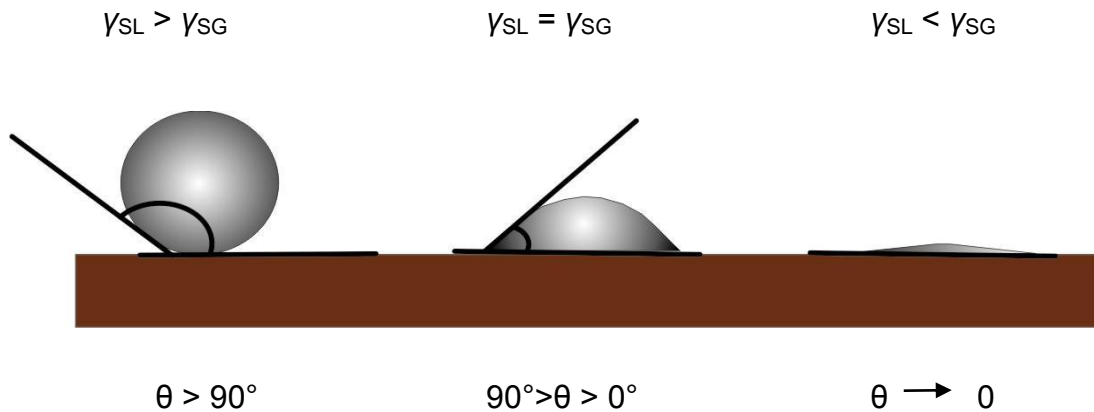


Figure 5-8: Contact angle measurement and wetting

Contact angle measurements are made on a goniometer (Figure 5-9), which has a sample stage to hold the substrate material, a syringe filled with the liquid to be dropped onto the substrate and a microscope objective with a protractor view in the eyepiece to magnify and measure the liquid droplet. In most cases, optics are connected to a CCD camera for recording and viewing droplet formation for better consistency in readings, also giving the option of performing static or dynamic measurements.



Figure 5-9: Data Physics OCA goniometer

A measurement is performed by placing a droplet of liquid (1-25 μL) from the syringe seen in Figure 5-9 onto the surface, the outline of the droplet is studied through the objective. The tangent angle between the droplet and the surface is determined to give the contact angle. Measurements are repeated as required to obtain an average that is statistically valid. Advancing angles are measured with a stable droplet before it starts to advance horizontally outwards. To measure the receding angle, the droplet is slowly sucked back into the syringe to the point where the droplet begins to horizontally recede then the tangent angle is recorded. Surface energy of the material increases compared to the liquid as the surface becomes more hydrophilic. The hysteresis between advancing and receding angles gives an indication of the surface quality of the material. Greater than 20° indicates that the surface is rough and/or chemically inhomogeneous and there are surface effects to be considered.

Contact angle measurements are sensitive to surface preparation: roughness, dirt or a heterogeneous surface, the chemical composition of the solid material and loose particles in the liquid that may produce a film on the surface (De Gennes, 1985) all influence measurement results to varying degrees.

In this work, dynamic contact angle measurements were made to screen materials for their suitability to be surface modified, measured as a reduction in contact angle (towards hydrophilic) signifying a reduced surface tension/energy

compared to distilled water and signifying an increase in the oxygen content on the surface, i.e. that a chemical change has been made to the polymer surface. By combining this with XPS measurement we will better determine the actual chemical composition of the modified material surface. The actual experimental set up used in this work is described in the following section.

5.2.2 Contact Angle Experiments – Dynamic Method

An OCA 15 Plus goniometer from DataPhysics (Filderstadt, Germany) with SCA 20 software which allows for static and dynamic contact angle measurement was used in this work. For dynamic contact angle measurement a droplet is placed on the substrate with dosing volume and rate, both variable, and recorded for a specific time by a CCD camera. A contact angle is determined for each individual photo taken. The dynamic contact angle is determined at between 5 and 15 seconds. Distilled water was used for these experiments with a surface energy of 72.8J/m (with a polar component of 51.1J/m and a dispersive component of 21.8J/m) (Gleich, 2004). Due to the interactions of the hydrogen bonds the polar component is larger than the dispersive component. To measure the advancing contact angle a drop of approx. 2 μ L was placed initially on the substrate and the pipette tip was positioned at the centre of the droplet and then water injected at a rate of 0.7 μ L/s until a droplet volume of 16 μ L was reached. Simultaneously the camera recorded this process with a speed of 16 photos per second for a total of 500 photos over a 20 second duration.

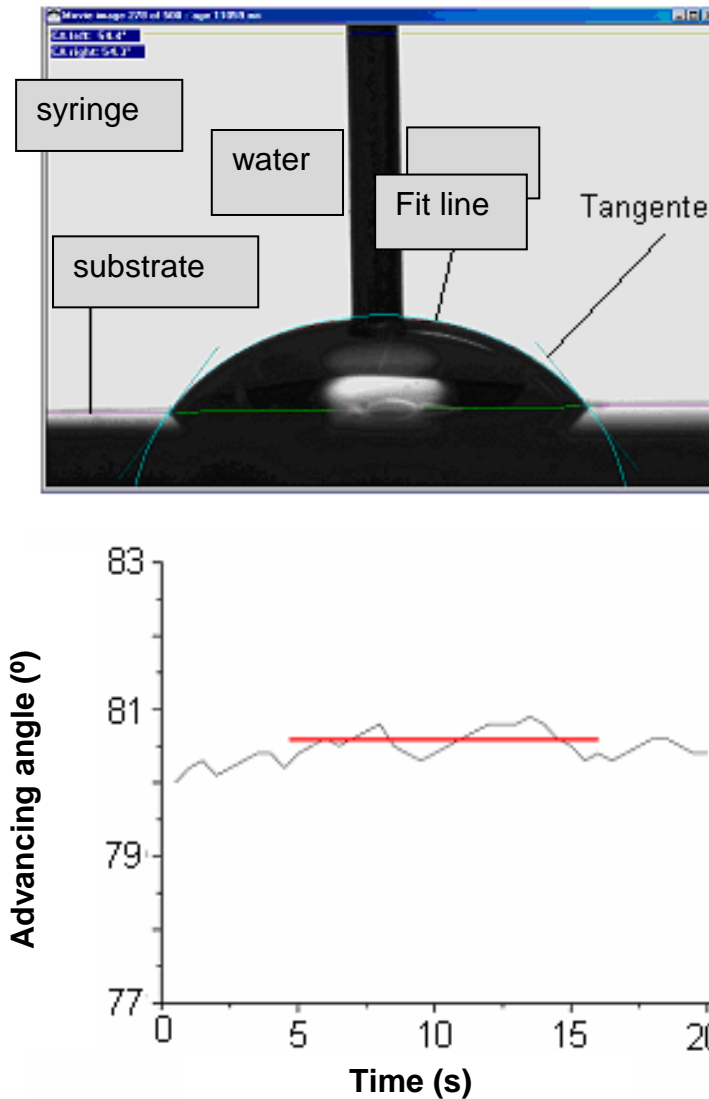


Figure 5-10: Dynamic contact angle measurement (above), ellipse fitting method, (below)

To measure the receding dynamic contact angle the reverse procedure was followed, the pipette tip was positioned in the middle of the droplet and water suctioned up at a rate of $0.7\mu\text{L/s}$, an angle obtained and documented.

Contact angles were analyzed using the ellipse method as shown in Figure 5-10. A baseline is set at the surface of the material and software creates a contour fit for the droplet. An angle is determined from the intersection of the ellipse to the baseline, and an average determined as shown by the red line in Figure 5-10, lower. Advancing and receding contact angle measurements were

performed 5 times for each exposure dose and on different surface locations to ensure an average surface response and prevent already hydrated surfaces being re-measured. The front and back of the foils were measured to determine surface differences due to manufacture or chemistry.

In combination with contact angle measurement, surface characteristics were also determined by X-ray Photon Spectroscopy.

5.2.3 X-ray Photon Spectroscopy (XPS) measurement

X-ray photon spectroscopy (XPS) is an electron spectroscopic for determining the chemical and elemental composition of a material's surface. The basic requirements for XPS are:

- a source of fixed energy radiation (a monochromatic x-ray source, typically soft – between 200 - 2000eV)
- an electron energy analyser, to disperse the emitted electrons according to kinetic energy and allow measurement of flux of emitted electrons of a specific energy
- a high vacuum environment (to enable emitted photoelectrons to be analysed without interference from gas phase collisions).

Figure 5-11 is a schematic diagram and photo of such a system.

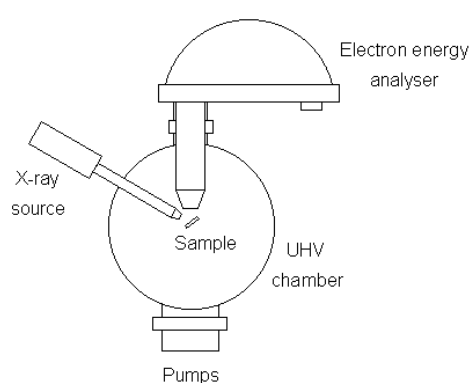


Figure 5-11: Simplified schematic of an X-ray Photon Spectroscopy (XPS) unit (left), an actual XPS unit (right)

Photoelectron spectroscopy is based upon a single photon in/electron out process this means a photon is absorbed by an atom in a molecule or solid, leading to ionization and emission of a core (inner shell) electron.

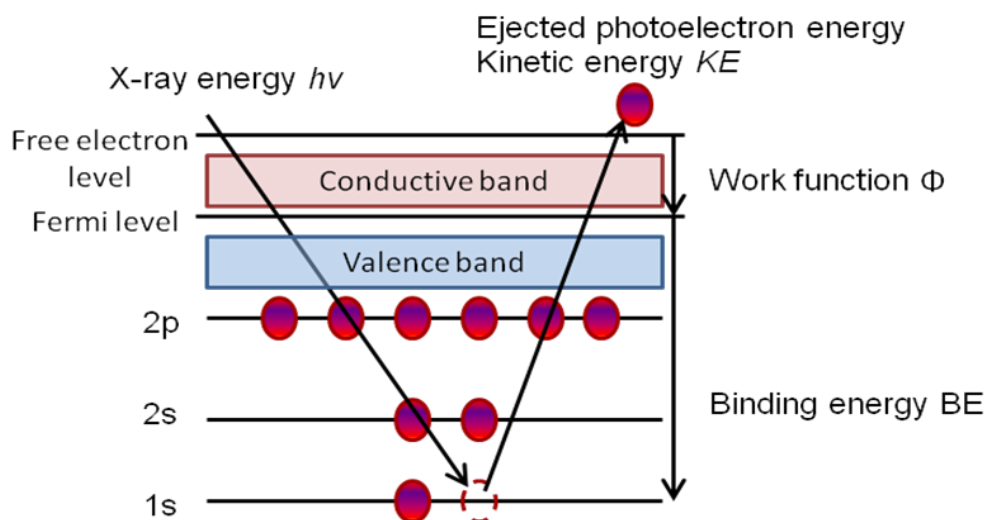


Figure 5-12: Schematic representation of a single photoelectron emission by X-ray for XPS measurement

The energy of a photon of all types of electromagnetic radiation is given by the Einstein relation:

$$E = h\nu$$

where:

h = Planck constant (6.62×10^{-34} J.s)

ν = frequency (Hertz) of the radiation

The kinetic energy distribution of the emitted photoelectrons (i.e. the number of emitted photoelectrons as a function of their kinetic energy) can be measured using an electron energy analyser and a photoelectron spectrum can then be recorded. The binding energy BE , of the electron is taken to be a direct measure of the energy required to just remove the electron concerned from its

initial level to the vacuum level and the KE , of the photoelectron is again given by:

$$KE = h\nu - BE$$

Because the photoelectrons are strongly attenuated by passage through the sample material itself, the information obtained comes from the sample surface, with a sampling depth on the order of 5 nm. Binding energies are characteristic of each element and can be used for identification. The peak heights allow for comparative quantification of the element. Chemical bonding will clearly have an effect on both the initial state energy of the atom and the final state energy of the ion created by emission of the photoelectron.

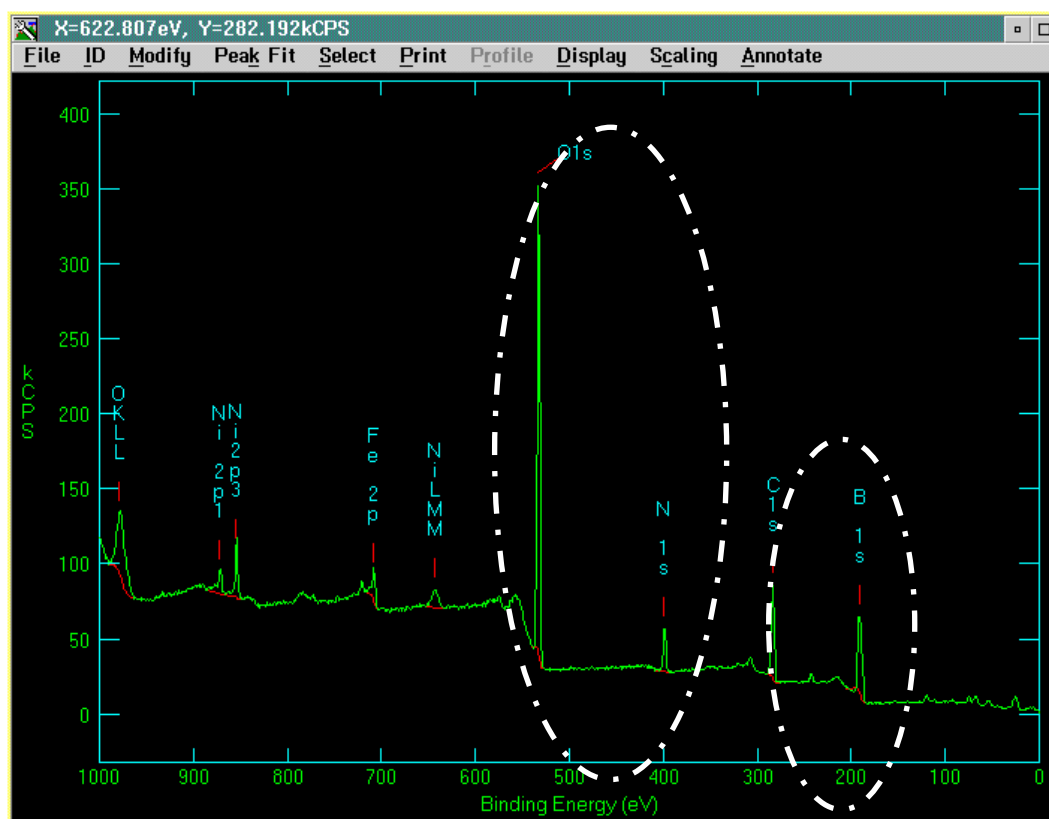


Figure 5-13 : Binding energy - example of an XPS result screenshot (INRS, Canada (Paynter,))

The presence of chemical bonding and surrounding atoms causes binding energy shifts that can be used to extract information of a chemical nature, such as oxidation state from the sample surface. For this reason, XPS is also known

as Electron Spectroscopy for Chemical Analysis (ESCA). Of interest for polymer materials are the C1S and O1S spectra (circled in white in Figure 5-13). Comparing the ratio of both spectra gives an idea of the ratio of types of carbon to oxygen bonds on the surface and further information can be obtained by carefully expanding the C1s spectra as shown in Figure 5-14.

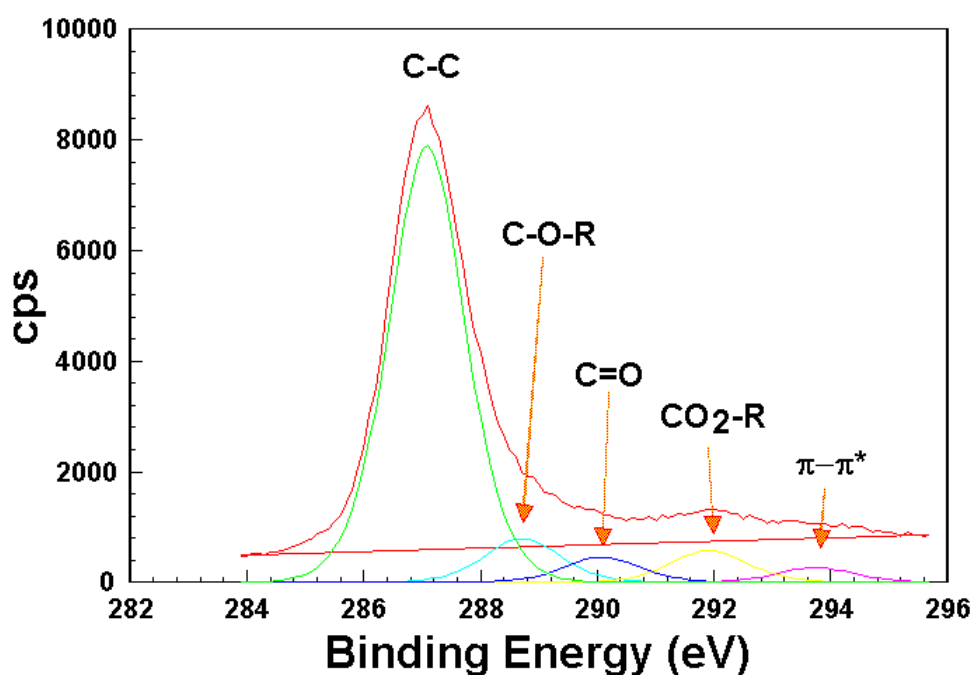


Figure 5-14: An example of polystyrene exposed to an oxygen plasma analyzed by XPS

In Figure 5-14 from L'Institut National de la recherche Scientifique - INRS, Quebec city, Canada (Paynter,), polystyrene exposed to oxygen plasma is used as an example of an XPS analysis. In this example the C1s envelope (see **Error! Reference source not found.**) has been resolved into five components showing the bond types determined by their binding energy. The spectrum was obtained from a sample of polystyrene exposed to an oxygen plasma, and displays components representative of the various types of carbon - oxygen bonds introduced into the sample surface (O-C=O at 289.1eV, or C=O here at 290 eV), shifts in the binding energy denote stronger or weaker bonds, the

height of the peaks form ratios that can be used to quantitatively determine how much of a particular bonding type is present on the surface, in this example C-O bonds are approx. 1/3 more than C=O bonds. This technique is used in this work to determine the ratio and type of bonds required for cell adhesion.

5.2.4 X-Ray Spectroscopy Experiments

X-ray photoelectron spectroscopy (XPS) measurements were carried out on an ESCALAB 5 spectrometer (Vacuum Generators, East Grinstead, UK) using non-monochromatized MgK α radiation (K α : 1253.6 eV) at a pressure of $<10^{-9}$ mbar. The binding energy scale was referenced to 285.0 eV for the main C1s (C-H bond) feature. The base pressure in the analysis chamber was $<10^{-10}$ mbar and increased to approx. 5×10^{-8} mbar during measurement. The photoelectrons were detected at a take-off angle of 60° with respect to the normal of the sample surface. This means that the informational depth of the measurements is equal to or lower than 5nm.

Exposed and unexposed reference foil materials are cut into 10x10 mm squares before placement into the measurement chamber. The preparation of SU-8 surfaces was somewhat more complex. A silicon wafer is laser engraved on the backside with a 10x10mm square matrix for easier sample sectioning after processing. SU-8 is processed as detailed in Section 5.9. Samples were measured as dried and after short oxygen plasma cleaning step (100W/5 mins) is performed after sample drying. The samples are separated into 10x10mm sections using gentle mechanical force before being placed into the measurement chamber.

The next section is a short literature review of surface modification methods for cell adhesion and is followed by a review of polymer surface modifications for cell adhesion and standard microsystems manufacturing methods used in this work.

5.3 Cell Adhesion and Competitive Protein Adsorption

For most applications biomaterials are in contact with cells and tissues, and for implants, often for prolonged periods. In typical automated patch clamping measurements, the maximum time cells are in contact with a surface (other than the storage bottle or tissue culture environment) is no longer than an hour or two. In this work, cells are cultured on a modified polymer substrate so it is useful to introduce some of the concepts behind cell adhesion or repellence as it is currently understood. Cell interactions with the external environment are mediated by receptors in the cell membrane which interact with proteins and other ligands which adsorb to the material surface from the surrounding fluidic environment. Once attached, multiple functional biochemical signals are triggered in the cell; it can be said then, that for most cell types attachment to a surface is important for cell viability, its growth, migration and differentiation (Griffith and Naughton, 2002) .

Cell adhesion is a balance of wettability, surface charge and surface roughness. (Goddard and Hotchkiss, 2007) (Ranella et al., 2010), (Yamazoe et al., 2010). However, many studies have been carried out measuring the influence of wetting behaviour on cell adhesion, whether a hydrophobic or hydrophilic surface is better suited and results are inconclusive. A study on polyethylene terephthalate (PET) modified by CO₂ laser demonstrated that cells attach to hydrophilic surfaces. This is due to changes in the chemical composition of the surface, as carboxyl groups are formed that lead to a reduction in contact angle (Mizradeh and Dadsetan, 2003). In contrast, a study on polymethyl methacrylate (PMMA) arrived at other conclusions. This study correlated cell adhesion with PMMA surface topographies which were mechanically changed, the result: hydrophobic surfaces are better for cell adhesion. (Lampin, 1997). There remains much debate on the surface characteristics required for cell adhesion, what is known is that it is mediated by cell adhesion molecules which are proteins (cadherins, integrins and selectins). It can be said that cell attachment is directly related to the adsorption of these molecules onto a surface.

5.4 Methods of surface modification for cell adhesion

There are many methods available to modify a material's surface to make it suitable for cell adhesion. The techniques can be subdivided into additive or subtractive processes which create chemical and/or mechanical changes to a material surface to functionalise it, either for direct cell adhesion, or to chemically bind with cell attractive proteins. In terms of physical size, modifications range from micrometer dimensions such as semiconductor lithography techniques to produce physical structures that act as channels in a biocompatible material for controlling cell growth along the channel,(Gomez et al., 2004)(Dowell Mesfin et al., 2004), or by etching into a material to form a channel(Roth et al., 2003)(E.A Roth et al., 2003). To produce finer structuring, other techniques involve the use of specialized equipment, such as adapted ink jet printers to deposit nanometer thick cell attractive proteins(Roth et al., 2003), or specially treated AFM tips (Sekula et al., 2008) can be used to graft proteins in a pattern onto substrates – this is known as Dip Pen Nanolithography, (DPN). Micro-contact printing techniques using inexpensive PDMS stamps can also be used to deposit cell attractive proteins in a tens of micrometer sized pattern onto a material (Xia and Whitesides, 1998). Other chemical techniques such as depositing silanes to define cell repellent areas, or depositing thiols onto gold to form cell attractive areas are also used (Bouafsoun et al., 2007); however there are many processing steps and chemicals involved which increase process complexity and increase the chances of contamination. For polymer materials, grafting is also an option and poly-l-lysine is commonly used as a backbone for grafting proteins onto other substrate materials to promote cell adhesion. There are a multitude of techniques available to aid cell placement, however it can be generally said that the more steps and chemicals involved, the more time consuming, complex and the greater the potential for error in the process, this is a common disadvantage of additive processes.

In this work, relatively simple one-step processes have been used to produce defined surface modification on polymer films.

5.4.1 Laser and Lamp modification below 200 nm

It has established that the application of UV radiation at wavelengths below 200nm, photons cleaves carbon-carbon bonds without a thermal influence; this technology has been in use for decades in laser eye surgery to reshape the cornea and improve vision.

In terms of polymers, commercially available UV-lamps at 185nm have been used to modify polycarbonate and polymethyl methacrylate (PMMA) as upon exposure to atmosphere the carbon and oxygen form carboxyl groups which are cell attractive. Cells began to adhere on the surface after 2 minutes after a selective protein adsorption process was carried out that is described in the following section. (Welle and Gottwald, 2002; Welle et al., 2005; Welle, 2003a).

In work by Sauerbrey and others, the influence of excimer laser irradiation (172nm) on the wettability of polyethylene (PE), polypropylene (PP), polyethylene terephthalate (PET) and Nylon 6. For all materials, irradiation resulted in a reduction of contact angle, an increase in oxygen content and a barely changed surface roughness. (Pettit and Sauerbrey, 1993)

The effects of surface modification using UV excimer laser (172nm) and UV lamp (172nm) were compared on PET and an increase in oxygen was found to improve cell adhesion (Cleve et al., 1999).

In this work, materials have been selected on the basis of their biocompatibility, formability and ability to have a good surface finish. A combination of UV lamp exposures at 185nm and UV laser at 193nm wavelength were studied and their influence on cell adhesion in this work.

5.4.2 The isoelectric point, Vroman effect and selective protein adsorption

The fundamentals of the isoelectric point were introduced in Section 2.2 and the attraction of cell adhesive proteins to hydrophilic COO⁻ groups was discussed. The use of a short UV wavelength UV laser or lamp to create hydrophilic carboxyl (COOH) groups has also been discussed.

The Vroman effect first observed that adsorption from plasma to serum (blood) occurred through a complex series of adsorption-displacement steps in which low molecular weight (MW) proteins arriving first at a surface are displaced by relatively higher MW proteins arriving later. Certain proteins such as albumin were seen to be relatively resistant to displacement at hydrophobic surfaces whereas others, such as high molecular weight kinogen readily displace fibrinogen {107 Derand 1998;}. The exact molecular mechanisms underlying the process remain unresolved.

In previous work done by Welle and Gottwald {18 Welle, A. 2003; 18 Welle, A. 2003;}, competitive protein adsorption using the Vroman effect was used effectively to create distinct areas of cell attraction and repulsion to guide cell adhesion and growth on hydrophilic (charged) surfaces. The proteins used for the studies were albumin and laminin on a polystyrene surface. This work was used as a basis for promoting cell attractive and repellent areas for cell types which are more sensitive to surface properties.

Bovine Serum albumin (BSA) is a large globular protein (66,000 Dal) with a good amino acid profile which is attracted to hydrophobic surfaces. Its properties have been well characterized and the physical properties are well known {{108 Feldhoff, R.C. 1975;}}. BSA is known to be cell repellent {{109 Tourovskaia,A. 2003;}}, and it has an isoelectric point of 4.7 to 5.6 which means that its affinity to COOH⁻ groups is lesser than that of the cell attractive protein, mouse laminin, used in this work. Laminin is an extremely large protein at 850,000 Daltons and has an isoelectric point of 6.28. It is evident then by using

the principles of the Vroman effect and the isoelectric point, that albumin would be displaced by laminin in areas where COOH⁻ groups are present.

5.5 Cell culture method

Cell culture is the process of growing cells under controlled conditions. There are two well-known methods to culture cells. Primary cell culture is the culture of cells taken directly from a subject (animal, person), with the exception of some tumour derived cells, most primary cultures have a limited lifetime. After a certain number of population doublings the cells senesce (grow older) and stop dividing. The second cell culture method is to use established or immortalized cell lines, these are more commonly found in cell culture labs. Cell lines have acquired the ability to proliferate indefinitely either by random mutation or by deliberate modification. Well defined cell lines have been used in this work to establish adhesion patterns on modified substrates.

Cells are grown and kept at an appropriate temperature and gas mixture, for mammalian cells this is generally 37°C with a 5%CO₂ supplement in a cell incubator at 100% humidity. Standard cell culture was performed in tissue culture flasks (Becton Dickinson Labware, Plymouth, England, Falcon Cat. No. 353024), and cells were passaged (a procedure to control number of cells in a flask) once per week. Good lab practice dictates that two flasks of each cell type are cultured simultaneously in case of unexpected cell degradation or contamination, for this work, each cell type has one flask containing 4x10⁶ cells and one containing 2x10⁶ cells. Cell culture experiments have accompanying reference petri dishes to verify cell viability, this work used 2 collagen coated tissue petri dishes and 2 UV-lamp surface modified bacterial petri dishes as references, the former to assess overall cell viability and the latter to compare the results of a petri dish modified surface to a foil modified surface in terms of cell behaviour.

Three cell types were chosen for this work partly based on their availability in the lab, but also because of their differences in terms of adhesion and growth patterns and finally for measurement, their robustness outside of the cell lab as

the patch clamping measurement rig used was located in a plant cell lab in another building, requiring cells to sit in a cold environment (18°C) for up to two hours before measurement.

L929 cells are a mouse derived (murine) fibroblast cell. Fibroblasts form the connective tissue and structural framework for animal tissue and they play a critical role in healing. This cell line is used often for assessing cytotoxicity. It is a cell line that prefers to adhere to surfaces and is used in this work to assess adhesion boundaries for surface modification. L929 medium is MEM (Minimum Essential Medium) (Life technologies, Karlsruhe, Germany, Cat. No. 21090-022) 2mM L-Glutamine (Life technologies, Cat. No. 25030-024), 1mM sodium pyruvate (Sigma Aldrich Cat. No. S836), 0.1mM amino acid (Life technologies, Cat. No. 11140-035), 100 units/mL penicillin, 100µg/mL streptomycin (Life technologies, Cat. No. 15140-114), 10 vol% horse serum (ATCC, Manassas, VA, USA Cat. No. 30-2040). During petri dish growth 1mg/mL Pluronic F68 (Sigma Aldrich Cat. No. S1300-500G) is added to the culture medium. Pluronic F68 is a di-block co-polymer [poly(ethylene oxide-poly(propylene oxide)-poly(ethylene oxide)] which has been shown to enhance the efficacy of cooperative effects of both albumin as a cell repellent agent and laminin as a cell-attractive agent. (Welle et al., 2005; Detrait et al., 1998)(Welle, 2003b)

HEPG2 cells are a liver tumour cell (human hepatocellular liver carcinoma cell) that have an epithelial (lining/ sheet) morphology and is a cell line that is often used as a model for the Hepatitis B virus (HBV). The line is also used for cancer and apoptosis studies. In this work HEP G2 cells are used as an alternative to L929 cells as their form is more suited to adhesion above a hole, unlike L929 cells which have a long spindle-like structure and tend to grow into vertical mounds. The culture medium for L929 cells is MEM (Minimum Essential Medium), supplemented with 1 vol% non essential amino acids solution (Life technologies), 2mM L-Glutamine (Life technologies), 100 units/mL penicillin, 100µg/mL streptomycin (Life technologies) and 10% foetal calf serum (PAA Laboratories GmbH, Linz, Austria, Cat. No. A15-649).

PC-12GFP (rat liver adrenal gland tumour cells) are the third cell type used in this work. This a cell line derived from a pheochromocytoma of the rat adrenal medulla. PC12 cells stop dividing and terminally differentiate when treated with a nerve growth factor (NGF). This makes PC12 cells useful as a model system for neuronal differentiation studies which is the application of this work. PC-12 GFP are genetically modified with a green fluorescent protein, with a major excitation peak at 488nm and emission peak at 509nm. PC12 cells are suspension cells that agglomerate PC12 culture medium is ATCC RPMI 1640 medium (cat # 30-2001), 50 units/mL penicillin, 50µg/mL streptomycin, 10 vol% heat inactivated foetal calf serum (Gibco BRL, Cat. No. 10082-147).

Cells are passaged (thinned out) once per week. Cells are passaged using 0.2 wt% trypsin (Life technologies, Cat. No. 17072-018) in a solution of 4.5 g/L sodium citrate ($\text{Na}_3\text{-citrate } 2 \text{ H}_2\text{O}$), 10g/L KCl, 3.85g/L EDTA and for L929 and HEPG2 cells 5mg/L phenol red to detach cells from the culture substrate after rinsing the culture flask with Ca/Mg free phosphate buffered solution. Cell counting was performed using a Coulter counter. A dilute number (4×10^6 and 2×10^6 cells) are returned to their respective tissue culture flasks and the 'discarded' cells are used to inoculate experimental petri dishes. Pre-tests on modified surfaces of 20x20 mm showed that inoculation of 0.5×10^6 cells in 4mL of medium into a 60mm petri dish provided the overall best coverage of the modified area with little deposition of cells in undesired areas and two days of cell medium. Medium is exchanged by aspiration every two days A more detailed cell passaging procedure is given in Appendix A.

5.6 .1 Micro-injection moulding and overmoulding

In this work, micro injection moulding (μIM) was used for forming the two part design and to assess whether it is possible to directly injection mould microfluidic structures to a polymer foil which has surface modifications and a measurement hole already in place. The technique of inserting a foil and injection moulding against it is known as overmoulding or insert moulding and is

done commercially for applying decals and labels to buttons for car dashboards and display elements for cell phones for example. In contrast to typical injection moulding for replicating parts, micro injection moulding enables the replication of smaller micrometre sized parts using precision moulds. The technology uses a thermoplastic granulate material which is heated to above its melting point and is then injected at high pressure into a mould which is the inverse of the desired shape. The molten polymer then solidifies into a part which can be ejected from the mould chamber by a set of pins. The entire process is very fast at just a few seconds per production cycle. In micro-injection moulding, the mould cavities are very small features in the micrometre range which need to be completely filled by the polymer melt, a typical molten polymer shot is only a cubic centimetre in size. In many cases, mould filling requires an adapted process to remove air trapped in the small features and the addition of heating elements to compensate for extremely fast cooling of injected material into small, cold mould features. Micro-injection moulding machines have the following characteristics:

- small plasticating units to avoid prolonged polymer melt dwell time which could result in changes in material properties or degradation
- precise and repeatable shot volume control to carefully metre the volume of material required. No material cushion must reside in the injection unit in order to ensure material uniformity.
- adjustable injection speed and pressure
- precise mould alignment and gentle open/close mould movements to avoid deformation of the small mould features.

Figure 5-15 shows the Cranfield Battenfeld 50 injection moulding set up.

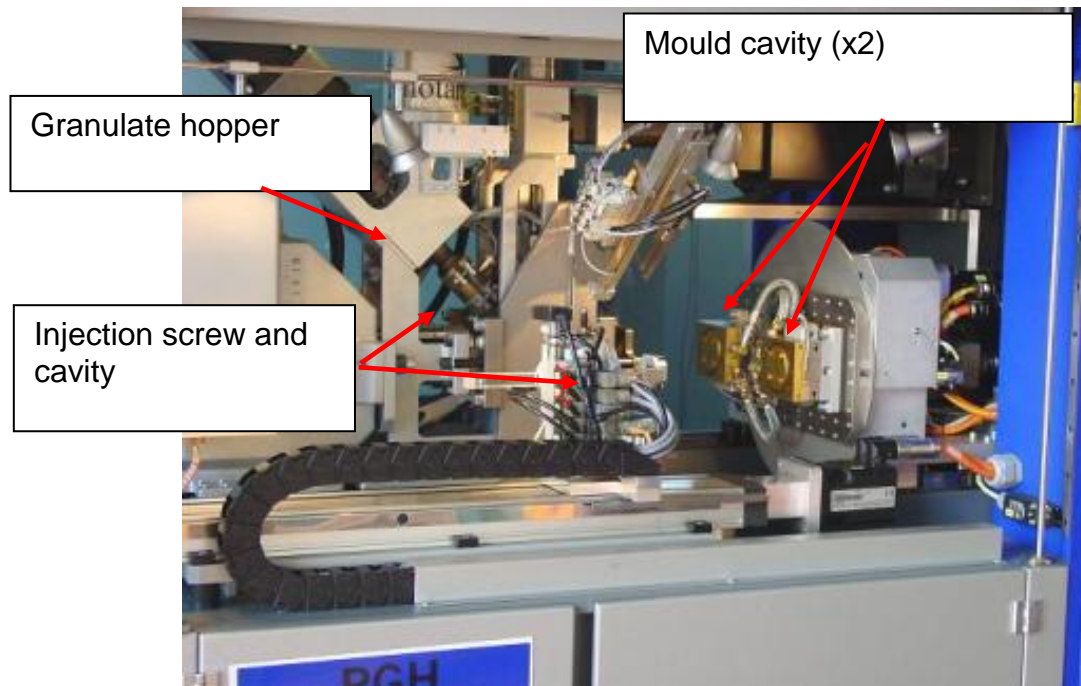


Figure 5-15: Battenfeld 50 micro-injection moulding system

5.7 Injection Moulding Experiments

To evaluate the feasibility of leak tight bonding of a polymer film/foil to a microfluidic structure using overmoulding, and to save on expensive mould making; an existing mould with meander type microfluidic structures was used for test injection moulding (see Figure 5-17). The injection moulding chamber set up was as in Figure 5-16. The foil was placed against the flat back plate of the mould cavity and held in place with high temperature vacuum grease applied to four corners. The mould was then closed and pressure applied. The cavity was heated and the polymer melt injected directly onto the foil. Trials varied melt and mould temperatures, injection pressures and rates. Parameters were adjusted until the best adhesion results were achieved. Adhesion was determined as satisfactory if the foil did not separate from the moulded part after manually pulling the foil at 90° to the moulded part with a reasonable force. The optimum adhesion result parameters were then injection moulded as test

series runs (each run producing a minimum of 20 parts).

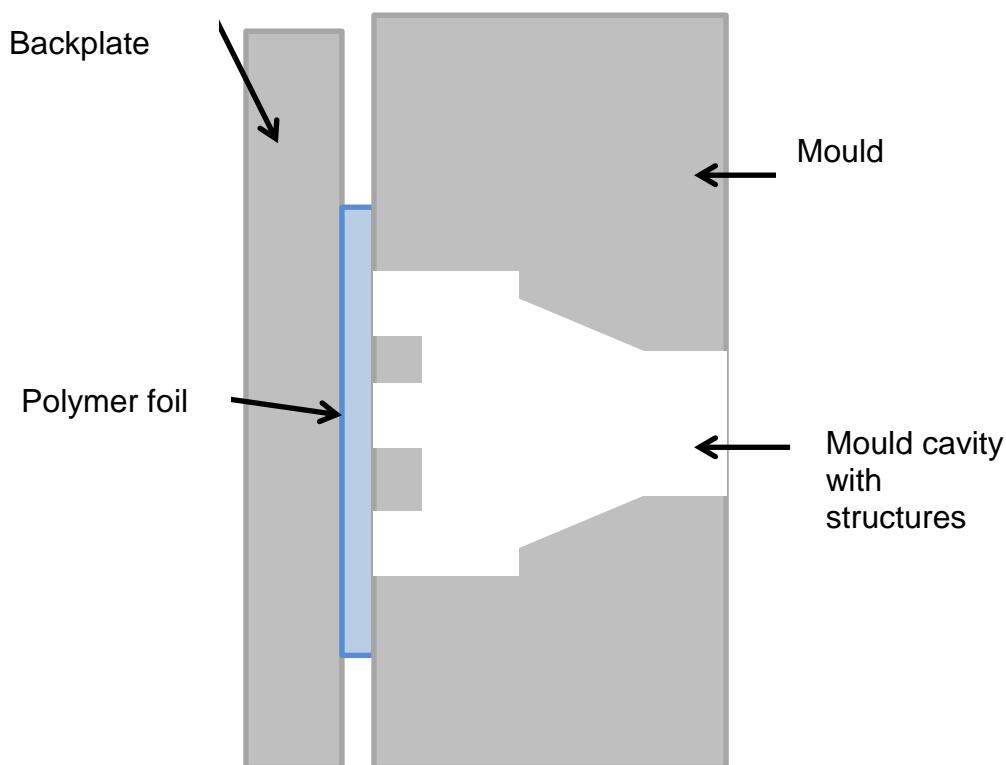


Figure 5-16 Injection moulding machine set up for overmoulding foil to microfluidic structures

To study the robustness of the interface formed between the polymer foil and injection moulded structure a realistic test would be to measure the electrical resistance between two thin walled cavities bonded to a foil placement where the cavities are filled with a conductive salt solution. However, the test mould did not have such thin walled or closely space structures available. For this reason, the approach used to determine the leak tightness was visual. A water based dye was placed into the cavities marked red in Figure 5-17. These cavities gave direct access to the interface between the foil and injection moulded structure. These red areas were photographed at the same magnification and distance with a digital camera (Panasonic Lumix, DMC-TZ5). The photos were imported into Image J free image analysis software available from the National Institute of Health) and image analysis was performed as a black/white contrast to determine the area of coverage of the ink. In the initial

test this was compared to the area specified in the parts drawing. The parts were then rinsed free of dye and then immersed in cell medium at 37°C up to ten days then rinsed with d.i. water, re-inked and photographed. A visual comparison was made between start and completion image analysis values to determine if a leak could be visualised.

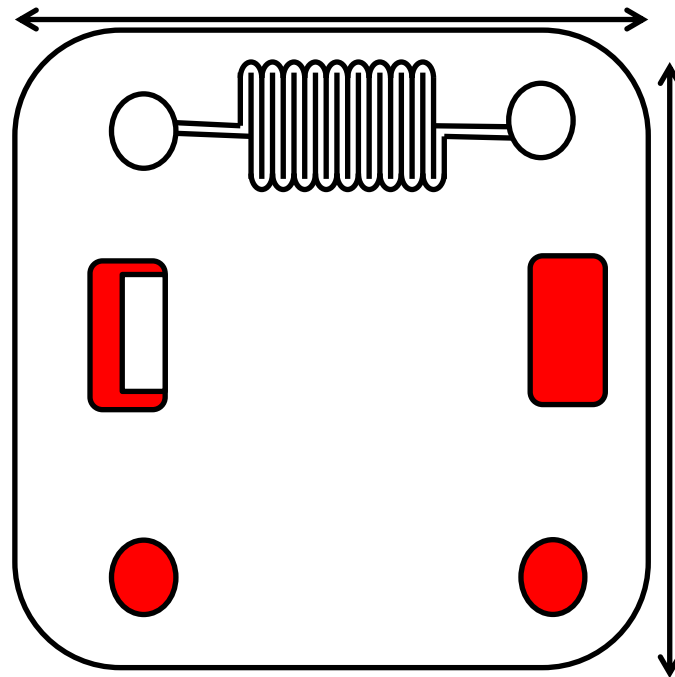


Figure 5-17 Test injection mould layout, red areas are through holes used for leak testing

5.8 Laser drilling and laser surface modification

Lasers have the capability of producing the holes required for patch clamping applications by removing or ablating small focused areas from a bulk material. When operating below the ablation threshold of a material, lasers can also be used to make surface modifications without surface roughening.

As small holes require very focussed optics and a surface modification does not require such demagnification, two lasers were used for this work with demagnifications of 10x and 4x for ablation and modification respectively

5.8.1 Laser hole ablation

A hole is created by many 'applied shots' of laser energy known as pulses. The depth over which the laser energy is absorbed and therefore, the amount of material removed by a single laser pulse depends on the material's optical properties and the wavelength of the laser.

Basic requirements must be met to structure polymers, such as a sufficient coefficient of absorption ($\alpha_{eff} > 1\mu m^{-1}$) for the laser wavelength used (Cleve et al., 1999). In order to drill holes into polymers, the ablation rate R , must be increased above an ablation threshold $\varepsilon \downarrow 1$, which is logarithmic to the energy fluence, ε (Beers Law)

$$R = \frac{1}{\alpha} \ln\left(\frac{\varepsilon}{\varepsilon_1}\right)$$

Very high energy densities and a fast dissolution of ablated fragments leads to a material vapour plasma. This plasma partially absorbs the laser radiation. This is the so-called saturation area (Pettit and Sauerbrey, 1993).

Figure 5-18 is a laser setup at 193nm for hole ablation. A laser source and mirrors reflect the light beam through a motorized quartz chrome mask (as used in traditional semi-conductor microlithography), through deflecting mirrors through a 10x reducing objective onto a positioning table where the sample part is placed. The exposure area is approx. 2x2 mm.

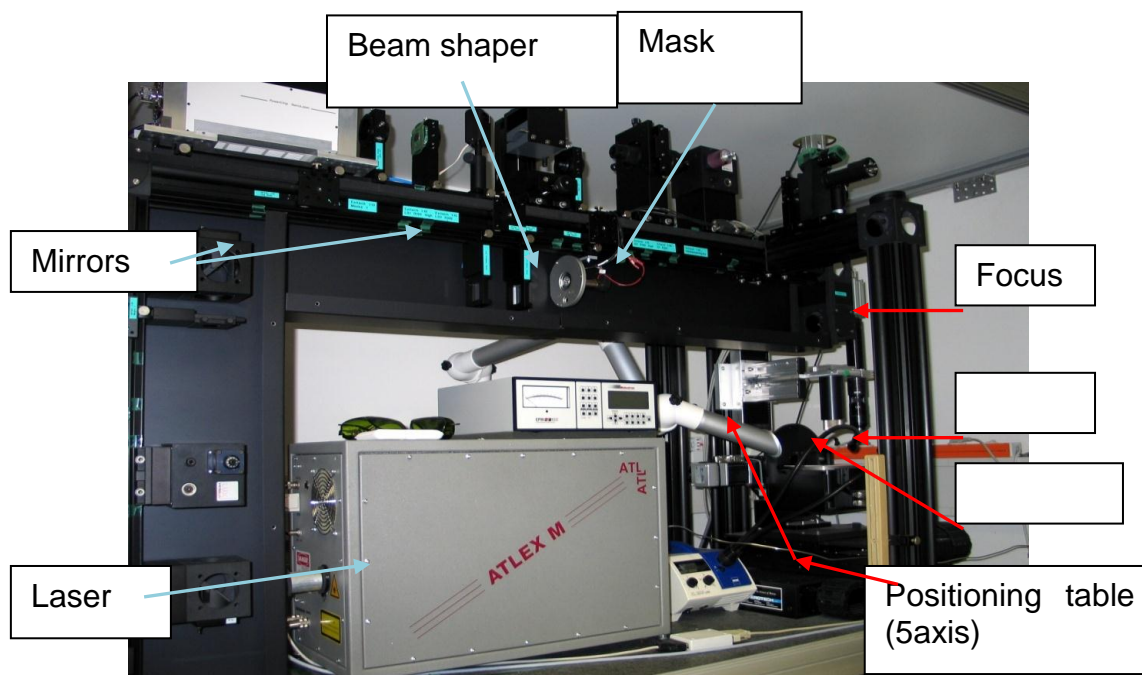


Figure 5-18: ATLEX 185nm laser set up

In terms of the influence of laser wavelength, a photochemical process happens at wavelengths $<200\text{nm}$ as covalent bonds are broken and material is ablated if energy applied is above the ablation threshold. Volatile fragments are then dissolved. The photon energy for 193nm is 6.4 eV . It is above the bond energy for most covalent bonds (Laurens, 2000).

At wavelengths $>248\text{nm}$ and depending on material, the electronic excitation does not lead to a break in molecular chains. In this case, rapid heating occurs followed by an explosive evaporation (Pettit and Sauerbrey, 1993).

For wavelengths $>300\text{nm}$ single and multiple pulses lead to heating in the energy absorption ranges resulting in a thermal decomposition. A single pulse is insufficient to break covalent bonds (Pettit and Sauerbrey, 1993). The laser work in this project remains below 200nm wavelengths for two main reasons; to break covalent bonds for surface modification inducing hydrophilic carboxyl group formation on the sidewalls of drilled holes to increase hydrophilicity for better capillary filling, and secondly in order to make sidewall surfaces cell attractive so they partially grow into the holes to provide a 'self seal' before measurement.

An additional surface modification is placed around the hole to provide a cell attractive area for the cell somas to adhere to during culture, this was produced either by exposure at 185nm through a chrome mask or by laser as described in the next section.

5.8.2 UV laser surface modification

Figure 5-19 shows the layout of an Exitech PS 2000 laser system. It is an ArF laser which operates at wavelengths of 193 or 248nm with a pulse width of 20 or 25ns and energies of 400 or 850 mJ/cm². The repetition rate (frequency) can be altered from 1-100 Hertz with laser fluencies from 0-40mJ/cm² at 193nm or 0.5-5J/cm² at 248nm. For this work, the 193nm wavelength was used with demagnification optics of 4x for surface modification.

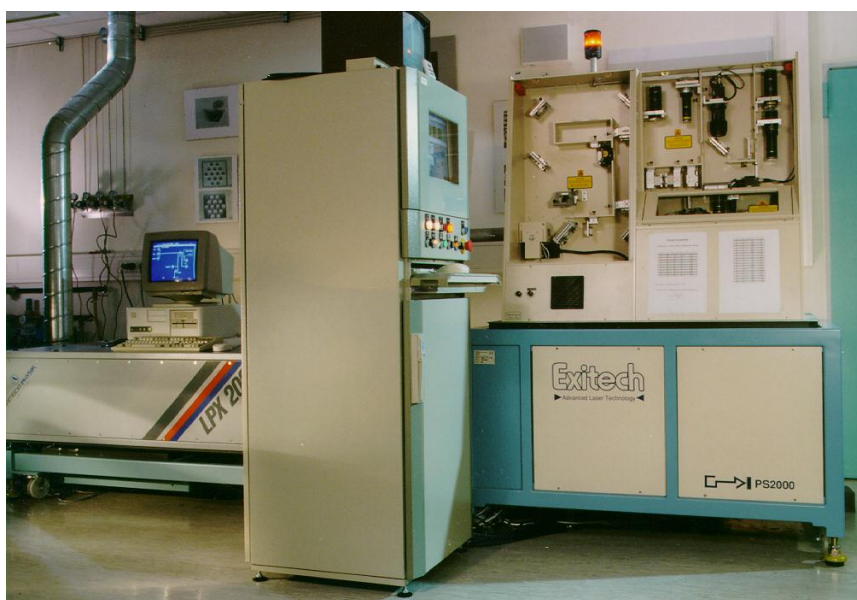


Figure 5-19: Exitech laser PS2000

By remaining below the ablation threshold for polystyrene, a patterned surface modification which breaks covalent bonds can be made by using a step and repeat beam process. A schematic representation of the chemistry is shown in Figure 5-20 a laser beam moves across a surface at an energy fluence below the ablation threshold. The ablation threshold is determined experimentally by number of pulses, laser frequency and applied energy. As previously discussed, the 193nm UV laser has the photonic energy sufficient to break covalent bonds

such as in benzene, and ambient air reacts with the broken C-H bonds with the goal of creating more COOH groups. By using a quartz chrome mask in the laser, and some reducing optics, very fine patterns can be 'written' into the surface of the material, and with optimized parameters no dry etching or ablation takes place.

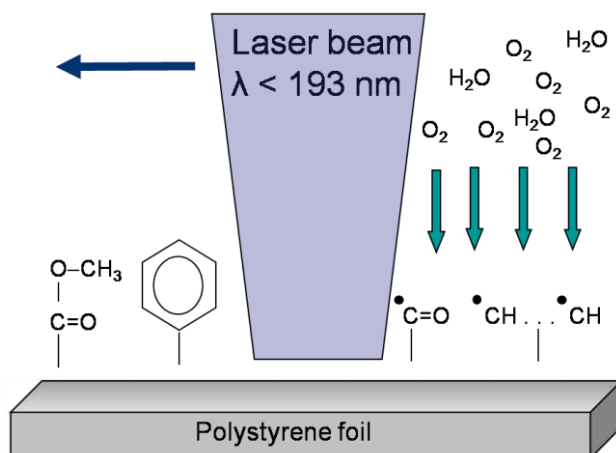


Figure 5-20: Schematic of laser surface modification, ambient air as process gas.

Experimentally, frequency, energy and pulse numbers were varied. Material assessments were done by contact angle measurement and XPS, and cells were cultured up to 48 hours to obtain a cell adhesion frame to place boundaries on the best conditions for cell attachment.

5.9 Microlithography

SU-8, the photo-sensitive epoxy resist introduced in Section 3.1 is processed using traditional microlithographic methods. Microlithography is the technology used in semiconductor manufacturing to image a pattern from a photomask onto a silicon wafer coated with a UV-light sensitive photoresist material. The photomask has a thin patterned chrome layer on the bottom which is nearly opaque to UV light wavelengths. UV light is passed through the photomask or reflected by the patterned chrome layer. The photoresist on the wafer is then exposed with the shadow pattern of the photomask and a blueprint is created in the resist forming the basic design of, for example, CMOS chips.

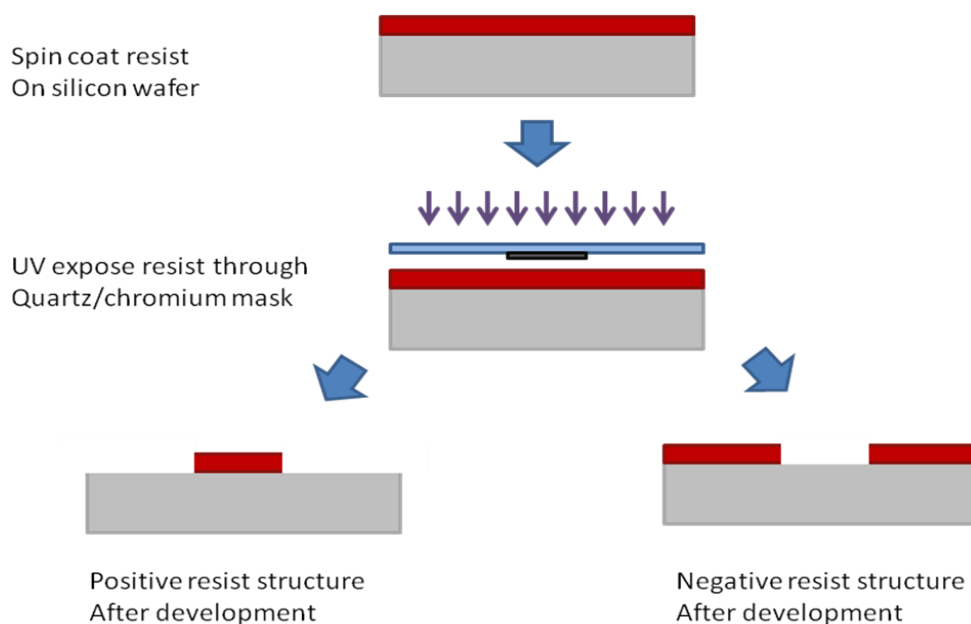


Figure 5-21: Schematic of microlithography processing

There are two basic types of photoresists; positive or negative. When exposed to UV light, the bonds of a positive photoresist such as Clariant AZ4533 are scissioned where subjected to UV light. A salt solution can be used to rinse away broken bond material leaving unexposed photoresist structures behind, this is shown in Figure 5-21, left. With a negative photoresist such as SU-8, the reverse occurs. Areas exposed to UV light crosslink and remain on the substrate, while non-crosslinked areas are removed by an organic solvent as seen in Figure 5-21, right. SU-8 has been used in this work as an alternative material to polystyrene and polycarbonate as small holes can be produced and the surface can be modified.

5.9.1 UV Lithography of holes

UV lithography holes were produced by spin coating a thin layer of SU-8,. A 5µm layer of SU-8 was spin coated onto a silicon substrate coated with titanium with etched alignment marks. A Gyrset RC8 unit spincoater (SUSS MicroTec, Sternenfels, Germany) was used at 2400 r.p.m. for 40 seconds, followed by a soft bake at 95°C for 2 minutes on the integrated hotplate. An exposure dose of 350mJ/cm² was applied to the substrate through a patterned chromium mask on an MA6 UV exposure unit (SUSS MicroTec Lithography GmbH, Garching,

Germany) with an i-line filter which is transparent at only 365nm. A post-exposure bake of 5 minutes at 95°C was also made on the RC8 hotplate. The holes were developed in a large glass dish (6 inch, 2 inch sidewall height), in PGMEA (2-[1-methyl]propyl acetate)). The large dish was set down onto a shaker at 100 r.p.m for agitation during a 15 minute development. The developed substrate was removed from the developing solution and allowed to dry suspended with the resist side facing down in a fumehood. After drying, a short plasma clean step was made, 100W at 5 minutes in an oxygen plasma.

5.10 Physical Vapour Deposition (PVD)

PVD is used to deposit thin layers of metals. In this work, planar micro-electrodes are deposited using a PVD method.

To explain PVD simply, a thin material film (some nanometres to a few micrometres), is physically transferred from a source (target material) to a substrate. During deposition the chemical composition of the target material is not altered. PVD processing takes place in a sub-atmospheric (vacuum) environment to reduce gas particle density thereby limiting gaseous contamination during deposition and additionally in PVD processes with gases, to establish partial pressures of inert or reactive gases, and control gas flow.

Physical vapour deposition technology is key in the creation of microelectronic devices and the more important technologies for thin-film deposition by physical vacuum deposition processes are listed in Table 6.

The two main methods, principles and main characteristics of PVD metal deposition have advantages and disadvantages. By its nature, sputtering is a highly kinetic deposition method which leads to less control of coating thickness and higher stress in deposited films, but increased adhesion properties. Sputter deposition processes can create heat in substrate material, so parameters for depositing on polymer films must be carefully controlled. For this reason evaporation was chosen as the main technique to pursue for this work. While evaporation actually melts the material to be deposited, distance from the target material to the substrate material can be changed and deposition thickness

better controlled. The following section is a short description of thermal evaporation.

Table 6: Survey and classification of PVD deposition techniques (Kern and Schuegraf, 1994)

EVAPORATIVE METHODS	GLOW DISCHARGE PROCESSES
Vacuum evaporation	Sputtering
Conventional vacuum evaporation	Diode sputtering
Electron beam evaporation(e-beam)	Reactive sputtering
Molecular beam epitaxy (MBE)	Bias sputtering (ion plating)
Reactive evaporation	Magnetron sputtering
Ion beam deposition	Ion beam sputter deposition
Cluster beam deposition	

Thermal evaporation is a lower energy deposition technique which relies on the vaporization of metals from thermal heating of a solid (sublimation) or a liquid (evaporation) to coat a substrate. Atoms or molecules from a thermal vaporization source reach the substrate without many collisions with residual gas molecules in the deposition chamber, travelling directly from the source to the substrate (line -of-sight). To allow this to happen efficiently, a relatively good vacuum, usually better than 10^{-4} Torr, is required.

Depending on the tolerable impurity level in the deposit a high (10^{-7} Torr) or ultrahigh (10^{-9} Torr) vacuum environment can be used. In order to achieve a reasonable deposition rate a minimum vapour pressure of the element to be deposited is needed, usually around 10^{-2} Torr as shown in Figure 5-22.

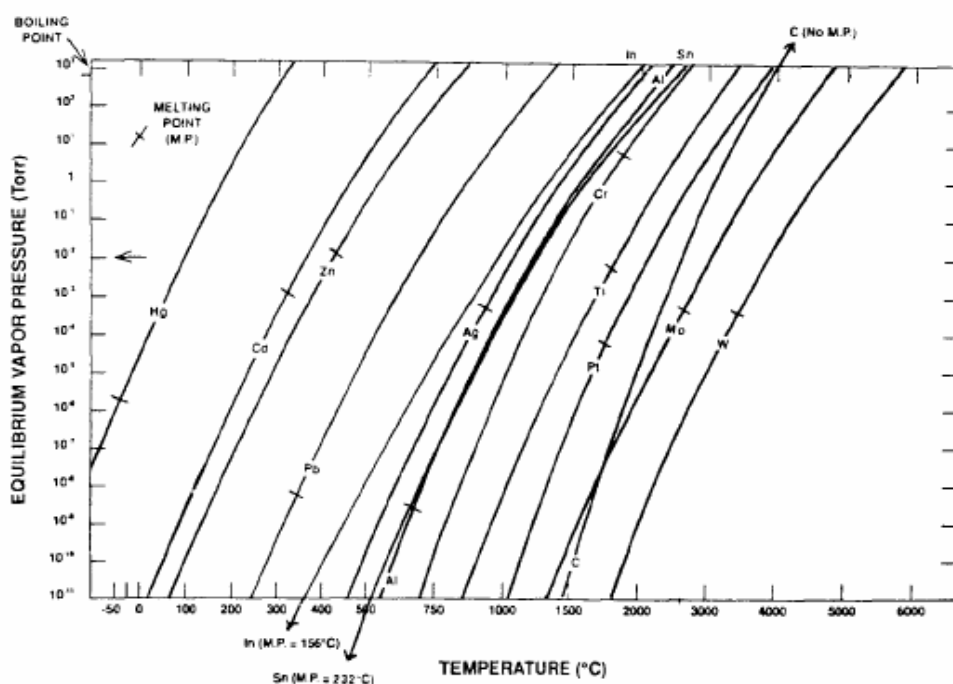


Figure 5-22: The dependence of vapour pressure on melting temperature for selected materials

Metals that reach this vapour pressure value in the solid state are considered subliming, whereas others reaching it above the liquid state are described as evaporating. In this work, silver was deposited by ebeam evaporation.

5.10.1 Electrode deposition experiments

In standard patch clamping measurements, the electrodes are silver wires with chlorated tips. The chloration process stabilizes the silver electrode for measurement purposes, and prevents loose silver ions in the solution which are cell toxic. For the design presented here, planar electrodes are intended, which are directly deposited to the design structure by using a patterned steel mask which is placed on top of the polymer film during evaporation.

The Edwards thermal evaporator chamber is 60x90cm with two boat positions. The sample was held 150 mm above the boat on a metallic plate as shown in Figure 5-23.



Figure 5-23: Edwards thermal evaporator, chamber exterior and interior (Cranfield)

Deposition rate and thickness were monitored during processing using a quartz sensor positioned 10 cm from the source and previously calibrated (tooling factor= real thickness/thickness sensed). Silver is evaporated by a resistance-heated thermal boat and the processing pressure was between 10^{-5} and 5×10^{-5} torr. The base pressure is 4×10^{-6} torr. For silver (98% + 2% Cu) deposition is carried out at 25A at a deposition rate of 50nm/min and thicknesses varied between 100 – 400nm. The deposition is carried out as a blanket coating of a piece of polymer foil for adhesion tests, or through a stainless steel mask (Figure 5-24) taped onto the foil for test electrode structures.

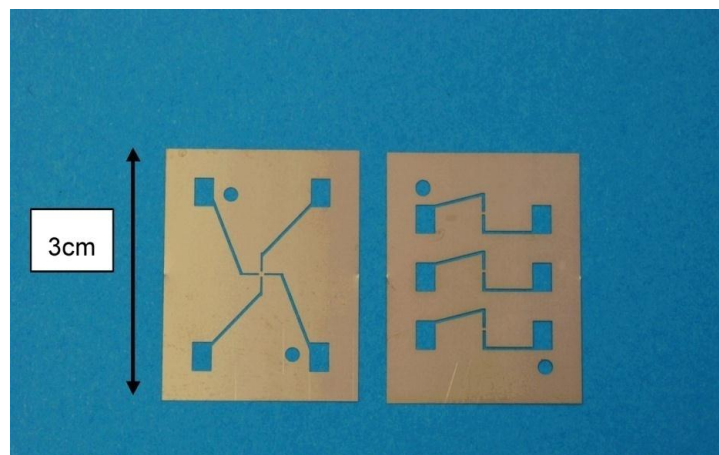


Figure 5-24: Sputter masks – test electrode design

Temperature was measured in all depositions. The maximum permissible temperature for the polymer foil was 90°C for polystyrene and the temperature of a sample was determined by means of temperature sensitive labels placed on a glass slide next to the coating sample. Labels give the maximum temperature reached during deposition. Two temperature label ranges were used, 37 to 65°C and 71 to 110°C, each with temperature increments of 5-6°C. Adhesion of the deposited coating was determined using DIN-EN Standard 58196-6, K2 Scotch tape test.

The silver layer, deposited at thicknesses 100nm, 200nm and 400 nm was then chlorated by submersion in a Clorox® bleach solution (3-6% NaClO), or electrolytically with a 30mM KCl solution. In the electrolytic method the evaporated electrode material is connected as the cathode of the reaction, and the counter electrode (silver wire) which sits in the KCl solution is the anode.



Voltage is applied from a voltage source (IET V1700) slowly until bubbles are seen on the anode (production of H₂O₂). The electrodes are evaluated for stability in a cell culture medium (with water as a reference) at 37°C up to ten days to mimic later cell culture conditions.

5.11 Resistance measurement set up

Resistance measurements are the first step towards making patch clamping measurements. In order to acquire the pico- to nanoampere signals of ion channels opening and closing, a high resistance seal is required. While a giga Ohm resistance is required for the physiological response of cells for patchers, for drug screening often a lower resistance seal beginning at 100 MOhms is sufficient to begin measurement (Comley, 2003). A test rig was develop as part of this work to enable the measurement of foils on a traditional patch clamping setup The test rig design is introduced in Section 6.8. The inherent resistance of this test rig filled with medium was measured, and then with foils with one hole, and eventually with cells.

To assess the system, patch clamping measurements were made using a HEKA patch clamping unit (with EPC 10 amplifier, Axiovent 200M microscope, Sutter MP 285 micromanipulator) shown in Figure 5-25

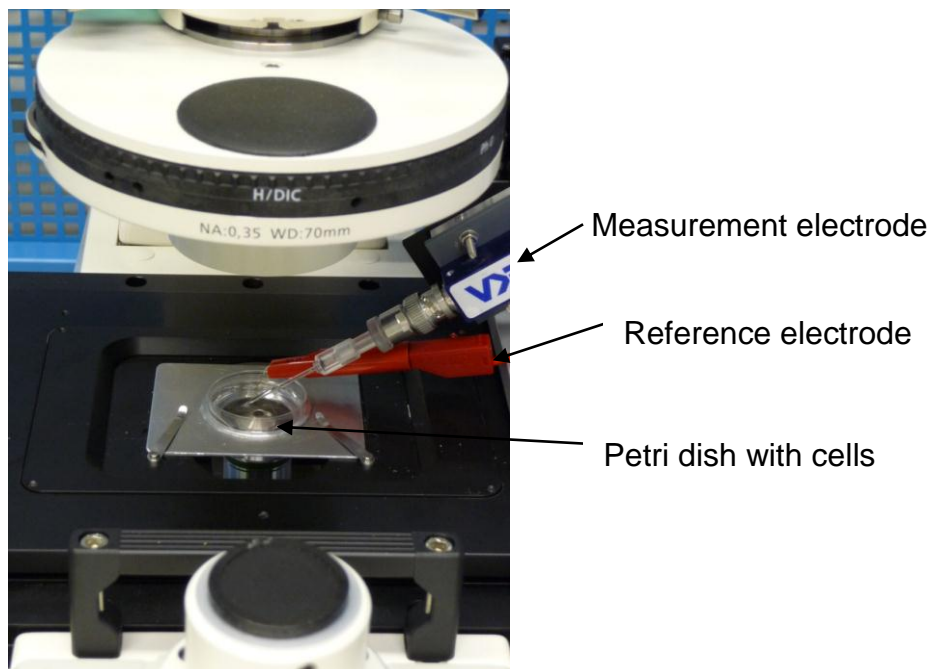


Figure 5-25: Patch clamping system used for measurement

Patch clamping scans are performed with a set test range between -200mV and +200 mV at 20mV increments. Amplifier gain was set at +5V but was adjusted as required to have the lowest possible system noise. Data was acquired and analyzed using Patchmaster™ software. Measurements were made with a fluid filled rig without foils and then with foils and foils with cells respectively.

5.12 Considerations for single part design and material bonding of two part design

For addressable measurement of each cell, this design requires many electrically separated microfluidic structures (chambers) each containing an electrode underneath the measurement hole. Sufficient sealing between adjacent measurement chambers must be obtained with a seal sufficiently good to withstand the cell medium at 37°C for a culture time up to 10 days, and withstand for example, any drug compounds used. Two designs were pursued

in this work, a cell chip shown in Figure 5-26 typically produced by hot embossing in PMMA was produced for this work in polystyrene, or for a two part design where a foil is bonded to supporting microfluidics. Solvent bonding and direct micro-injection moulding are used in this work.

The single part design could make use of the Institute for Biological Interfaces (IBG) bioreactor which has fluidic flow to both the top and bottom chambers separately; however consideration would have to be given to isolate the electrodes/fluids to prevent electrical signal cross-talk and loss of signal.

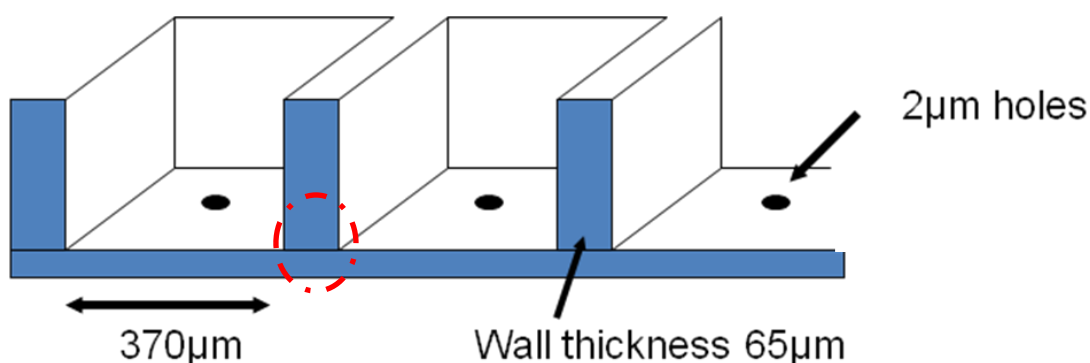


Figure 5-26: Section of a cell chip showing a drilled hole for patch clamping

The dimensions of each chamber of the cell chip are 370x370µm with a height of 400µm. Wall thickness is 65µm. The chip has two side by side arrays of 11x22 chambers, for a total of 484 chambers. The design intended for patch clamping is an array of 10x10, using approximately a quarter of the cell chip. The residual layer from hot embossing (the bottom of the cell chip well), is flipped over in this design (Figure 5-27) to allow the culture of cells on the flat surface, particularly neuronal cells which physically grow and connect to each other. The residual layer from hot embossing is typically from 500µm thick up to several millimetres, and must be reduced to less than 100µm in order to laser drill holes of a size suitable for cell culture.

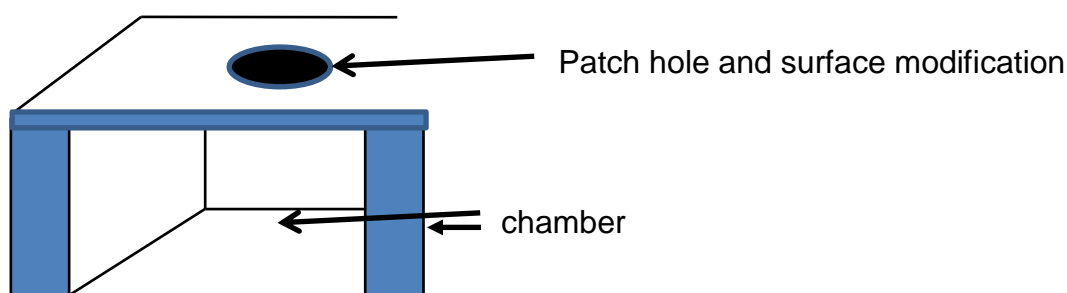


Figure 5-27: Inverted cell chip well structure as a microfluidic chamber permitting surface modification for single or neuronal cells

In a two part system a foil must be bonded to a microfluidic frame and be of sufficient quality that any liquid leaks between chambers are prevented as they cause loss of addressability to single cells and signal loss, this is shown in Figure 5-26 as the leak-tight area. Possible approaches are thermal bonding (application of heat to around the glass transition temperature of the material, and pressure applied to form a mechanical bond). Thermal bonding was attempted on polystyrene at KIT, however the test rig could not be sufficiently temperature controlled to permit good bonding of polystyrene to polystyrene. This could be pursued with a better rig and by increasing the surface energy of polystyrene to increase it from its native 30 Dynes/cm to at least 50 Dynes/cm

Lamination of foil is a similar technique, where pressure and heat are applied and foils rolled together.

In this work, two methods of bonding were pursued, solvent bonding and overmoulding (direct injection moulding). Solvent bonding uses solvents to form a chemical and mechanical bond between materials.

A solvent bonding rig at the Institute for Biological Interfaces uses gas phase solvents introduced into a chamber where foil and supporting structure are pressed against each other. Figure 5-28 shows a section through the chamber. The foil to be bonded is placed on cellulose (a non-stick surface) and the cell chip placed on top. The rubber press is closed and a pressure of 370-380 mbar applied to seal the chamber. Acetone is heated in a coil (60°C) and introduced

into the chamber through small channels in the silicone in the gas phase for a set time period, to soften the polymer surfaces enough that a seal is formed. Chamber pressure is released and the bonded structure is removed.

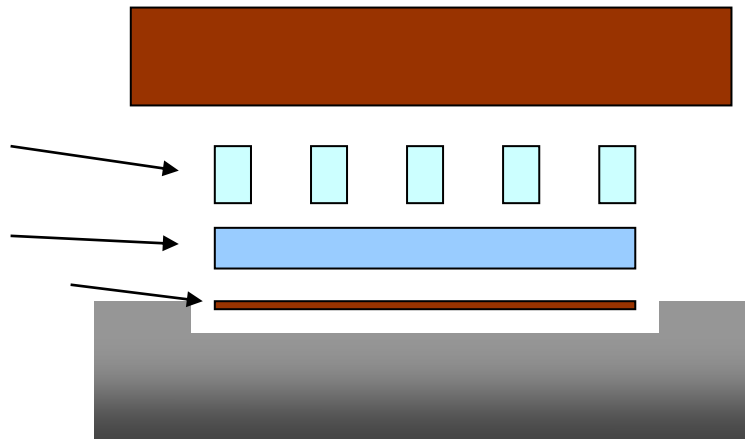


Figure 5-28: Solvent bonding unit chamber

This completes the introduction of the technologies and approaches used in this work. The next section is the results and discussion.

6 Results and discussion

Figure 6-1 for review purposes, shows the overview of the approach used in this work. As much of the work was carried out in parallel, for example, materials were assessed for biocompatibility, laser drilling of holes and modification for cell attachments at the same time, the results and discussion section does not strictly follow the outline of Figure 6-1.

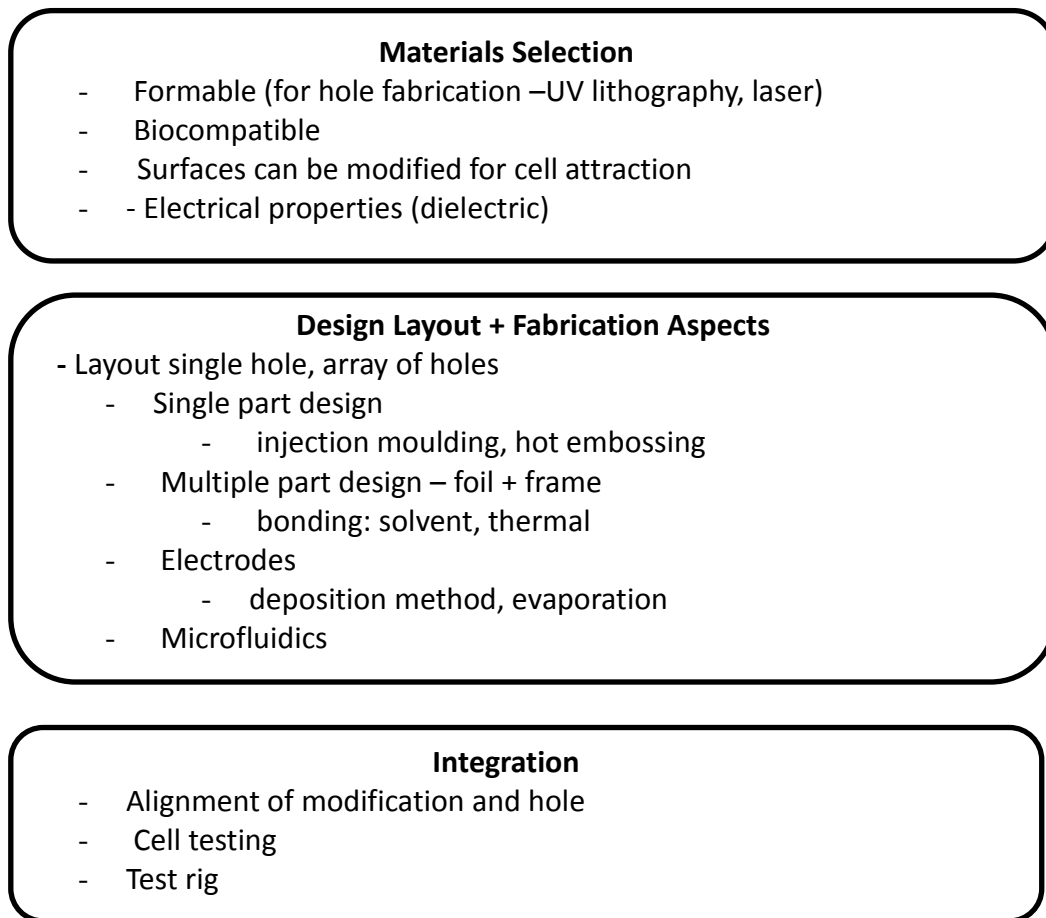


Figure 6-1 Layout of this work

6.1 Hole drilling

Materials must be selected on their ability to have holes formed, either by laser or UV-lithography. To enable adhesion of cells onto/into the holes these must show specific geometries. The drilled holes must have a diameter on the laser exit side of 1-5 μ m to prevent the cell falling through the hole. The diameter of

the hole on the laser entrance side should allow electrolyte penetration to the bottom of the cell. Ideally, the hole should be conical as calculated in Section 3.3.

The energy fluence and the focus level of the laser have significant influence on the geometry of the holes. They were varied to create a desirable form (small exit diameter and larger entrance diameter to form a conical hole shape for optimal cell culture medium penetration to the cell from below). At a fluence of $0.5\text{mJ}/\text{cm}^2$ the best desired result was achieved. The cells sit on the exit side of the hole with a diameter of between 1 and $4\text{ }\mu\text{m}$. For optimum penetration of cell culture medium, the laser entrance side diameters are between $5\text{--}9\text{ }\mu\text{m}$ on average.

Laser pulse frequency has no influence on the hole shape or quality (de Oliveira et al., 2008). For the 193nm laser the thermal influence is small. In contrast to other wavelengths (248nm) the bonds between molecules are photolytically replaced. Other laser types or excimer lasers working with longer wavelengths ($>200\text{nm}$) evaporate the ablation area or require sufficient energy to melt and then evaporate material.

Laser tests were initially performed on both foil and the milled polycarbonate at 248nm to verify the possibility of machining. Three energy doses were applied with a different number of pulses until the hole formed through the membrane. The target hole diameter was $3\text{ }\mu\text{m}$.

As expected, lower energy with increasing numbers of pulses result in a wider spread in hole diameter data, as more scattering occurs. At $0.31\text{ J}/\text{cm}$, 250 pulses results in a hole diameter of $2.5\text{ }\mu\text{m}$ (Figure 6-2). Increasing the pulse number to 6000 increases the diameter to $4\text{ }\mu\text{m}$. Increasing the energy to $2\text{J}/\text{cm}^2$ reduces the diameter spread to zero, although there is a cost in accuracy; the holes at $2\text{J}/\text{cm}^2$ are $5\text{ }\mu\text{m}$, some $2\text{ }\mu\text{m}$ wider than the intended goal of $3\text{ }\mu\text{m}$.

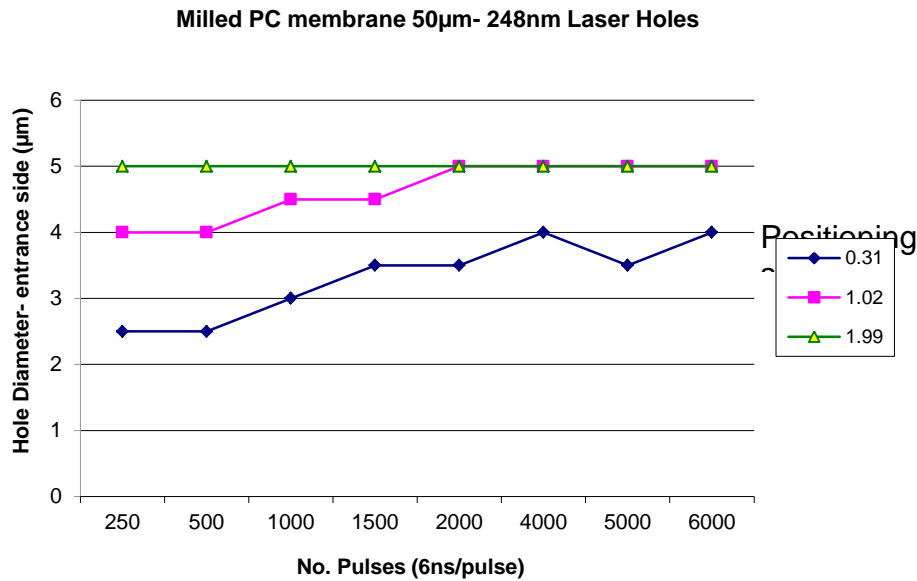


Figure 6-2 248nm UV laser holes in polycarbonate

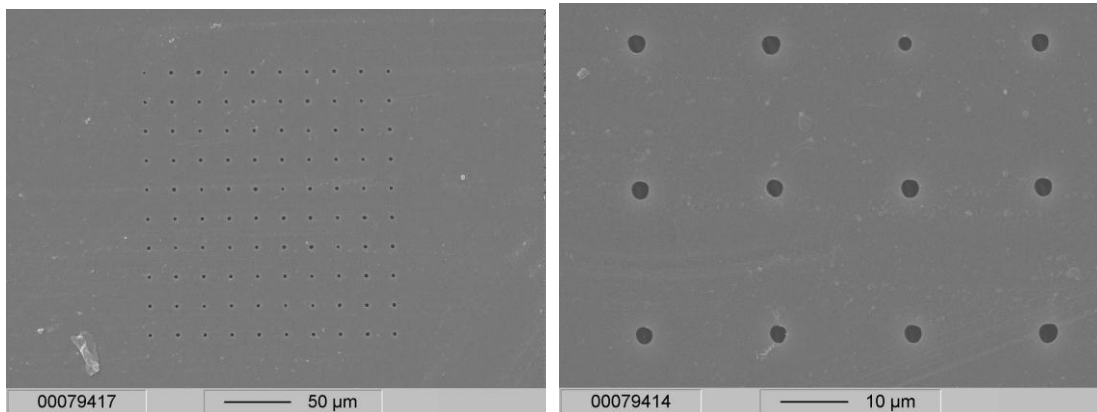


Figure 6-3 PC foil, 2J/cm² 25ns duration: 300 pulses (left), 250 pulses (right)

The measurements above suggest that for uniformity in hole diameter, pulse numbers under 500 produce the best results. It was observed that diffraction effects (Figure 6-3) were seen when pulse numbers increased (above 2000 pulses). These effects can be minimised by adjusting the distance from the metal mask to the workpiece. Above 1J/cm² energy input, the holes begin to show an oval form, this only occurs on the milled polycarbonate and is most

likely due to anisotropy in the material surface due to thermal effects during milling. (Figure 6-4)

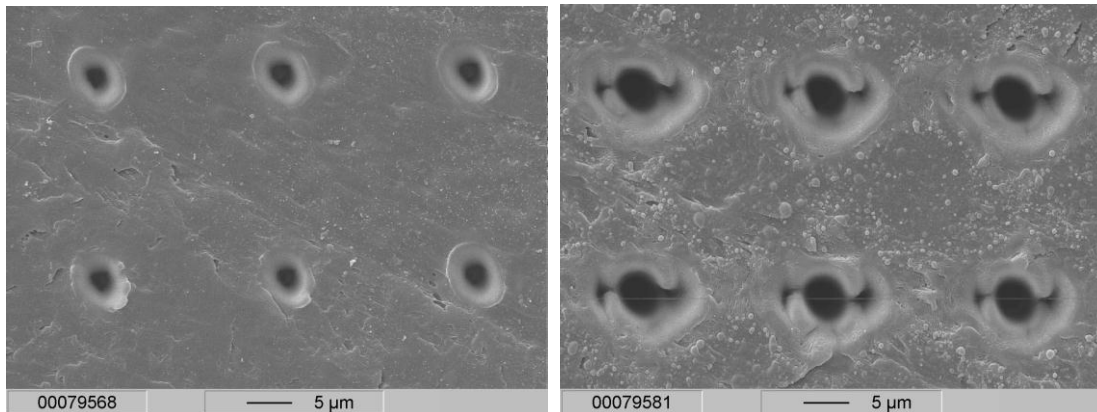


Figure 6-4 3J/cm² 250 pulses (left) 1J/cm² 1500 pulses (right)

The focus level has a large influence on the geometry of the hole. A deviation of a few micrometers from the optimum delta z (z-axis) leads to a geometry difference such as an elongated hole. The optimum for a 50µm foil was placed at $-0.14 \text{ mm} < \Delta z < -0.18 \text{ mm}$.

This work was then repeated with polystyrene, and repeated once again with a 193nm laser, which is preferred due to the type of bonds produced. The results of drilling were in general of a slightly higher visual quality than at 248nm, although work remains to be done to determine if there is a functional difference.

A cross-sectional view, Figure 6-5, of a hole drilled at 193nm in polystyrene, shows the hole from top to bottom with the conical shape. At laser fluences of 0.8mJ/cm² and 1.5mJ/cm² the holes are less conical in shape and show an entrance diameter of 5µm and exit diameter of 3µm. Increasing the energy fluence shows another behaviour than at 0.5mJ/cm². At 0.8mJ/cm² the exit diameter is oval and at 1.5mJ/cm² the holes are round but at >8µm too large for cell analysis.

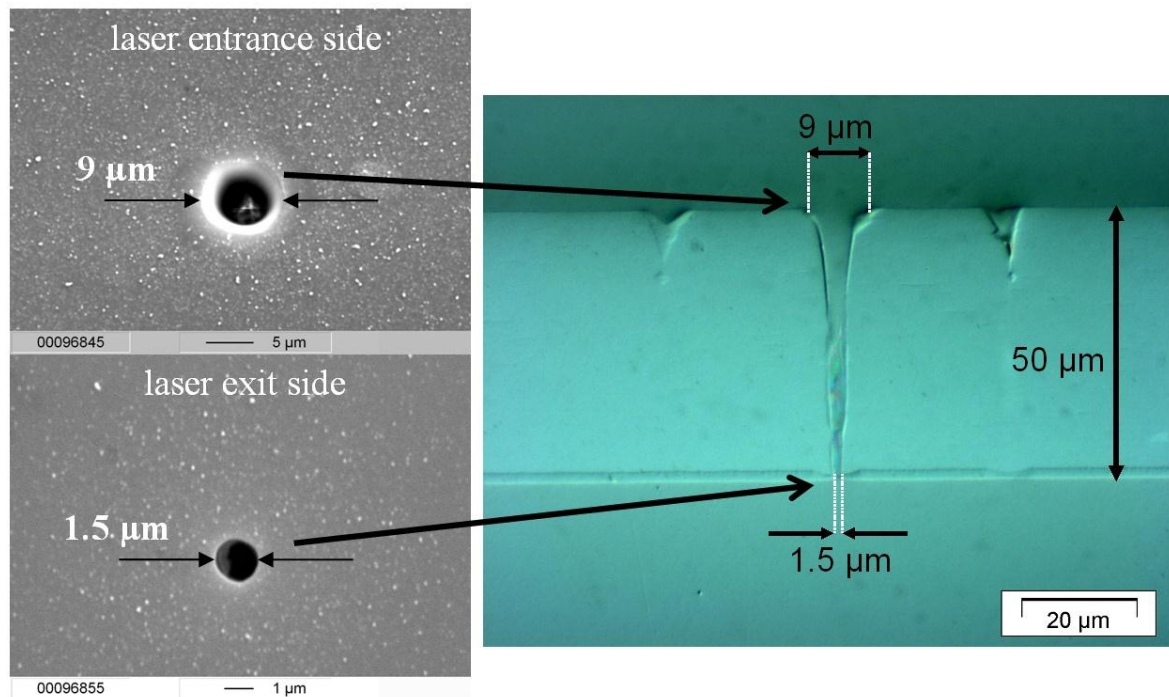


Figure 6-5 Cross-section of a 1.5µm hole drilled in 50µm thick norflex polystyrene foil, 0.5J/cm² laser fluence (image also shows partially cleaved neighbouring holes)

With a combination of correct wavelength selection, laser energy fluencies, pulse numbers and frequency, it is possible to produce holes suitable for patch clamping in polystyrene and polycarbonate, although polycarbonate is much more thermally sensitive (foils from Lofotech High Tech).

The smallest diameter of the hole, the laser exit side is used for cell placement. To produce foils with cell modification and drilled hole, the hole is drilled first followed by an aligned modification.

6.2 Biocompatible polymer selection

Initially, materials were pre-selected on the basis of their ability to form stable carboxyl (COOH) groups. As these groups are hydrophilic, contact angle measurements are the first screening criteria used to verify that a surface change had taken place on a material

Surface modifications were made on polystyrene petri dishes, a commercially available polystyrene foil and on a spincoated layer of SU-8. For handling purposes forty and fifty micrometer thick polystyrene foils were purchased from Goodfellow (Cambridge, UK), and norflex© foils (Norflex, Nordenhein, Germany) respectively, and exposures performed with an 185nm UV-lamp (NNQ low pressure mercury lamp, $\lambda = 185\text{nm}$, 15W Heraeus Noblelight, Filderstadt, Germany) in five minute increments up to 60 minutes at a 10cm distance below the lamp, which corresponds to a range of exposure energy doses (Lamp intensity in $\mu\text{W}/\text{cm}^2 \times \text{time (s)} = \text{Exposure dose (mJ}/\text{cm}^2))$ up to $1\text{J}/\text{cm}^2$.

For patterned lamp exposures a chromium/quartz mask was placed onto the bottom surface of the petri dish with the chrome pattern contacting the polymer surface.

The biocompatibility of SU-8 (Wilson, 2005) and polystyrene petri dishes has already been determined and those polystyrene foils were then irradiated with a UV lamp and UV laser modification at a range of exposure doses to assess their surface modification capabilities. To vary energy, UV lamp exposures were made at 5 minute increments to provide a cumulative timed dose from 5 to 60 minutes UV laser modifications were performed at different fluencies and a range of pulse numbers below the ablation threshold for the material. The ablation threshold for norflex© polystyrene and polystyrene petri dishes was determined between 9 and $10\text{mJ}/\text{cm}^2$ (de Oliveira et al., 2008).

Laser surface modifications were performed at 193nm using an ArF ATLEX laser (ATL Laser Technik, Wermelskirchen, Germany) at different energy fluencies, frequencies, and number of pulses and in ambient air. A chromium/quartz mask is also used in this work but as a projection mask not in contact with the material. The mask feature size demagnification factor to the final achieved feature size is 4:1.

Polymers were exposed under a UV lamp as described in the experimental method section and contact angle measured at 5 points for each exposure time. The averages were calculated and are shown in Figure 6-6 below.

Contact angle as a function of exposure time under a UV lamp at 193nm

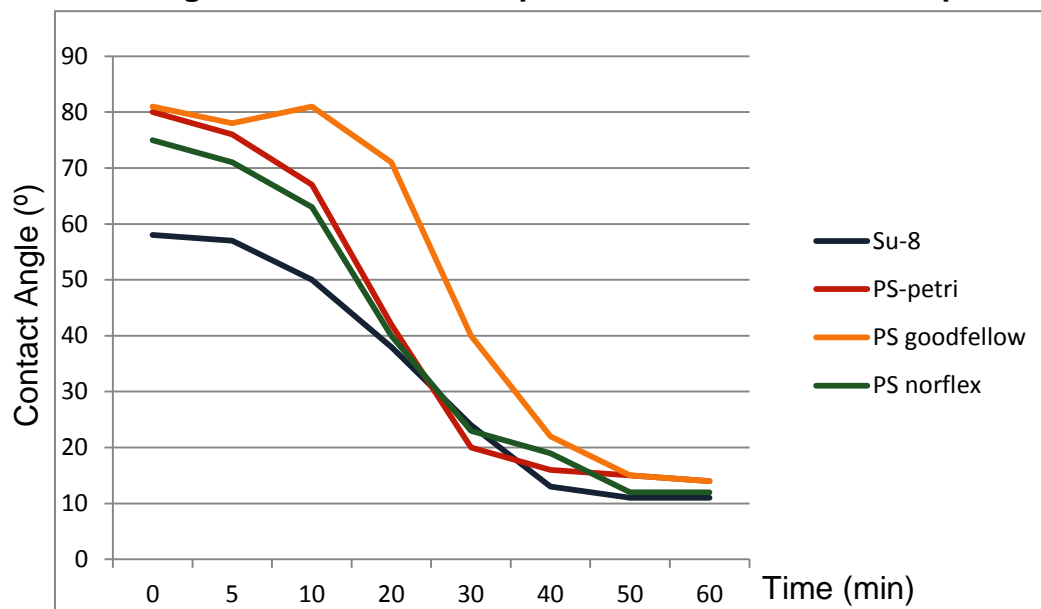


Figure 6-6: Advancing contact angle measurements for a range of polymers

The 5 μ m SU-8 film, polystyrene petri dish material and both the goodfellow and norflex polystyrene foils show a good hydrophilic shift (below 15 degrees) indicating a chemical surface change that begins within the first 5 minutes and starts to stabilize from about 45 minutes. Polycarbonate was measured previously (Welle and Gottwald, 2002) and also showed a good shift to <15°. After 55 minutes the contact angles have reached a plateau so the surface chemistry is assumed as stable. All of these materials show some kind of chemical surface modification.

The biocompatibility of polystyrene is evidenced by its use in many biocompatible applications such as petri dishes and culture flasks. However, polystyrene materials from different manufacturers have different proprietary additives to provide better forming or other properties such as toughness, may not result in a truly biocompatible end product.


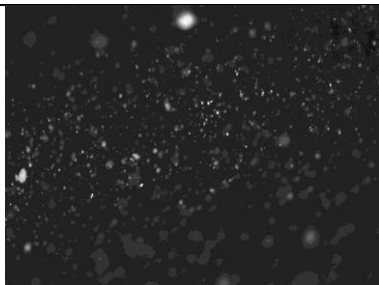




With this in mind, polystyrene foils were purchased which did not have obvious additions such as anti-static coatings. They were initially screened by inspection under a fluorescent microscope (Apotome Axiovert, Zeiss, Wetzlar, Germany) to determine the presence of fluorescing particles, specifically for concentrated areas and volume of filler materials different to the majority of the chemistry, which is assumed to be polystyrene. Foils with large amounts of poorly distributed particles or randomly spaced agglomerates as a rule will respond inconsistently to modification processes and subsequent cell culture results and are not considered suitable materials. Excessively fluorescing materials may also interfere with the visualization of cells dyed with fluorescing proteins. Before microscopy all foils were rinsed using isopropyl alcohol in an ultrasonic bath for 10 minutes, followed by 10 minutes ultrasonication in d.i. water, then a d.i. water rinse and nitrogen gun blow dry. This step should remove any loosely adhering surface particles before inspection.

From previous work (Wilson 2009), neither the petri dish material nor SU-8 have auto-fluorescence in the DAPI and FITC filtered regions (important for GFP labelled cell lines) so these were not included in the inspection here, however Table 7 shows a selection of microscopy images of commercially available polystyrene.

Inspection under an Apotome fluorescence microscope with DAPI (excitation peak = 359nm, emission peak = 461nm) and FITC (excitation peak = 494nm, emission peak = 518nm) filters (Carl Zeiss, Wetzlar, Germany) was very revealing. Goodfellow (www.goodfellow.com) and norflex© interweave foils have many large fluorescing particles in irregular agglomerations which may make it difficult to view fluorescing cells later, also it is assumed that these additions to the polymer blend may influence cell adhesion, at the very least because surface chemistry may not be consistent if these particles are close to the surface of the material. It is also unknown if these polymer additions are cell toxic. From this analysis, the Goodfellow foil and norflex interweave foils are then not suitable for this work. The norflex© glasklar (norflex, Nordenhein, Germany) on the other hand shows little fluorescence and no large

agglomerates, and so it was chosen as the polystyrene of choice due to its more unified composition. To summarize, work proceeded on SU-8, norflex© glasklar polystyrene and polystyrene petri dishes as a reference substrate material.

Table 7: Apotome microscope analysis of purchased polystyrene foil materials

Material	Illumination/filter: DIC/DAPI	Filter: FITC
Goodfellow polystyrene (40µm)		
Norflex interweave glasklar (50µm)		
Norflex glasklar (50µm)		

6.3 Single or two part design analysis

Hot embossing was used to assess whether a “one piece” cell chip could be manufactured in PS, thereby removing the need for an extra bonding step for a foil.

Ten cell chips were manufactured by hot embossing to a chamber height of 400 μm with a residual bottom layer intended as the layer used for drilling a measurement hole (target thickness <100 μm). First investigations looked at milling the residual layer down to 50 μm to achieve a thickness suitable for laser drilling purposes. During milling, cell chips are placed into a specially designed fixture and gradually covered with thin layers water and chilled to -17°C to secure parts during processing and also to stiffen the rather soft polystyrene material. Figure 6-7 shows a cross-sectional view of a milled cell chip, the average thickness of this section of the chip is, at 109.5 μm , thicker than the targeted maximum of 100 μm , unfortunately no further milling can be done as there are sections of the chip where there is no remaining residual layer and the cell chip bottoms are open.

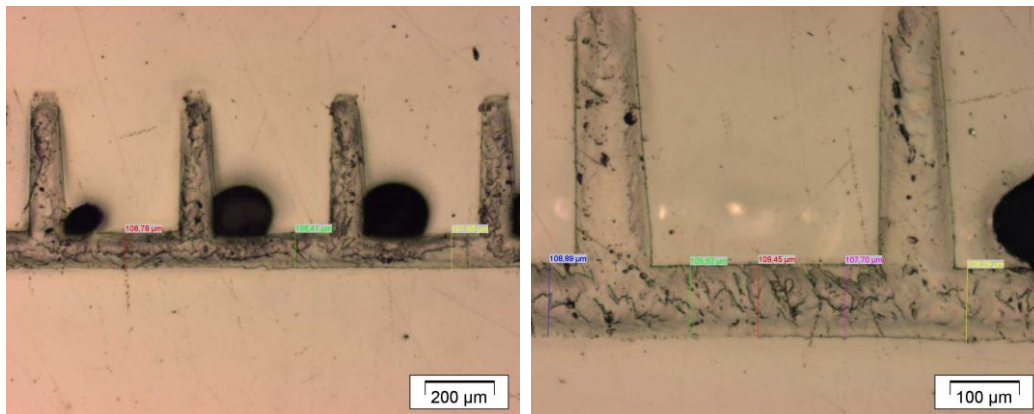


Figure 6-7: Milled cell chip

Parameters such as temperature (reduced) and machining parameters (number of bit passes, bit rotation speeds) were adjusted; however the cell chip could not be milled with consistent residual layer thickness suitable for laser drilling. The disadvantage of this is clear, if material thickness varies, the focus level of the laser must be adjusted for each change of more than a few micrometres, making the process time-consuming and no longer cost-effective. Added to this,

the mechanical nature of the milling step on a soft material increases surface roughness considerably, subsequent surface modifications will be distorted and it is also likely that thermally induced surface effects may alter surface chemistry which could detract from the patterning effects of surface modifications. Also, as roughness is a factor in cell adhesion this would also be influenced. Figure 6-8 shows the exit sides (milled surface) of two laser drilled holes in embossed well structures.

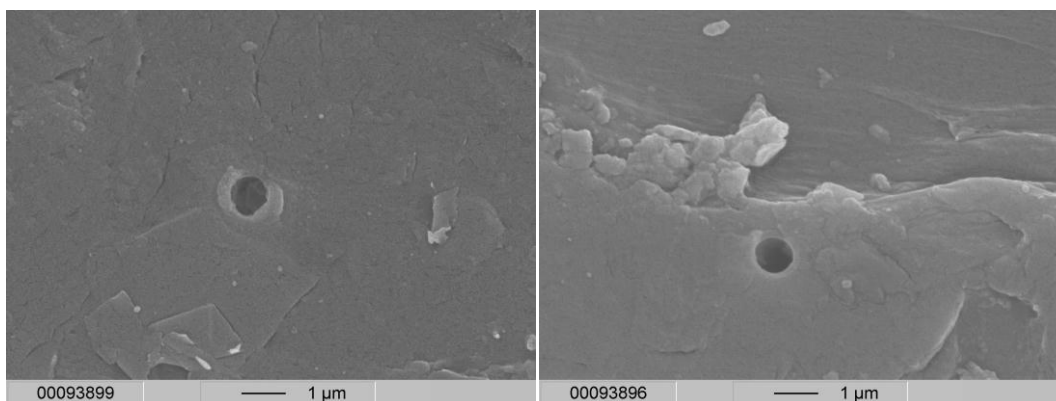


Figure 6-8: A sectional view of a milled and drilled well around laser drilled holes showing surface roughness effects

As the figure reveals, the surface appears flaky and rough after milling and unsuitable for surface modification. It appears that a single design part cannot be achieved using current hot embossing technology. The chips produced were then salvaged for use in a two part chip, by milling the bottoms open completely (no residual layer) and they were used in both thermal and solvent bonding tests as described in the next section.

6.3.1 Solvent bonding

Bonding experiments were performed on polystyrene foils and frames. As a starting point, gas phase solvent injection time (acetone) was set to 17 seconds which is the standard time used for typical PMMA / PMMA bonding performed in the custom made bonding machine at KIT / IBG. The results in Figure 6-9, right, show severe blistering of the foil at 17 seconds (opaque areas), so time was reduced to 10s and then 5s. The time reduction did decrease the effects of blistering, to about 40% area coverage at 10s, to very minimal blistering at 5

seconds, however adhesion was also deleteriously impacted. Foils showed good adhesion at 17s but at 5 and 10 seconds could easily be manually pulled away from the frame. Acetone clearly reacts quickly and aggressively in the vapour phase against polystyrene. These experiments, do however, show principle viability of solvent bonding as an approach for polystyrene, but less aggressive solvents with similar boiling points must be selected, such as ethyl acetate (boiling point 77°C) or other ketones. Care must be taken to select a solvent that is not explosive in an essentially closed circuit. None of the alternative solvents could be tried in this work due to processing restrictions on the bonding unit used.

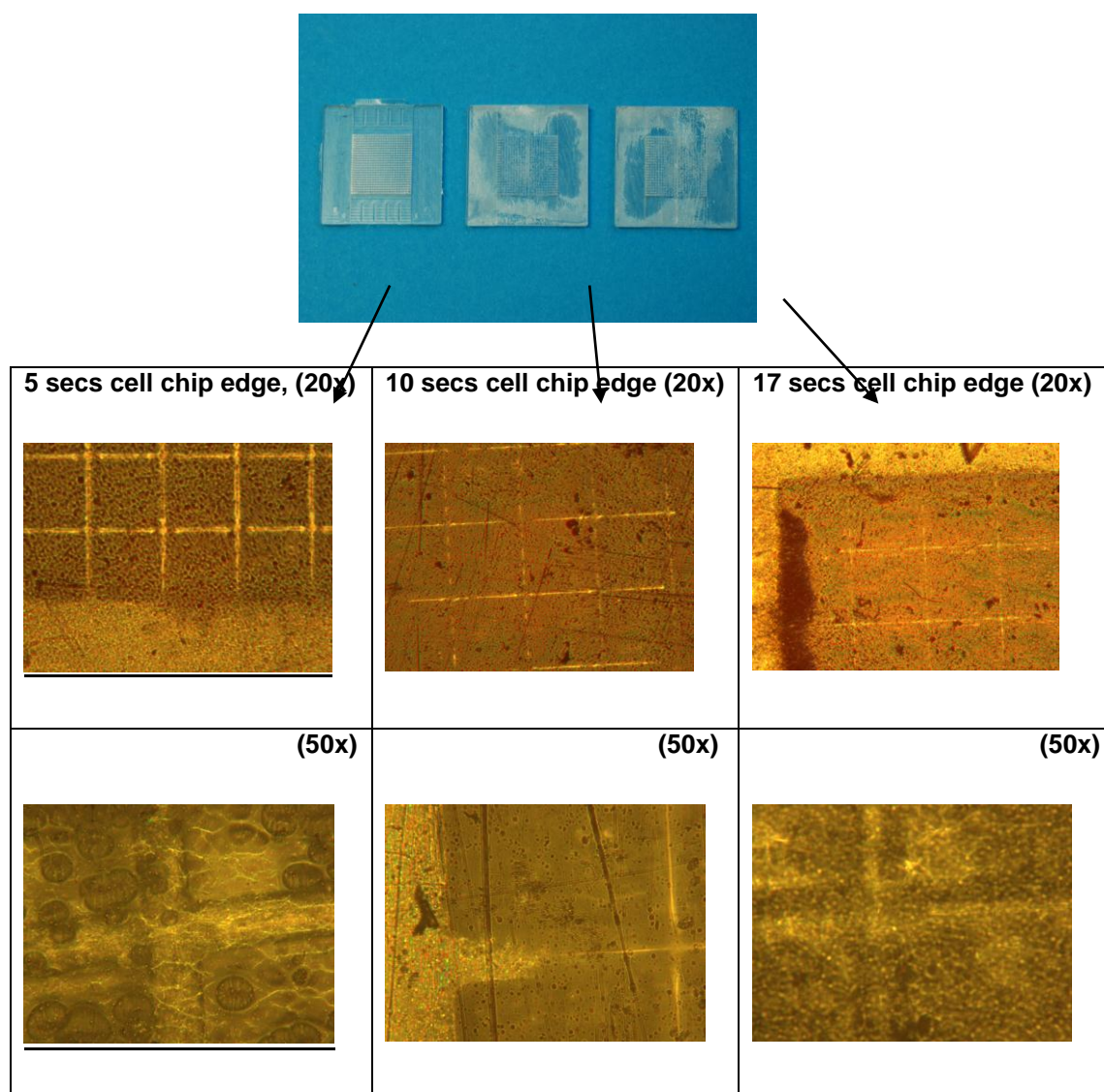


Figure 6-9: From left to right, 5 sec, 10 sec and 17 seconds gas phase acetone solvent bonding on polystyrene

In future work, lamination and thermal bonding with the appropriate equipment, for example heated rollers or pressure plates, could be pursued.

6.3.2 Direct injection moulding

For the two-part design with planar electrode arrays, the approach was to injection mould a support structure directly onto the drilled and modified polystyrene foil. The glass transition temperatures between the polystyrene foil (101°C) and the polystyrene granulate (93°C) are quite close to each other, which requires that granulate melt temperature, injection speed, mould temperature and injection pressure be very well controlled. A Battenfeld 50 micro-injection moulding machine with a 1cm² maximum melt shot size was used to control the melt volume and temperature as closely as possible.

Before injection moulding, the foil was placed against the back plate and held in place using high temperature grease at the corners, then the mould was closed over it. A pressure of 300 to 400 bars was applied over the 4 inch squared mould. A 500mm² shot of molten polymer was injected to fill the test moulds (2 cavities), while the mould which was maintained at a temperature of 80°C. This following section is the results and discussion of the experimental aspects of this work

Three initial test runs were performed to identify melt parameters for polystyrene and the best operating pressure and temperature for injection moulding to the polystyrene foil established (parameters are shown in Table 8). A test mould structure comprising of microfluidic meander structures and two through holes and two through c-shaped structures was used for initial tests to evaluate the feasibility of an injection moulding approach to bonding foils. Peel test results show that it is possible to successfully bond the foil with injection moulded material, The best parameters are run 4 and higher (not shown, but with the same parameters as test run 4) with a melt temperature of 200°C, mould temperature of 85°C and an applied pressure of 300bar. The two-cavity mould could be filled with a 500mm³ shot of polymer melt and a filling time of two seconds. From run 4 onwards, parameters were maintained and a total of

40 runs were performed all had intact foils attached to the microfluidic structures without any apparent damage to the foil.

Table 8: Injection moulding results BASF PS granulate onto 50µm Norflex foil

	run 1	run 2	run 3	run 4
Injection				
Temp (°C)	230	230	230	200
Speed profile (mm/s)	300	300	300	300
Pressure (bar)	300	300	300	300
Metering				
Volume (mm ³)	500	500	500	500
Speed (mm/s)				
Holding				
Pressure (MPa)	40	40	40	40
Time (s)	2	2	2	2
Mould				
Temp (°C)	88	85	85	85
Cooling time	10	10	10	10
Other parameters				
Total cycle time (s)	20	20	20	20
Notes	Bare PS foil	Bare PS foil	Bare PS foil	Bare PS foil

To evaluate the bonding between the injection moulded structure and the foil, immersion tests were performed over 1, 2, 5, 7 and 10 days to assess the stability of bonding over time in the cell culture medium. As the test design had only two through-holes (see Figure 5-17), and two 'C' shaped cavities which are spaced far apart, no electrical measurements could be used to assess bond quality. So an optical method was developed.

The procedure, shown visually in Figure 6-10, was developed as a method of comparing the potential leakage area of a through structure (hole or c-shape) before and after immersion to observe the possible deterioration of the bond; if the bonding degraded the leakage would have increased allowing more ink flow

between the PS sheet and the support, increasing the effective coloured area. Image analysis software (ImageJ® software, National Institute of Health, Bethesda, USA) enabled determination of the number of pixels of each picture and the number of black pixels, corresponding to the inked area. However to get the end value the image was slightly improved because software functionality only works with black and white (B&W) images, without grey tones.

The through hole and C-shaped through structures were inked and photographed, then put into the test medium for the allocated amount of time, rinsed with d.i. water, dried, and then ink reapplied. The samples were then re-photographed, and a comparison made between before and after assessed using image analysis as shown in Figure 6-10.

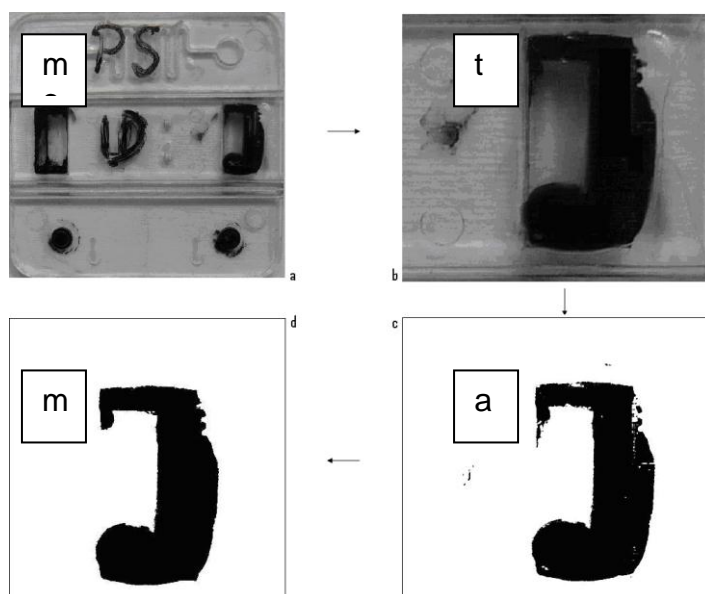


Figure 6-10: Photographs (1,2) plus raw and adjusted ImageJ® image analysis (3,4)

To obtain a black and white only image, a threshold function is available in the ImageJ® software, however, if only this function was applied to the picture, the result was not always representative as sometimes parts of the inked area disappeared or shadow was included in the inked surface. For this reason, some manual adjustments were made on the images.

Figure 6-10 shows the process using image analysis software. In 1, a photo of the whole sample was taken using a Panasonic Lumix DMX-TZ5 camera on a tripod at high resolution (460,000 pixels). A zoom was made of the structure of interest and markers on the structure ensured that the same position was photographed each time (2). Contrast and brightness were adjusted in the image analysis software until a black/white image was obtained (3). The outline was refit to fill any obvious areas of ink filling using the image analysis software (4). Finally a ratio was made between the numbers of black pixels to the total number of pixels in the photo. This was done before and after submersion in medium.

The results of this are difficult to interpret given that step 3 of the image analysis procedure is subjective; however initial results did not give conclusive evidence of significant bond deterioration even up to 10 days. Some visual observations of foils could be made; namely that wetting behaviour changes over time, initially the polystyrene foil is hydrophobic and cavities are difficult to fill with water based ink solutions. The foil becomes more hydrophilic after time in the cell medium; this may be due to amphiphilic proteins in the media coating the surface giving it a hydrophilic appearance, as well as general reduction in surface energy due to immersion in a water based solution. For future work, use of a more applicable mould with closer 'through' features that would enable the electrical measurement (resistance) between electrodes would be a better measure of leak-tight bonding.

To summarize the bonding work, a one-part system may be possible with a process which produces better controlled features that do not require milling, such as micro injection moulding – however there would be a challenge filling a mould to produce the thin layer for laser hole drilling ($<100\mu\text{m}$) over a large area, so some design changes would be required. Solvent bonding work could not be successfully applied to work here as the only solvent available for use in the equipment, acetone, is not compatible with polystyrene. Other solvents with a boiling point similar to acetone which are less aggressive to polystyrene may be more suitable if their flashpoint and vapour pressure allows

use in an essentially closed circuit configuration. A two-part design with microfluidic structures directly injection moulded to the foil structure is of interest, but more study is required to validate the initial findings, specifically visualizing the interface between the foil material and the microfluidic structures, and also to assess the effects of bonding on the hole structures electrically over time.

The next section contains the results of surface modification work and its analysis.

6.4 Surface Modification

One of the unique features of this approach to patch clamping uses a surface modification to attract cells to the holes, so conditions required to achieve a stable and cell attractive surface modification were investigated and parameters established for both a UV laser and a UV lamp.

Surface modifications by UV lamp and UV laser were carried out on norflex® polystyrene foil, polystyrene petridish material, and SU-8. The modifications were analyzed using contact angle measurements and XPS to determine the surface chemistry, and roughness was measured using a contact profilometer (Tencor). The pre-modification advancing contact angles for all three PS types lies within values cited in literature of between $82^\circ \pm 3.3^\circ$ (Pfleging et al., 2007), although some literature states values as high as approx. 92° (Goddard and Hotchkiss, 2007). SU-8 is known to be hydrophobic and contact angles of an average of 68° were measured at the beginning of this work.

Contact angle measurements used in this work were performed with an ambient humidity of between 38.8% and 49.4% and temperature ranges between 21.1° and 25° . As these variables are within a narrow range their influences on measurement are considered negligible. A comparison of different types of polystyrene showed differences in contact angle, in surface roughness and in SEM photos of surface quality. The causes of this are the chemistry of the materials themselves and their production methods creating different responses to surface modification techniques. Sheets and foils are produced using

extrusion processes, where petri dishes are produced by injection moulding processes. (Vieweg and Daumiller, 1969).

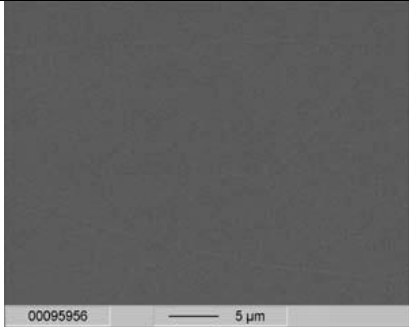
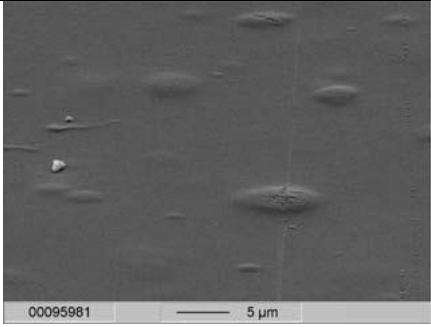
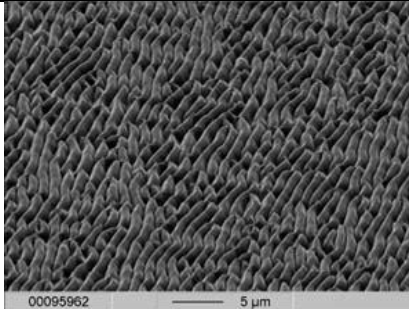
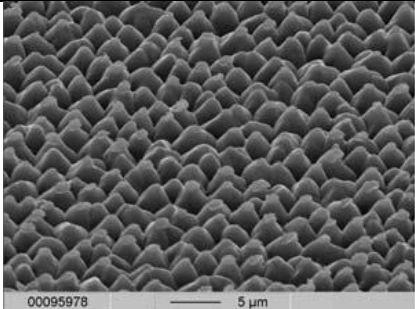
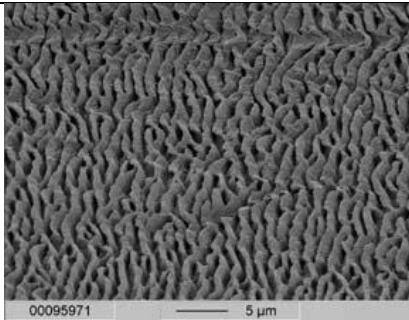
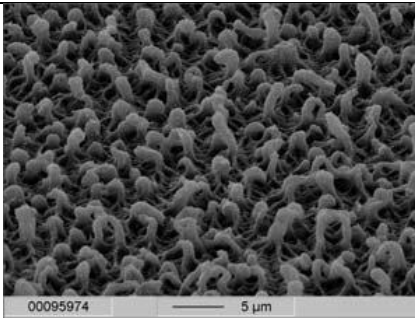
These processing influences can be highlighted particularly clearly using laser ablation. Petri dishes show a ridge type structure if they are structured by UV laser above the ablation threshold. This ridge type structure is considered a material artefact as it cannot be altered by laser radiation density or number of pulses and is also independent of laser direction (parallel or perpendicular to the ridges). For energy fluencies of 20mJ/cm^2 , selective material removal occurs in the amorphous areas, Semi-crystalline areas have a higher removal rate leading to the ridge type structure as shown in Table 9.

A significant change in roughness measured by profilometer was not observed. The largest difference was found for Norflex foils at an energy fluence of 100mJ/cm^2 and oxygen as a process gas. The difference in roughness between the reference measurements and the foils modified at 4mJ/cm^2 is very small. The SEM photos show no significant difference. The reason for this is that the 4mJ/cm^2 fluence is below the ablation threshold.

A comparison of the effects of different laser pulse widths showed no significant difference in contact angle. Both 20ns and 4ns pulse widths only a very small difference was seen in contact angle hysteresis which can be considered negligible.

No measurable change in roughness was seen for UV lamp modified materials as material is not removed during exposure, however at exposure times of above 180 minutes the norflex© foil material begins to show opacity and a slight increase in roughness as micro-cracks begin to form and the material begins to degrade.

Table 9: Influence of laser exposure on surface roughness of polystyrene

Material	Bacterial petri dish (PS)	Norflex© polystyrene
Laser exposure 4mJ/cm ² - 200 pulses, ambient air		
Laser exposure 20mJ/cm ² - 200 pulses, ambient air		
Laser exposure – 100mJ/cm ² - 40 pulses, O ₂ atmosphere		

Spin coated SU-8 showed a similar response, with surface roughening and opacity beginning at 300 minutes under the UV lamp.

The contact angle response for UV lamp exposures compared to UV laser exposures using the example of norflex© polystyrene shows a significantly different behaviour as seen in Figure 6-11. Figure 6-11: Contact angle measurements advancing and receding for norflex© polystyrene. As roughness effects are considered negligible for UV lamp exposed material, and laser treatments remain below the laser ablation threshold for the material during modification, contact angle measurements are assumed to be directly related to

chemical changes and not due to surface roughening influences. The upper graph in Figure 6-11 shows that for total exposure doses up to $E_{\text{tot}} = 1.2\text{J}/\text{cm}^2$, laser modified surfaces show no significant change in advancing contact angle with respect to the untreated PS surface. However the receding contact angle was significantly reduced from 74° to 22° . In contrast to this behaviour, the UV lamp modified surfaces leads to a significant reduction in both the advancing and receding contact angles. Even after an exposure dose of $0.3\text{J}/\text{cm}^2$ the receding angle has measured its largest decrease and achieves a value of 8° . The advancing contact angle has reduced to about 40° at a dose of $0.3\text{J}/\text{cm}^2$, but continues to decrease reaching approximately 16° after an exposure dose of $0.7\text{J}/\text{cm}^2$. The contact angle hysteresis $\Delta\Theta$, the difference between the advancing and receding contact angles illustrates the different mechanisms of laser and UV lamp modifications. While for the laser modification $\Delta\Theta$ increases with increasing exposure dose up to values of $\Delta\Theta=63^\circ$ at $E_{\text{tot}}=1.2\text{J}/\text{cm}^2$, the curve for the UV lamp modification passes an absolute maximum at $\Delta\Theta=64^\circ$ at $0.075\text{J}/\text{cm}^2$ and shows a sharp decrease in $\Delta\Theta$ down to $\Delta\Theta=10^\circ$ at $E_{\text{tot}}=0.65\text{J}/\text{cm}^2$ were detected. The existence of significant contact angle hysteresis after laser processing indicates that the polymer surface is not homogeneous with respect to chemical properties. Surface domains with different wetting behaviour exist concurrently. Laser pulse length variations of 5 or 19 seconds seem to be equivalent in terms of surface properties. Receding contact angle and advancing contact angles show almost the same behaviour as a function of total exposure dose.

The difference between the laser and lamp assisted polymer modification as a function of E_{tot} can be explained by time dependent surface reaction processes. Short laser pulses offer a high number of photons within a very short time. Each photon can react with the polymer bonds and compared to UV lamp exposure which operates at constant intensity, an obviously significantly higher density of radicals will be formed. These radicals run through different kinds of competitive reactions such as recombination processes, formation of new bonds in the polymer texture or reactions with oxygen from ambient air. Due to time-dependent diffusion processes in the gas phase and in the oxide layer created,

laser generated radicals cannot be completely saturated by reactions with oxygen and therefore other recombinant processes become more important.

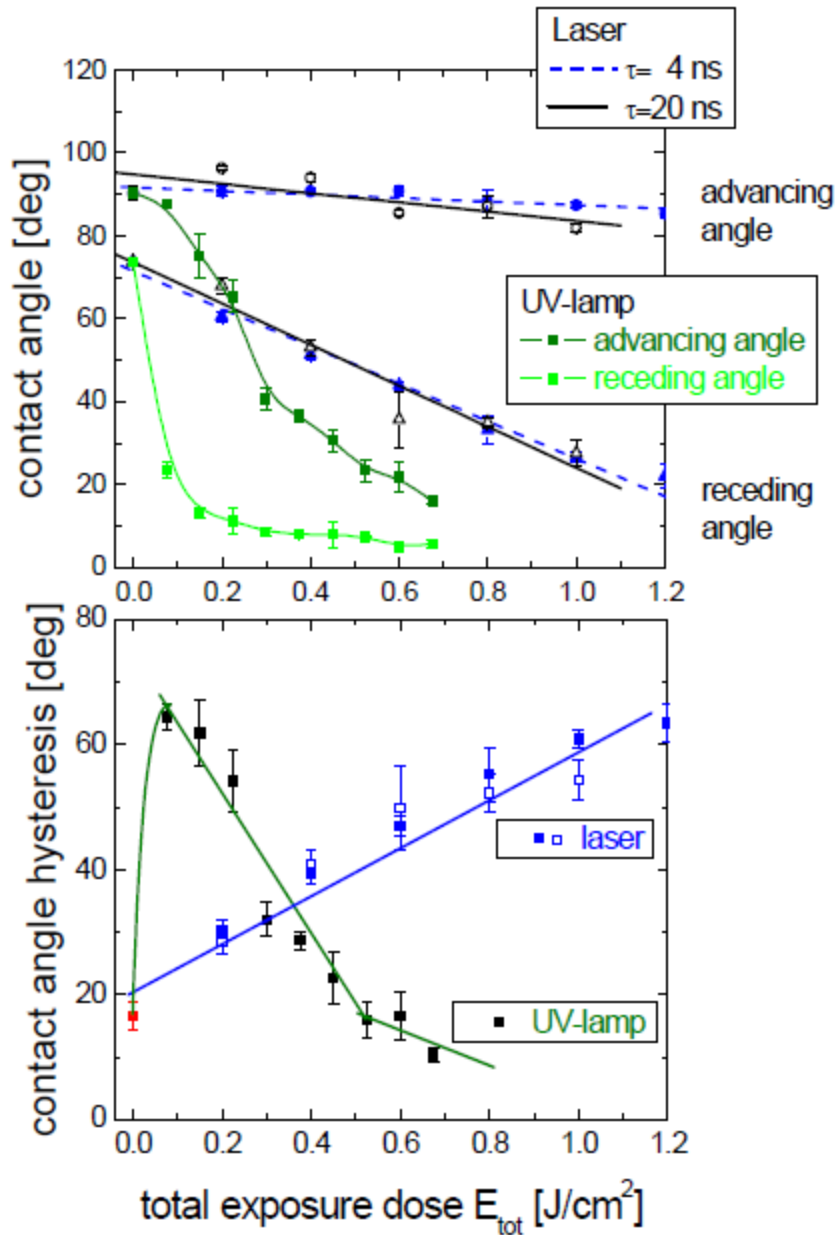


Figure 6-11: Contact angle measurements advancing and receding for norflex® polystyrene

The surface energy γ , of untreated and modified norflex® polystyrene was measured as a function of total exposure dose E_{tot} . Untreated PS has an almost completely non-polar surface with a dispersive component of $\gamma^d = 31.7 \text{ mN/m}$

and a polar component of $\gamma^p = 2.2 \text{ mN/m}$. Even after a laser exposure of 1 J/cm^2 (pulse length 19ns, 20 Hz, $\varepsilon = 4 \text{ mJ/cm}^2$) it is remarkable that the polar component remains small and nearly unchanged in comparison to the unmodified polymer surface. After laser modification with $E_{\text{tot}} = 2.5 \text{ J/cm}^2$ the polar component of surface energy slightly increases up to $\gamma^p = 8.6 \text{ mN/m}$ ($\gamma^d = 34.9 \text{ mN/m}$). In the case of the UV lamp treatment, the polar component of surface energy increases from $\gamma^p = 6.8 \text{ mN/m}$ ($E_{\text{tot}} = 0.5 \text{ J/cm}^2$, $\gamma^d = 32.8 \text{ mN/m}$) up to 49.0 mN/m ($E_{\text{tot}} = 1 \text{ J/cm}^2$, $\gamma^d = 12.2 \text{ mN/m}$) and becomes dominant. The laser process requires an exposure dose four times higher ($E_{\text{tot}} = 4 \text{ J/cm}^2$) to achieve a comparable surface energy composition ($\gamma^p = 43.7 \text{ mN/m}$, $\gamma^d = 5.0 \text{ mN/m}$) indicating that a significant amount of polar groups were generated at the PS surface.

Chemical analysis using XPS measurements show that for $\varepsilon = 4 \text{ mJ/cm}^2$ the amount of oxygen on PS surfaces increases logarithmically with laser pulse number and total exposure dose (Figure 6-12 left). After 150 laser pulses ($E_{\text{tot}} = 0.6 \text{ J/cm}^2$) and even after 300 laser pulses ($E_{\text{tot}} = 1.2 \text{ J/cm}^2$) no difference between the used laser pulse lengths could be observed. After 150 laser pulses the amount of oxygen at the surface was 12at% and after 300 pulses the content of oxygen was 17-18 at%. For both laser pulse lengths and for UV-lamp assisted processing the C1s (Figure 6-12, right) and O1s line shape of the modified polystyrene surface corresponds very well with the line shape of the chemical group $-\text{COOH}$.

UV-lamp modification also leads to a logarithmic increase in oxygen stoichiometry as a function of exposure time T and total exposure dose E_{tot} (Figure 6-12). After long-term exposure ($T = 90 \text{ minutes}$, $E_{\text{tot}} = 1.5 \text{ J/cm}^2$) oxygen content reaches a value of about 34 at%. After 4000 laser pulses ($E_{\text{tot}} = 16 \text{ J/cm}^2$) and with oxygen as processing gas a similar oxygen stoichiometry can be reached. This means that laser modification with 150 or 300 laser pulses leads to a polystyrene surface which is not fully oxidized, this

agrees very well with the results which were obtained by contact angle measurements (Figure 6-11).

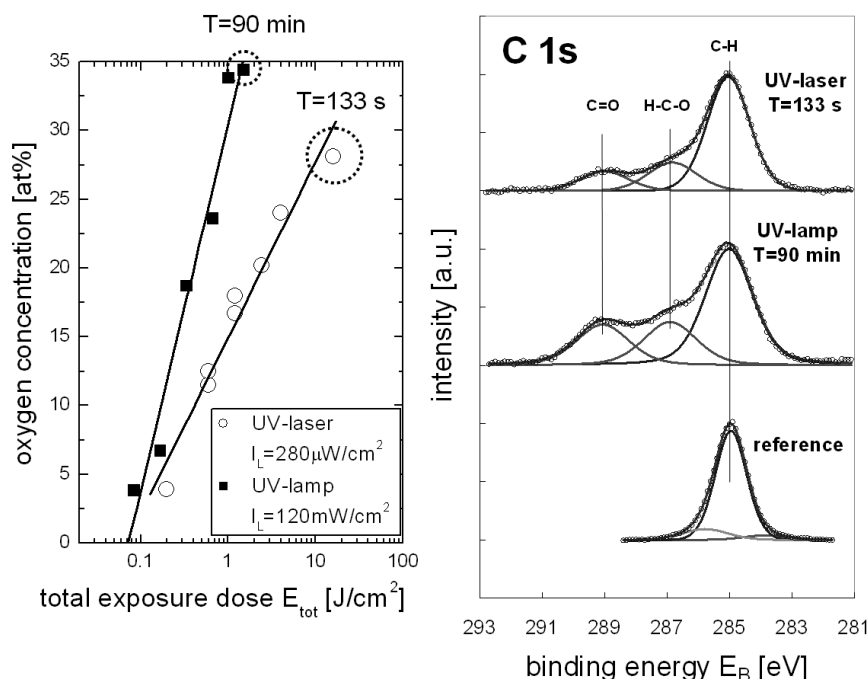


Figure 6-12: oxygen concentration compared to total exposure dose (E_{tot}) for laser and lamp surface modification

The logarithmic increase in oxide layer thickness (Figure 6-12) is typical for physisorption and subsequent chemisorption processes at the surface. The reaction zone is limited to the nanometer-scale and bulk diffusion of oxygen can be neglected.

Now that the surface chemistry has been defined, the next step is to define the parameters required for cell adhesion, firstly by laser modification followed by lamp modification.

6.4.1 Defining laser modification parameters using cells

L929 cells (murine fibroblast) were chosen for first cell adhesion tests as they are a robust cell type and generally show consistently good adhesion to attractive surfaces. Laser surface modifications were performed directly on the bottom interior surface of a bacterial petridish (polystyrene). For laser

modification, a quartz chrome mask was placed into the laser optics beam path with a 4:1 mask to end feature magnification reduction (the feature is 4x larger on the mask than the final structure obtained) and focused onto the petri dish. Each petri dish was exposed at one fluence from 1mJ/cm² up to 8 mJ/cm² but with a pulse numbers varied from 50 to 1200 in steps as shown in Figure 6-13 and Figure 6-14. After modification, 0.5x10⁶ cells in 4mL of medium were inoculated onto the surface and cultured for 48 hours, then dried and stained (procedure in Appendix A) and inspected under the microscope. Images of cells were analyzed optically and cell adhesion of 50% of an exposed area is considered adherent (Figure 6-13, Figure 6-14).

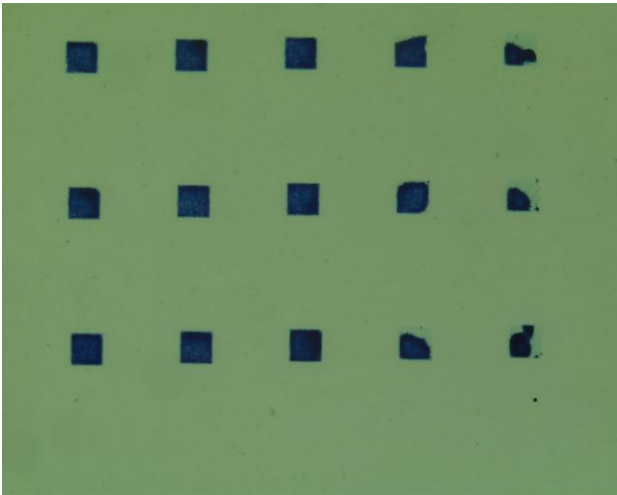


Figure 6-13: Stained cells on exposed petri dish material (polystyrene)

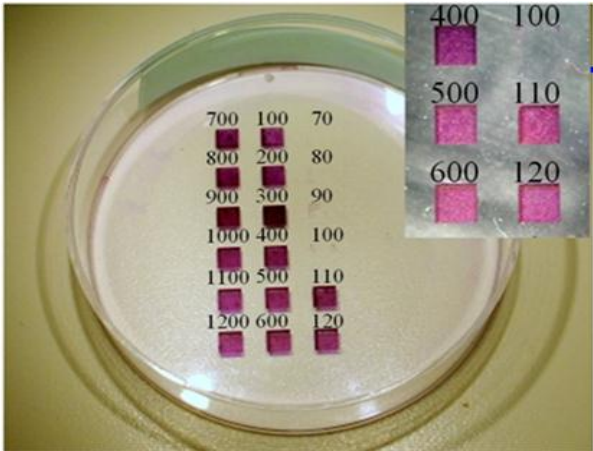


Figure 6-14: Laser modified petridish, 5mJ/cm² energy, number of pulses and cell adhesion

Laser fluencies of 9-10 mJ/cm² are a threshold value where polymer ablation begins to occur, functional polar groups required for cell adhesion are removed and material debris is spread over the polymer surface making defined patterned areas no longer possible, for this reason no tests were performed above this value.

The threshold of laser pulse number varies with laser fluence as shown in Figure 6-15. For a laser fluence of 6 mJ/cm², 250 laser pulses are necessary for subsequent cell adhesion while for laser fluencies of 4 mJ/cm² 150 pulses are required while the range of 110 to 1100 pulses show cell adhesion. Cell adhesion is observed within a range of 100 to 1100 laser pulses. It seems that an increasing irradiation dose represented by an increasing laser pulse number has no negative effect on the efficiency of cell adhesion if laser fluencies smaller than 10 mJ/cm² are selected. Modification of PS with ArF excimer radiation at low laser fluencies enables high resolution control of cell adhesion. The error bars are plus or minus 100 pulses due to laser calibration; it would be possible to define the error bars more tightly after a tighter control calibration.

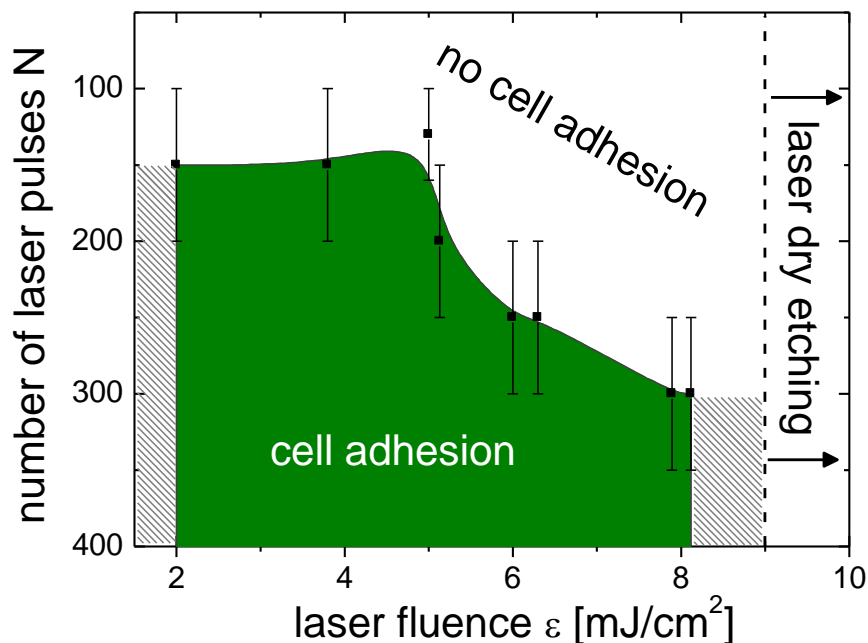


Figure 6-15: Cell adhesion as a function of laser pulse number and laser fluence

6.4.2 Defining lamp modification parameters using cells

Previous work with a UV lamp showed that a 10-12cm distance between the UV lamp (185nm) and the polymer surface and an exposure time above 30 minutes produces cell adhesion of L929 cells (Welle and Gottwald, 2002). Both norflex© and Goodfellow polystyrene foils were exposed for 35 minutes and L929 cells cultured for 48 hours, as detailed in Appendix A.

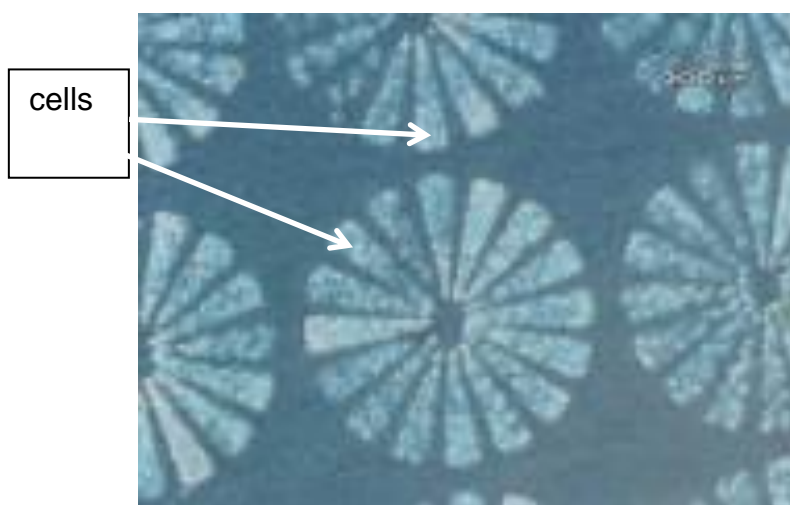


Figure 6-16: L929 cells on norflex© polystyrene , 48 hours after inoculation, diameter of circle 1mm



Figure 6-17: L929 cells on Goodfellow polystyrene foils, 48 hours after cell inoculation (magnification as in figure above)

UV lamp modification on polystyrene petri dishes and polystyrene foil show that cell adhesion of L929 cells also begins at 30-35 minutes (Figure 6-18); however for best cell coverage an exposure time of 60 minutes provided more consistent results. This equates to an exposure dose of approximately 1400mJ/cm^2 at 185nm . Figure 6-16 and Figure 6-17 above were exposed for 60 minutes. The difference in behaviour of the foils is significant. Goodfellow foils did not show any kind of cell response to patterning which may be due to irregularities in surface chemistry perhaps due to the fluorescing particles seen in earlier microscopy work or outgassing of additives over time in the media. To understand the mechanism of this requires further study, but for the purposes of this work Goodfellow polystyrene was no longer pursued as a possible material.

XPS results of a UV lamp modification (lamp intensity $280\mu\text{W/cm}^2$) where energy dose applied is varied in terms of time and cell modification has already been discussed but is summarized visually in Figure 6-18 compared to cell adhesion. Cell adhesion begins at 35 minutes (this equates to a dose of 0.5mJ/cm^2) at an oxygen content of approx. 23at.%. Cell adhesion continues and a maximum oxygen content is achieved by 90 minutes (33-34at.%) ($E_{\text{max}}=1.5\text{J/cm}^2$). Adhesion of L929 cells remained stable up to the maximum applied energy dose E_{max} . The actual XPS data is shown in Appendix A (Table 1)

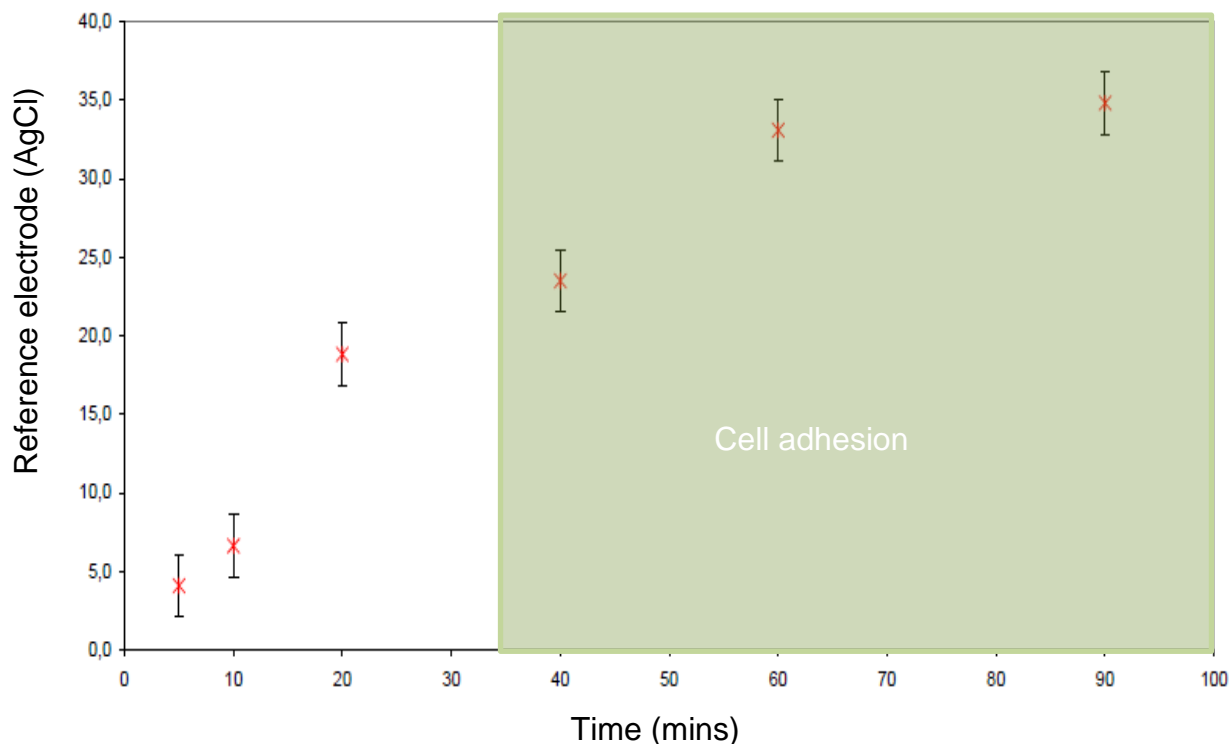


Figure 6-18: Cell adhesion for UV lamp exposure in terms of oxygen content (%) and exposure time

The XPS data summary in Figure 6-19 shows the photolytic breaking of C-H bonds as the PS material is exposed under the UV lamp at 185 nm. As expected in an ambient air environment, O_2 and H_2O interact with the broken bonds and the atomic percentage of C-O-H and C=O bonds increases with increasing energy to a maximum of 14.5 at% for C-O-H bonds and 13.4 at% for C=O bonds. The surface chemistry begins to plateau at 60 minutes of exposure time where the ratio of C-O to C=O bonds is almost 1:1.

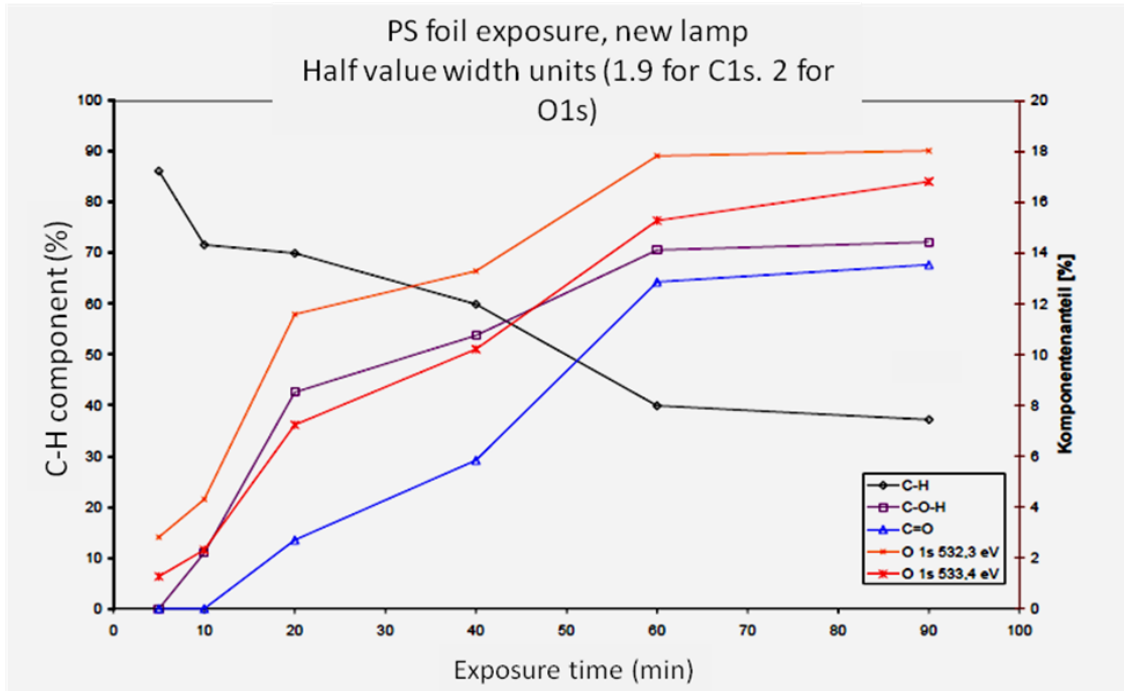


Figure 6-19: XPS data summary, C-H binding over UV exposure time norflex© PS foil

Interestingly the XPS data correlates well with the findings of cell adhesion experiments and contact angle data. Cell culture results showed better cell coverage to modified areas at 60 minute exposure times compared to 35 minutes, and contact angle data also shows less hysteresis at this same dose ($\Delta\Theta = 10^\circ$). These results indicate a much more homogeneous surface chemistry at 60 minutes compared to 35 -40 minutes.

The results of this work were then applied to the selective cell adhesion on the design layout for the patch clamping system.

6.5 Patterned / selective cell culture

Once the best cell adhesion parameters were determined, cells were cultured in patterned arrays and then eventually over the measurement holes. In any standard cell culture trial, reference cells are cultured alongside those of interest. In this case, 2 petri dishes coated with collagen were inoculated with the same cells as those being evaluated. Figure 6-20 shows a reference collagen coated petri dish of PC-12 GFP with an added 1% NGF to support cell

differentiation. The benchmark for viable cells is an approximately 85% cell differentiation on a micrograph taken a 200x magnification.

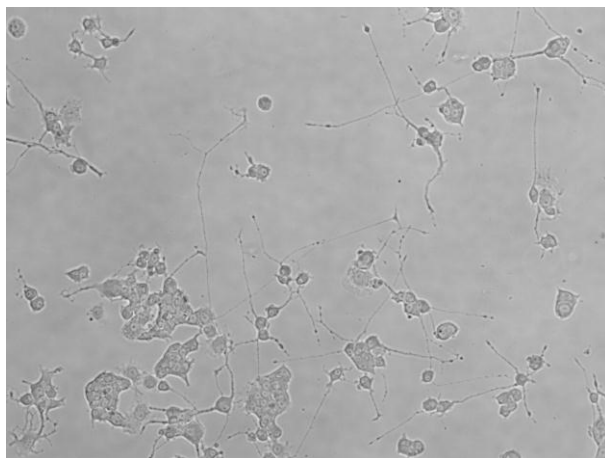


Figure 6-20 Collagen control petridish, culture day 7, showing greater than 85% neurite growth of PC-12 GFP cells (200x)

In addition to collagen coated reference petri dishes, UV mask patterned petri dishes were used following the same preparation protocol as the cells inoculated onto foils to give a direct reference of surface modification quality between foils and polystyrene petridish. The PC12 GFP cells in Figure 6-21 are growing in a clear pattern on the petridish indicating good modification and cell health after 9 days.

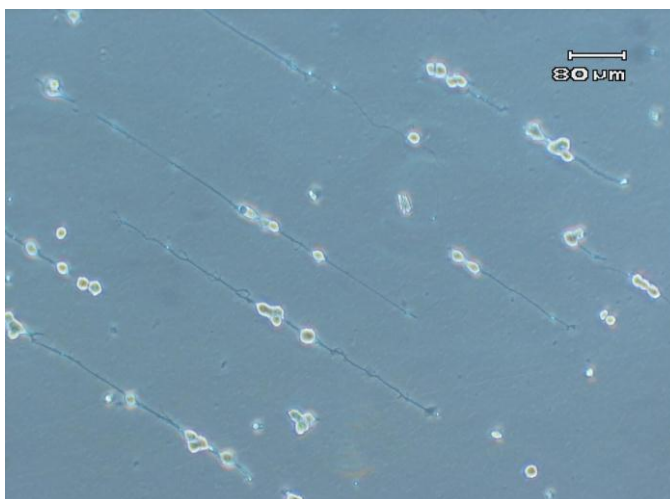


Figure 6-21 PC12 GFP cells, cultured on a lamp modified petridish, 9 days line/space pattern 10μm/100μm

L929 cells were cultured on laser and lamp modified bacterial petri dishes and Norflex© foils. Laser modifications were made at 4mJ/cm² and 1000 pulses and lamp modifications at 0.6J/cm² (an exposure time of one hour). Cells were cultured for 5 days and then viewed in an ESEM (Environmental Scanning Electron Microscope). Figure 6-22 shows well defined areas of cell adhesion and no cell adhesion

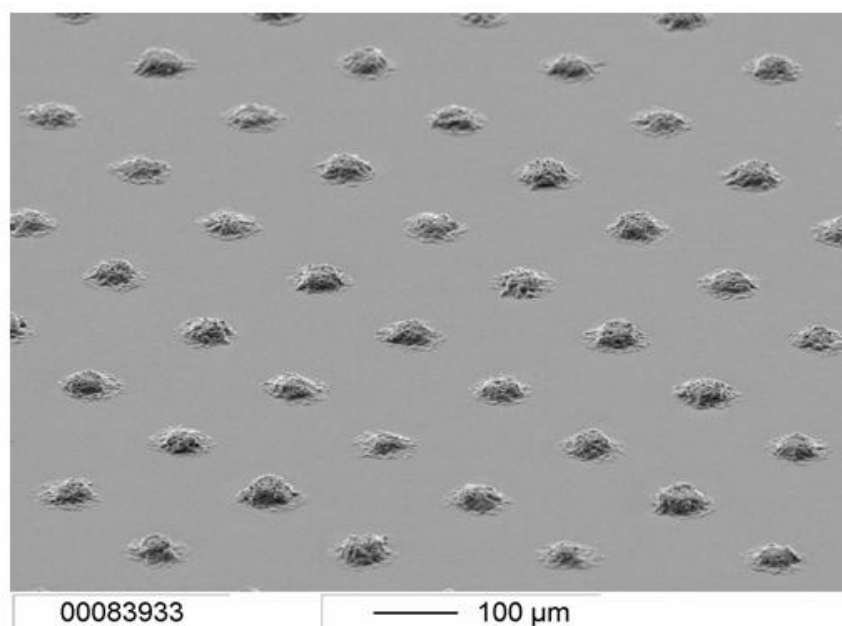


Figure 6-22 L929 cells cultured 5 days onto UV patterned norflex© foil

PC-12GFP cells are suspension cells that require some “incentive” to sit on a surface. For this reason a preferential protein adsorption step was made (see Appendix 1) to induce the cells to sit on the foil surface. The preferential protein adsorption procedure is based on the Vroman effect – proteins with different motilities are adsorbed on to surfaces preferentially, high motility proteins arrive at binding sites first, to be later replaced by lower motility proteins which have a higher affinity for the surface. Albumin is a high motility protein deposited first as a cell repellent protein – it does not present any cell attractive peptides, and is later displaced by laminin, a cell attractive protein, which has a higher affinity for carboxyl groups. PC-12 cells were inoculated into the petridish after the protein adsorption treatment and cultured up to 7 days. The results are seen in Figure 6-23.

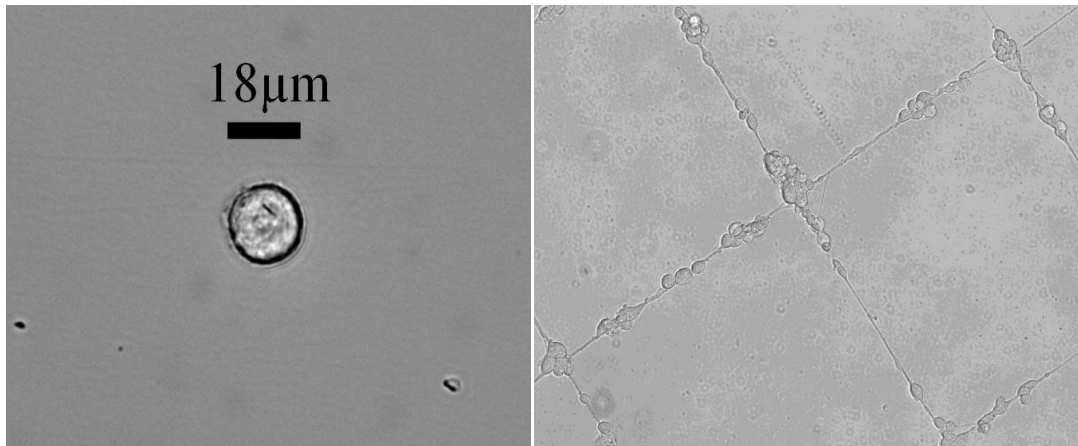


Figure 6-23 PC-12 GFP cells after 7 days of culture, left a modified circle with no modified tracks sits isolated, right, modification with tracks shows the development of a neural network 10x10, spacing of tracks is 435μm

PC-12 GFP cell culture includes a nerve growth factor (NGF) to differentiate this cell line into a neuronal type cell. In Figure 6-23 left, a 20μm modified circle was produced with no guiding tracks for neurite growth. The cell adhered well to the surface, cultured for 7 days but neurite growth was completely restricted by the modification and albumin repellency. On the right, a 25μm modified circle was made at the cross-section of lines (each of which are 435μm long and 8μm wide) shows very well-defined neurite growth between cells.

To visualize the surface modification albumin which was ex-situ labelled with a fluorescing ester according to manufacturer's protocols (see Appendix A) to produce a red contrast seen in Figure 6-24 left. As albumin loosely adheres to surface modified areas, it is displaced by laminin which has a greater affinity for the carboxyl groups. Laminin has been stained using an immunofluorescence protocol, also detailed in Appendix A. The result is a green fluorescing laminin adhering to modified surface areas; see Figure 6-24 right, surrounded by the red labelled albumin. The pattern consists of tracks which are 8μm wide and form a square that is 435μmx435μm in a 10x10 array. A modified circle of 25μm diameter is placed at each intersection of lines, and it is here that the holes would be drilled for cell attachment. The laser can direct write a section of 5 x 5 line segments (corresponding to an approx. 2x2mm area), so a step and repeat process with alignment is required. A slight misalignment in x and y can be seen

in Figure 6-24 right, however this is not detrimental to the function of the system as the lines connect with the circle.

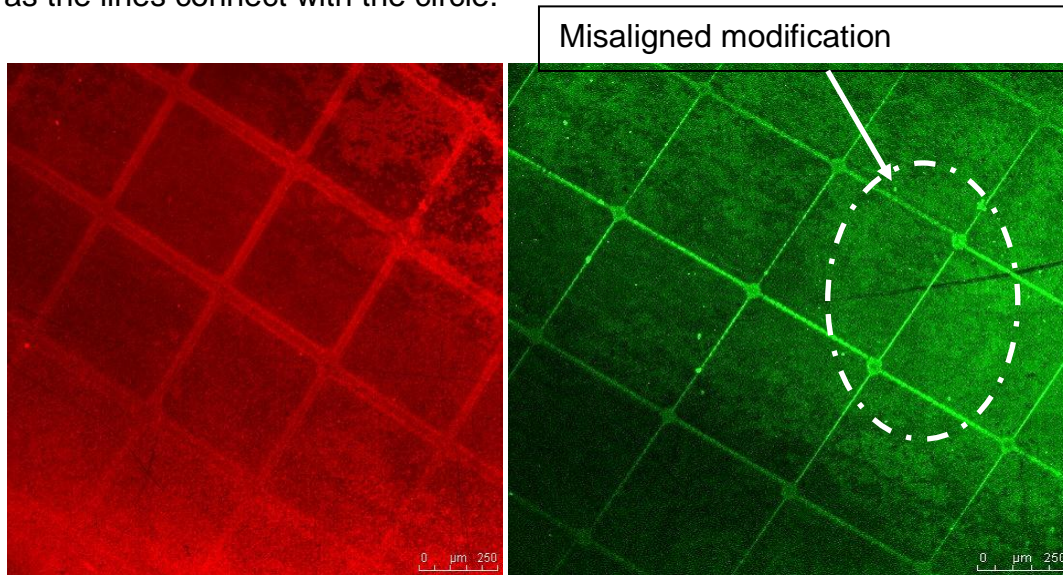


Figure 6-24 Fluorescence micrographs: left, labelled albumin, right, labelled laminin on laser patterned norflex foils. High brightness indicates a high concentration of adherent proteins (squares $435 \times 435 \mu\text{m}^2$)

In summary, it is possible to produce surface modifications that are cell attractive, but also to increase the effective range of cell adhesion and repellency by using a preferential protein adsorption procedure. The next section deals with the production of measurement holes.

Cell culture on the modified surfaces with holes is covered in the next section.

6.6 Integration of cell culture on modified surfaces over holes

In the development of the system, individually addressed components were combined, holes, aligned surface modification and cell culture. Before work began it was unknown if and how well cells would culture over holes and also if there was an electrical leak path due to the adhesion of cells on the surface. Figure 6-25 shows drilled holes and a misaligned surface modification (+x direction) showing cell growth (PC-12-GFP) confined to the modified areas next to the holes with cell somas mostly confined to the $25\mu\text{m}$ diameter modification and the modified tracks between them allow growth for neurites. On the left of

the image, the tracks are wider (due to a mask error) allowing both cell somas and neurites to grow along the tracks.

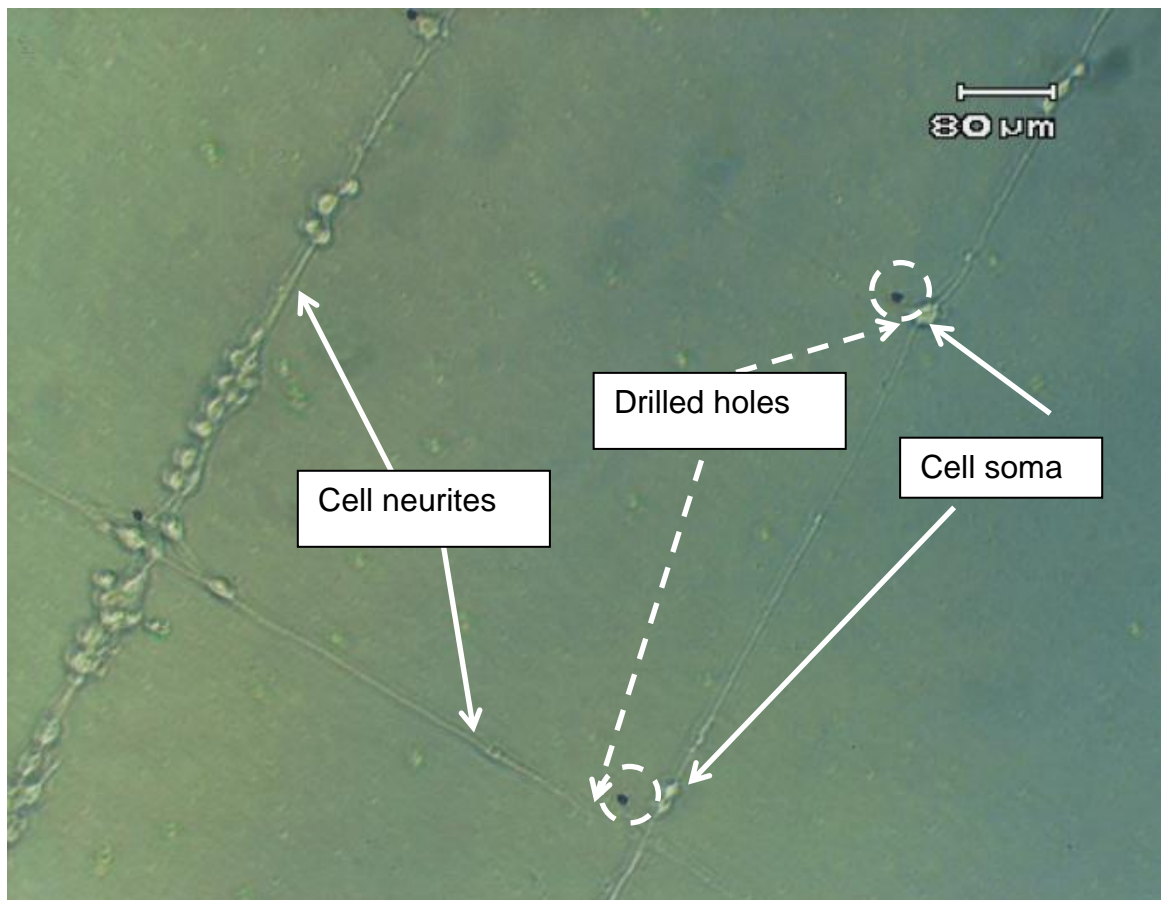


Figure 6-25: PC12 GFP misaligned surface modification to holes, and cell culture

Figure 6-26 shows a properly aligned surface modification with cells grown over the holes (after 7 days culture). The holes are completely covered by the cells. It was possible over more than 30 trials to have a minimum of 85% coverage on a 10x10 array of holes, demonstrating a good degree of process robustness.

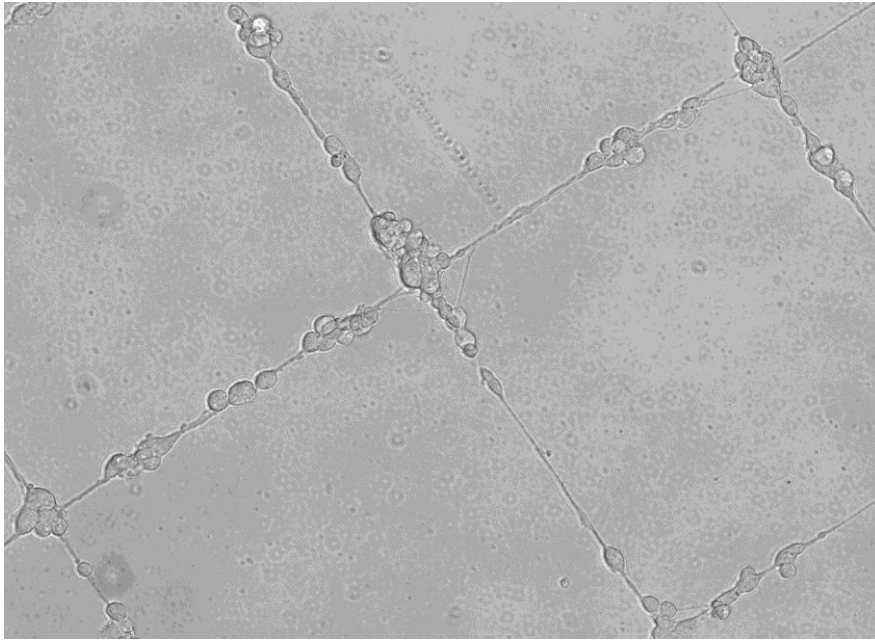


Figure 6-26: PC12-GFP cells cultured over holes

The next section evaluates electrode fabrication and chloration

6.7 Electrode fabrication

Chlorated silver electrodes are required for each cell hole for individually addressable signalling. For the single part design silver wire with chlorated tips could be implemented, however the methods to produce a single part design were unsuccessful. For a two part design, silver planar electrodes could be deposited by evaporation onto the underside (larger hole diameter) of a measurement hole in a foil. A section of a principle design shows electrodes in green in Figure 6-27 which would be placed onto the bottom side of a foil, and bonded to the microfluidic chambers below, which are shown in grey.

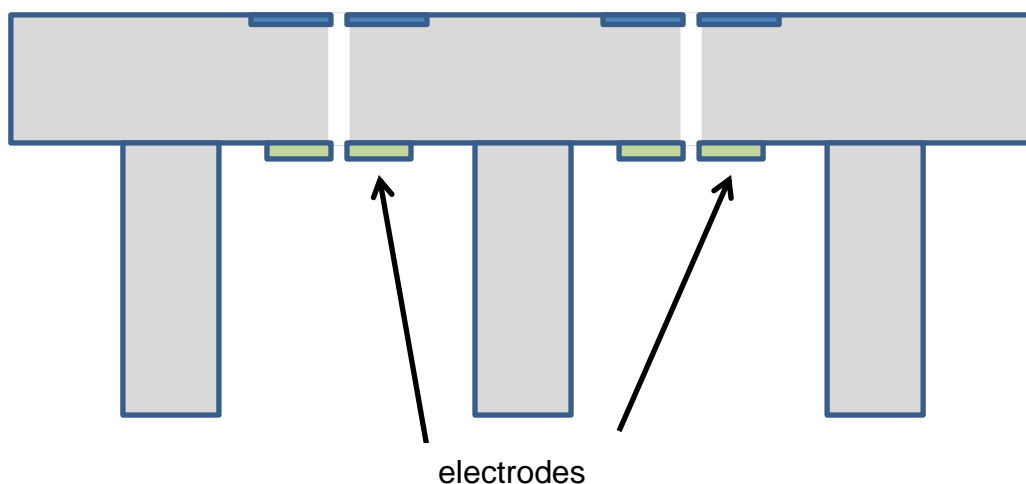


Figure 6-27: Electrodes (green) on the lower side of a microfluidic chamber.

Electrodes were deposited by evaporation for better thickness and temperature control. The deposition rate and thickness were monitored during the deposition by means of a quartz sensor positioned 10 cm from the source and previously calibrated (tooling factor= real thickness/thickness sensed). Silver was evaporated by a resistance-heated thermal boat and the processing pressure was between 10^{-5} and 5×10^{-5} torr. The base pressure was 4×10^{-6} torr. For silver (98% + 2% Cu) deposition was carried out at 25A at a deposition rate of 50nm/min and thicknesses were varied between 100 – 400nm. The deposition was carried out as a full coating of a piece of polymer foil, or through a stainless steel test electrode mask (Figure 6-28) which is taped onto the foil.

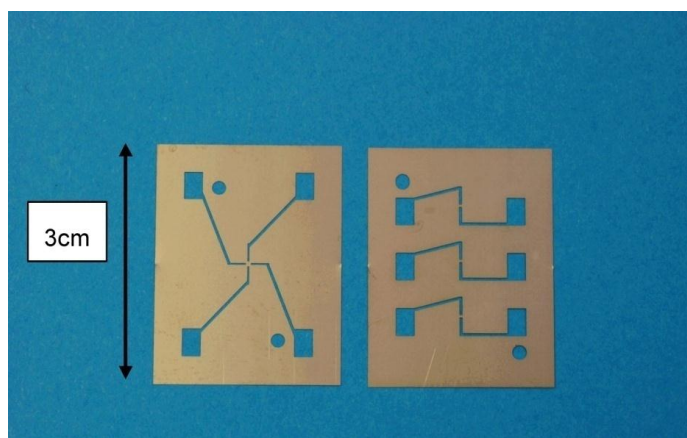


Figure 6-28: Steel VD masks with a test electrode design

Temperature was measured in all depositions and a maximum permissible temperature for the polymer foil was 90°C for polystyrene. Temperature was determined by temperature sensitive labels placed on a glass slide next to the sample. Labels give the maximum temperature reached during deposition. Two temperature label ranges were used, 37 to 65°C and 71 to 110°C, each with temperature increments of 5-6°C.

Adhesion of the deposited coating was determined using DIN-EN Standard 58196-6, K2 Scotch tape test after 2, 4 16 hours, 10 days and 30 days in cell culture medium with water as a reference (to compare results in the event that cell proteins on the surface interfere with measurements). The silver layer, deposited at thicknesses 100nm, 200nm and 400 nm onto a 20x20mm piece of polystyrene foil, was then chlorated by dipping in a diluted bleach solution (4.6 wt% ammonium chloride) or electrolytically in a 30mM KCl solution. In the electrolytic cell, the evaporated electrode material was connected as the cathode of the reaction, and the counter electrode (silver wire) which sits in the KCl solution is the anode. Voltage (IET VI700 voltage generator) was increased slowly until bubbles were seen on the anode (H_2O_2). Measurements were made with samples in a cell culture medium with water as a reference, at 37°C. Immersions of samples in pure bleach for 5 minutes resulted in the total dissolution of the silver for thicknesses from 100-400nm. Immersion of another group of samples into the solution with the same concentration resulted in a partial dissolution of the silver as shown in Figure 6-29.



Figure 6-29: Chloration of silver after two minutes in a diluted bleach solution.

At 100nm thickness and electro-chloration, however, the thickness is insufficient and silver is dissolved into the solution leaving gaps in the electrode as seen in Figure 6-30.

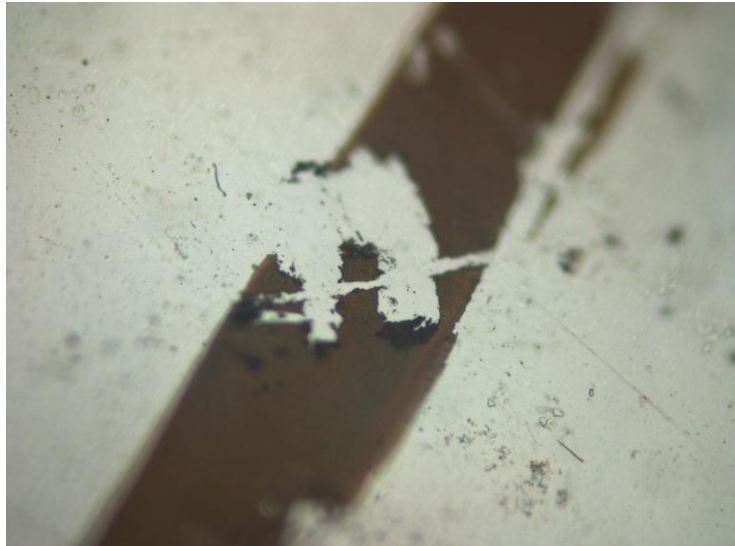


Figure 6-30 100nm deposited silver electrode after chloration

At 400nm the thickness is sufficient that the silver can be chlorated as can be seen in Figure 6-31. The silver has turned black through chloration indicating a reaction has taken place and that a silver/silver chloride electrode has been produced.

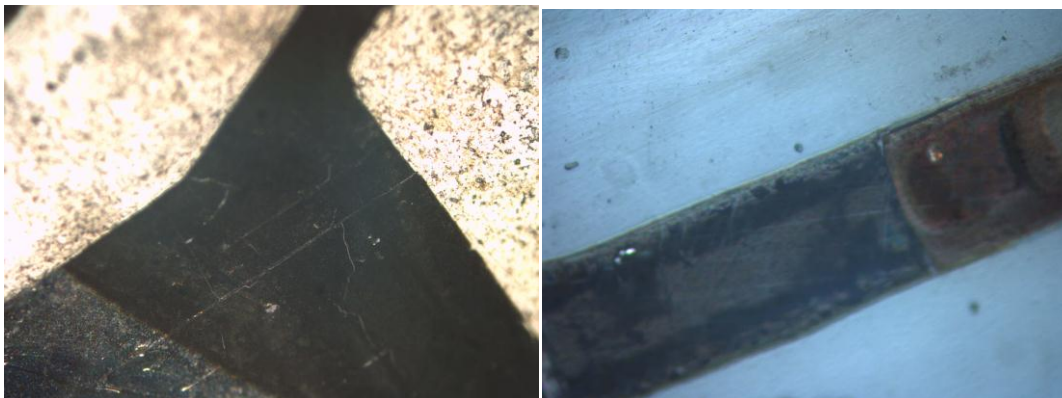


Figure 6-31 400nm silver after electrolytic chloration, left, a contact pad, right an electrode path

The 400nm thick chlorated electrodes were placed into an extracellular solution for 10 days and measured once per day, the average resistance per mm^2 was

8.10 Ohms at the beginning of measurement, and was 10 Ohms after 10 days – this may be due to the deposition of some salts or proteins, but is considered a negligible increase, electrodes can be considered stable.

6.8 Resistance Measurement

The culture of cells over holes, specifically PC12-GFP networks did not result in 100% coverage, but an average coverage of 85% was achieved in most cases. As the uncovered holes would significantly reduce any resistance values, a 10x10 array of surface modification was made but only one central hole drilled in the foil as seen in Figure 6-32.

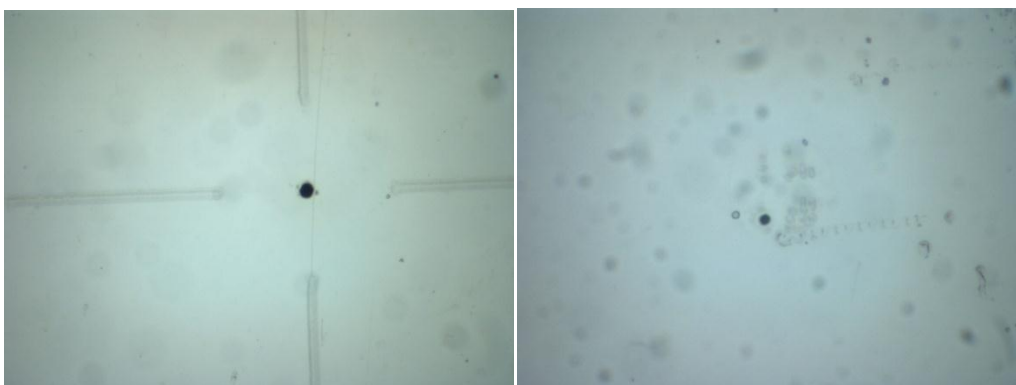


Figure 6-32 Single hole and alignment marks drilled in 50 μ m thick polystyrene, left laser entrance side (9 μ m) and right, laser exit side (4 μ m)

The holes drilled have a laser entrance diameter of 9 μ m and a laser exit diameter of 4-5 μ m. Modifications are made to the smaller diameter hole side. Two measurement rigs were developed in this work, the first design in PDMS (Figure 6-33, left) cast into a petri dish with two plastic tubes for measurement media delivery below the foil and placement for the reference electrode; and a top PMMA section with a hole to serve as a bath for measurement media above the foil. The rig is seen in Figure 6-33, left from the top and on the right with a foil and measurement media (cell culture media) with the glass pipette and measurement electrode on top and the reference electrode fed in from below on the right.

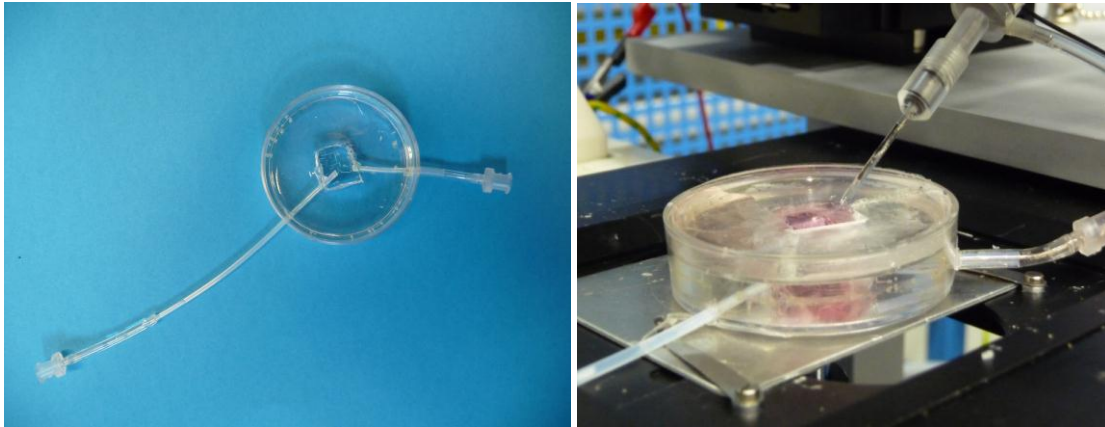


Figure 6-33: on left, PDMS measurement rig top view, right, rig with foil during measurement

Initial measurements to establish the baseline values of system setup resistances were carried out on a patch clamping unit (HEKA EPC 10 amplifier, Axiovent 200M microscope, Sutter MP 285 micromanipulator, Patchmaster software, from HEKA, Lambrecht, Germany). Voltages were applied in steps of 20mV in a range from -200mV to +200mV and the current measured. Cell culture medium (conductivity measured at 57 Ω .cm) and a baseline reading made after each measurement to check for drift in the baseline 'system' resistance which was measured at 0.14M Ω ms @ 25°C. AgCl electrodes were used for measurement filled with 3M KCl. The cell medium is a salty water solution and highly conductive, the system resistance of 0.14M Ω is a measure of the rig resistance filled with cell medium without foil and can be considered the background resistance present in all measurements.

By pre-wetting the holes in water in an ultrasonic bath (Branson ultrasonic bath 3510) for 10 minutes more consistent measurements were achieved as air bubbles and any trapped debris from drilling was removed. The foils were kept wet until measurement. Foils with a range of diameters from 2 – 10 μ were measured in the rig at a range of voltages from -200mV to +200mV at 20mV increments and their VI curves acquired.

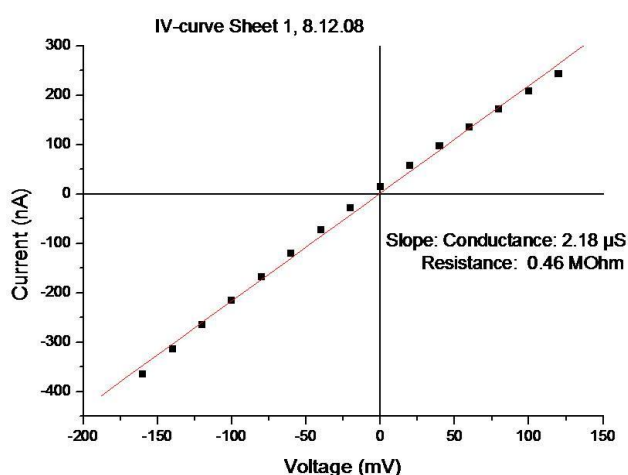


Figure 6-34: IV curve results for PS foil drilled with one hole (dia. top = 4-5 μ m, bot. 12 μ m)

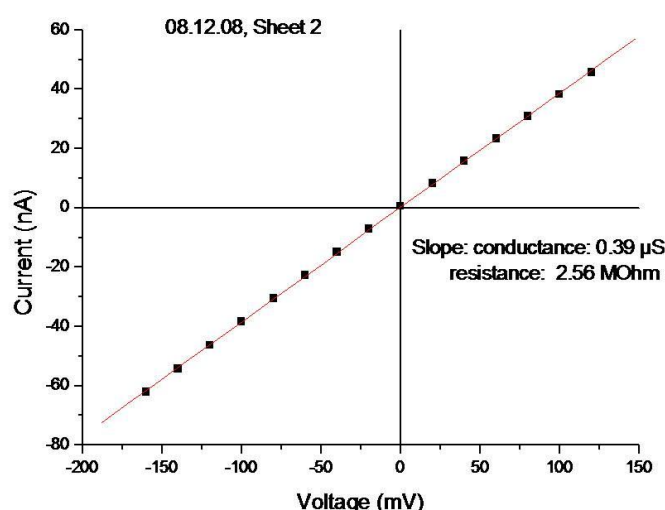


Figure 6-35: IV curve results for PS foil drilled with one hole (dia. top 2 μ m, bot. 8-9 μ m hole)

The results shown in Figure 6-34 and Figure 6-35 show resistances well below the maximum stated 10MOhm resistance for feasible patch clamping measurements, they also show a stable resistance response to voltage shown by the linear gradient which shows holes are filled with media and clear, i.e. not

filled with debris. The holes are stable enough for measurement. Figure 6-36 is a summary of measurements over a range of hole diameters from 2 to 10 μm . As expected, resistance increases with smaller hole diameters and decreases with larger holes. The measured resistance values are lower than the calculated values. The calculated values are based on a solution resistivity of 55 Ohms.cm which is a conductivity of approximately 2S/m, and very close to the actual solution. According to calculations a conical pore of 50 μm thickness with a 1.8 exit diameter should have a resistivity of 4.7M Ω which is much higher than the actual measured 2 μm exit diameter resistivity of 2.36M Ω (Figure 6-36) but this is an acceptable first approximation given the 2 μm difference in exit hole diameter, surface effects and given that it was concluded in Section 3.3 that sidewall angle has a significant impact on the resistivity of the pore. As can be seen in Figure 6-32, the laser entrance diameter is actually 9 μm and not 12 μm as calculated, giving a linear sidewall angle of 3.43°, and also there is a significant taper on the hole which reduces the accuracy of the calculation. A higher exit hole diameter is generally created by using a higher laser pulse energy, and correspondingly the sidewall angle gradient becomes more constant which brings the measured values closer to the calculated values, as seen for the 4 μm exit holes, where the calculated value of 675M Ω is very close to the measured value of 450M Ω .

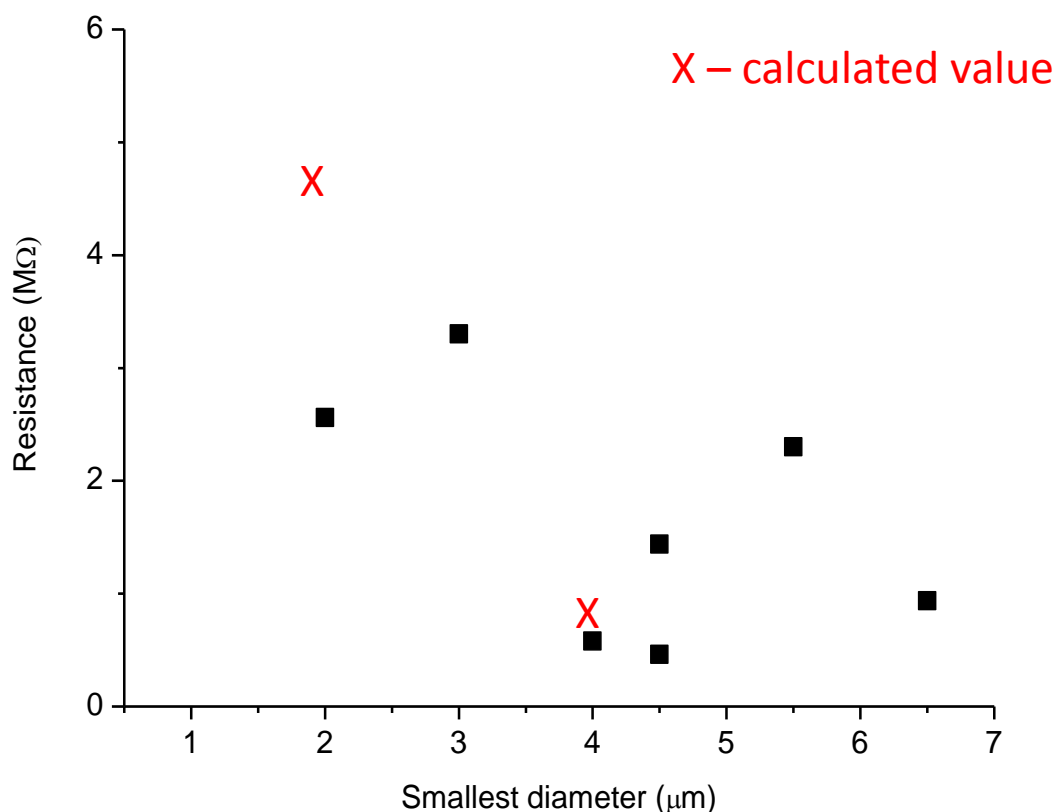


Figure 6-36: Patch clamp resistance measurements over hole diameter in Norflex© polystyrene – red crosses denote calculated values from Section 3.3

The next step in the work was to measure cells over holes. The patch clamping system at the Institute for Pulsed Power and Microwave Technology (IHM, www.fzk.de/ihm) has been setup for plant cells which, unlike mammalian cells, do not require temperatures of 37°C with a 5% CO_2 supplement. PC12-GFP cells are very sensitive to ambient conditions and are by nature a suspension type cell. During measurement this cell type did not remain viable long enough to establish good seal measurements likely due to temperature sensitivity. Future work using this cell type should include the provision of a heater and CO_2 supply to the cell measurement area (approx. cost 10k Euros). The more robust cell type HEP G2 was then cultured over holes for initial measurement and a new rig with increased stiffness and the option of clamping and slightly

pulling suction was fabricated as seen in Figure 6-37. In order to pull suction tightly, the reference electrode is placed into a rubber stopper for sealing.

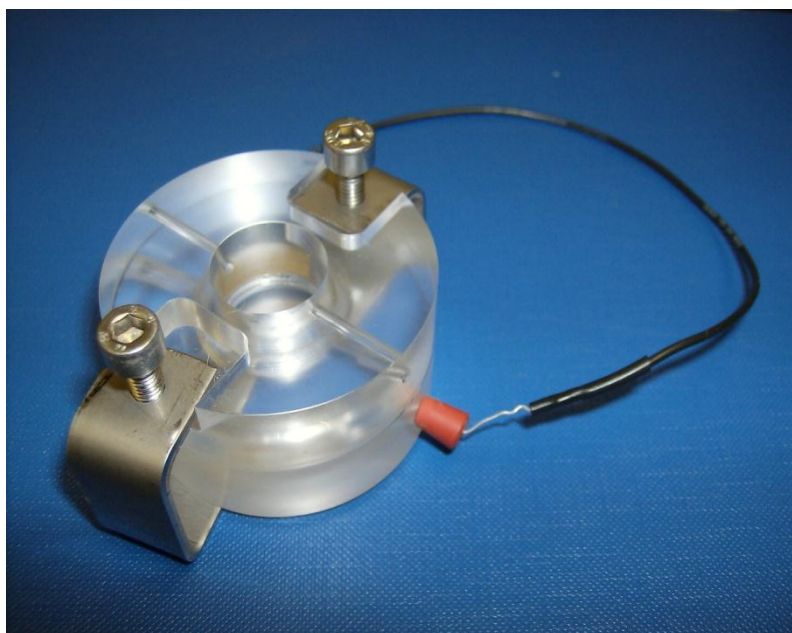


Figure 6-37: PMMA measurement rig (rig version 2) with measurement electrode inserted into a rubber stopper and clamps to ensure no leak around the foil

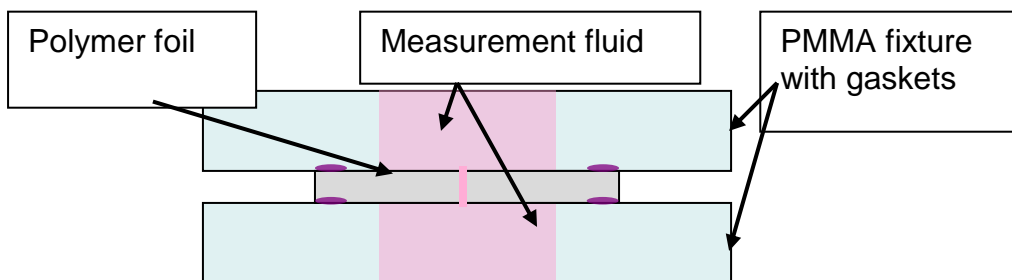


Figure 6-38: Cross-sectional schematic view of the measurement rig setup

Figure 6-38 is a cross-sectional view of the measurement rig. The rig is a two piece design, the bottom and top sections are PMMA, the foil is placed in the middle (lilac), suspended between wells which are filled with measurement fluid. The reference electrode is placed into the bottom well through a rubber stopper to enable the application of suction to the bottom area for improved seal resistance. The measurement electrode can be placed into the well area above the cell. In order to pull suction, the exit tube opposite the electrode in the

bottom well, was fitted with a 3-way valve, with one end attached to a simple syringe for pulling suction, the other end of the valve is open to atmosphere for bleeding air bubbles from the system during filling.

For measurement, voltages were applied as previously (steps of 20mV in a range from -200mV to +200mV) and the current measured. Cell culture medium was used as a conducting medium, and a baseline reading made after each measurement to check for drift in the baseline 'system' resistance. AgCl electrodes were used for measurement filled with 3M KCl.

HEP G2 cells were cultured for 5 days over a single hole drilled centrally in a surface modified array of 10x10. The average resistance of foils drilled from the same lot (laser entrance diameter 9 μ m and exit diameter 4-5 μ m) was measured at an average of 640 kOhms +/- 20 kOhms. It was possible to measure 3 cells over holes at resistances of 8, 12 and 16 MOhms, indicating that there is an increase in resistance with the cell sitting over the hole, however a significant leak path remains which should be addressed in future work. Using the syringe apparatus, which is very crude, it was possible to apply suction and measure a resistance of 84, 86 and 112MOhms. These measurements show that the approach is principally viable as the Molecular Devices systems begins to measure cell activity at a measured resistance of 100MOhms.

The next section is the conclusions and the outlook from this work.

7 Conclusions and Outlook

To summarize the key accomplishments of this work, a polymer patch clamping concept and design was produced with a single part and two part design.

A range of materials were selected and tested for biocompatibility, suitability for laser drilling and surface modification by laser and lamp. A polystyrene foil was pursued as the most promising candidate, although other materials and types of polystyrene could be revisited in future work.

In terms of the design approach, a one-part design of hot embossed frames were produced which required milling of the residual layer to a maximum of 100µm for laser drilling. Due to thickness variations and roughness in the residual layer this method was unsuitable for polystyrene and a two-part design was pursued, with the integration of a polystyrene foil using solvent bonding was investigated. Solvent bonding is in principle a viable approach, however the solvent bonding system used is limited to the use of acetone, which is not suitable for polystyrene. Other solvent systems with similar vapour pressures which are less aggressive to polystyrene can be considered in future work.

Holes from 1-10µm in diameter can be drilled into 50µm thick polystyrene foils successfully using a 193nm excimer laser. The holes could be filled easily with salt solutions needed for cell nutrition and measurement.

A surface modification technique around the exit side of the drilled holes could be used for cell guidance. This simple modification technique enables the culture of cells in patterns above measurement holes and expands the range of cell types and numbers of interacting cells (10 x 10 array of cells) that can be used in patch clamping. The modifications, produced by both UV lamp and UV laser, were evaluated and characterized by contact angle and XPS measurement and by cell culture work for optimum cell placement.

Cells could be cultured up to 10 days over the holes with an average coverage of 85% (over 100 holes), and resistances of holes were measured at 8, 12 and 16MΩ without suction. With the addition of primitive suction, this value could be increased to over 100MΩ which is sufficient to be able to measure. Cell recordings could unfortunately not be made due to non-optimal measuring environment (room temperature 18 degrees and no addition of carbon dioxide), and cell lines which were not particularly suited for large expression signals. Addition of a heating system and a CO₂ addition or alternatively the use of more stable cell lines could lead to better measurements. Additional shielding within the Faraday cage could also lower noise seen during measurements.

A silver electrode system could be deposited by evaporation that is suitable for chloration and enables the signal acquisition over an x-y field, and a supporting microfluidics system was designed to allow the exchange of fluids necessary for cell culture and measurement. Bonding techniques were also evaluated and a promising candidate indicated (direct injection moulding of microfluidic structures to foil)

The development of this patch clamping system has overcome many risks including the most significant unknown of whether a cell would actually sit above a hole and culture in a viable way to enable measurement. The encouraging response of significant increase in resistance (from 650 kΩ without cell to 12 MΩ with cell) and with the addition of suction increasing resistance to 86MΩ validates the approach used in this work. However, with this in mind, there are still significant challenges and risks.

Measured resistance must be increased to above 100 MΩ to enable first actual ion channel recordings. This requires an improved suction arrangement underneath the cell.

It must be possible to bond or structure microfluidics such that no leak path exists between chambers below the cells which would cause signal loss or

cross-talk. In the currently proposed design a 10x10 array of holes with a maximum separation of 1mm (to allow for cell to cell neuronal networks) means that microfluidic system tolerances are extremely tight (in some cases only 25 micrometres). Direct injection moulding of microfluidic structures to the modified and drilled foils may be a method of generating very precise structures if the alignment tolerances can be achieved and a hollow moulded or sacrificial hollow structure made.

Surface modification for some cell types requires the use of a preferential protein adsorption process using expensive proteins such as laminin. It would be useful to have a range of surface modifications which are simple and cost effective and do not require the addition of proteins. An understanding of the actual mechanisms of the gigaseal remains for further study and understanding.

The current measurement apparatus used is optimized for plant cells which prefer cooler temperatures and do not require the addition of CO₂. To prolong cell life and thus measurement durations for mammalian cells, a heater (37°C) with the capacity for the addition of 5% gas must be provided. The measurement rig currently used requires a more stable form of suction for stable patch membrane resistances during measurement.

A microsystem system must also be developed which will provide medium exchange to the cells to provide nutrition and also remove waste, as well as deliver drug compounds to the cells quickly.

Toxicology in drug screening is not highly relevant on a planar substrate, as only a limited range of single cells can be measured, a future move in patch clamping will be from 2-dimensions to 3-dimensions to make patch clamping more physiologically relevant – closer to actual tissue. None of the materials currently being used in HTS patch clamping technology can be cost-effectively or feasibly processed into a 3 dimensional shape suitable for patch clamping – polymers are definitely the material of choice for future HTS systems.

8 List of Publications

Wilson, S.; Pfleging, W.; Bruns, M.; Welle, A.; Kirby, P. “*Novel material processing for patch clamping applications*”. IEEE Sensors 2009 Conf., Christchurch, NZ, October 25-28, 2009

Trouillet, V.; Torge, M.; Pfleging, W.; Wilson, S.; Bruns, M. “*Characterisation of UV-modified polymer surfaces for cell adhesion*”. 13th European Conf.on Applications of Surface and Interface Analysis, (ECASIA'09), Antalya, Turkey, October 18-23, 2009

Pfleging, W.; Bruns, M.; Danneil, F.; Kohler, R.; Stüber, M.; Ulrich, S.; Welle, A.; Wilson, S. „*Surface modification and functionalization of polymers and thin films on mm-scale*”. Ostendorf, A. [Hrsg.] Lasers in Manufacturing 2009 : Proc.of the 5th Internat.WLT-Conf., Munich, June 15-18, 2009 Stuttgart : AT-Fachverl., 2009 S.683-89 ISBN 978-3-00-027994-2

Wilson, S.; Welle, A.; Gottwald, E.; Molleman, A.; Kirby, P.B.; Pfleging, W.; Ramsden, J.J.; Heckeke, M. “*Automated patch clamping systems design using novel materials*”. Dimov, S. [Hrsg.] 4M2007 : 3rd Internat.Conf.on Multi-Material Micro Manufacture, Borovets, BG, October 3-5, 2007 Dunbeath : Whittles Publ., 2007 S.339-42 ISBN 978-1904445-53-1

Pfleging, W.; Torge, M.; Bruns, M.; Trouillet, V.; Welle, A.; Wilson, S. “*Laser- and UV-assisted modification of polystyrene surfaces for control of protein adsorption and cell adhesion*”. Applied Surface Science, 255(2009) S.5453-57 DOI:10.1016/j.apsusc.2008.08.053

Wilson, S.; Pfleging, W.; Welle, A.; Torge, M.; Trouillet, V.; Bruns, M.; Kirby, P. “*Novel material processing for patch clamping applications*”. 5th

Internat.Conf.on Microtechnologies in Medicine and Biology (MMB 2009),
Quebec City, CDN, April 1-3, 2009

Wilson, S.; Pfleging, W.; Welle, A.; Saint-Martin, S.; Kirby, P. "*An automated polymer patch clamping system for high throughput screening and cell network measurement*". Galvanotechnik, 99(2008) pp.2578-84

Wilson, S.; Pfleging, W.; Welle, A.; Kirby, P.; Przybylski, M. "*Machining of polystyrene by UV laser radiation for patch clamping device fabrication*". Dimov, S. [Hrsg.] 4M 2008 : Proc.of the 4th Internat.Conf.on Multi-Material Micro Manufacture, Cardiff, GB, September 9-11, 2008 Dunbeath : Whittles Publ., 2008 S.167-70 ISBN 978-1-904445-76-0

Trouillet, V.; Pfleging, W.; Torge, M.; Wilson, S.; Bruns, M.
„*Oberflächenanalytische Charakterisierung Laser- und UV-modifizierter Polymeroberflächen*“. 15.Arbeitstagung Angewandte Oberflächenanalytik (AOFA), Soest, September 8-10, 2008

Pfleging, W.; Bruns, M.; Welle, A.; Wilson, S. "*Laser-assisted modification of polystyrene surfaces for cell culture applications*". Applied Surface Science, 253(2007) S.9177-84 DOI:10.1016/j.apsusc.2007.05.047

Pfleging, W.; Torge, M.; Bruns, M.; Trouillet, V.; Welle, A.; Wilson, S. "*Laser- and UV-assisted modification of polystyrene surfaces for control of protein adsorption and cell adhesion*". European Materials Research Society Spring Meeting, Strasbourg, F, May 26-30, 2008

Wilson, S.; Pfleging, M.; Welle, A.; Ramsden, J.J., Kirby, P. *Design and fabrication of a polymer device for patch clamping applications*. Cranfield Multi-Strand Conf.: Creating Wealth Through Research and Innovation (CMC 2008), Cranfield, GB, May 6-7, 2008

Pfleging, W.; Bruns, M.; Przybylski, M.; Welle, A.; Wilson, S. "*Patterning of polystyrene by UV-laser radiation for the fabrication of devices for patch clamping*".

Pfleging, W. [Hrsg.] Laser-Based Micro- and Nanopackaging and Assembly II : Proc.of the Conf., San Jose, Calif., January 22-24, 2008 Bellingham, Wash. : SPIE, 2008 68800D/1-11 (SPIE Proceedings Series ; 6880) ISBN 978-0-8194-7055-3

Pfleging, W.; Lorenz, J.; Schierjott, P.; Welle, A.; Wilson, S. „*Lasergestützte Prozesse für Polymerwerkstoffe in der Mikro- und Nanotechnik. Strukturierung, Modifizierung und Verbindungstechnik*“. Technologien und Werkstoffe in der Mikro- und Nanosystemtechnik: GMM-Workshop, Karlsruhe, 7.-8.Mai 2007 Berlin [u.a.] : VDE-Verl., 2007 S.131-38 (GMM-Fachbericht ; 53) ISBN 978-3-8007-3033-9

Wilson, S.; Welle, A.; Gottwald, E.; Mollemann, A.; Kirby, P.B.; Pfleging, W.; Ramsden, J.J. "*Novel materials processing for automated patch clamping*". Lab-on-a-Chip World Congress: Microfluidics for the Life Sciences, Edinburgh, GB, May 15-16, 2007

9 References

- Altmann, B., Giselbrecht, S., Weibezahn, K. F., Welle, A. and Gottwald, E. (2008), "The three dimensional cultivation of the carcinoma cell line HepG2 in a perfused chip system leads to a more differentiated phenotype of the cells compared to monolayer culture", *Biomedical Materials*, vol. 3, pp. 1-10.
- Benitah, J. P., Gomez, A. M., Fauconnier, J., Kerfant, B. G., Perrier, B., Vassort, G. and Richard, S. (2002), "Voltage-gated Ca^{2+} currents in the human pathophysiologic heart: a review", *Basic research in cardiology*, vol. 97, no. 7.
- Birault, V., Cox, B., Giblin, G., Gosling, M., Gunthorpe, M. and McFazdean, I. (2009), "Ion Channels as Therapeutic Targets", Royal Society of Chemistry British Pharmacological Society, .
- Bouafsoun, A., Helali, S., Mebarek, S., Zeiller, C., Prigent, A. F., Othmane, A., Kerkeni, A., Jaffrezic-Renault, N. and Ponsonnet, L. (2007), "Electrical probing of endothelial cell behaviour on a fibronectin/polystyrene/thiol/gold electrode by Faradaic electrochemical impedance spectroscopy (EIS)", *Bioelectrochemistry*, vol. 70, no. 2, pp. 401-407.
- Cellectricon (2008), *Cellectricon website*, available at: www.cellectricon.com (accessed 12/06).
- Cho, S. H., Lu, H. M., Cauller, L., Romero-Ortega, M. I., Lee, J. B. and Hughes, G. B. (2008), "Biocompatible SU-8 based Microprobes for recording neural spike signals from regenerated peripheral nerve fibers", *IEEE Sensors Journal*, vol. 8, no. 11.
- Cleve, E., Schollmeyer, H., Schlosser, U. and Schollmeyer, E. (1999), "Oberflaechen strukturierung polymeren Fasern durch UV-Laserbestrahlung", *Die Angewandte Makromolekulare Chemie*, vol. 270, pp. 87-93.
- Cole, K. S. (1949), "Dynamic electrical characteristics of the squid axon membrane", *Arch. Sci. Physiol*, vol. 3, pp. 253-258.
- Comley, J. (2003), "Patchers v. Screeners divergent opinion on high throughput electrophysiology", *Drug Discovery World*, .
- Cytocentrics (2008), *Cytocentrics*, available at: www.cytocentrics.com (accessed 12/06).
- De Gennes, P. G. (1985), "Wetting: Statics and Dynamics", *Revised Modern Physics*, vol. 57, no. 3 part 1, pp. 827-863.

- de Oliveira, A., Pfleging, W. and zum Gahr, K. H. (2008), *Excimer-Laserstrukturierung und Oberflächefunktionalisierung von Polystyrol zur Erzeugung von biologischer Grenzflächen* University of Karlsruhe, University of Karlsruhe.
- Detrait, E., Lhoest, J. B., Knoops, B. and Bertrand, P. (1998), "Orientation of cell adhesion and growth on patterned heterogeneous polystyrene surface", *Journal of Neuroscience Methods*, vol. 84, pp. 193-204.
- Dowell Mesfin, N. M., Abdul Karim, M. A., Turner, A. M., Schanz, S., Craighead, H. G., Roysam, B., Turner, J. N. and Shain, W. (2004), "Topographically modified surfaces affect orientation and growth of hippocampal neurons", *Journal of Neural Engineering*, vol. 1, no. 2, pp. 78-90.
- Duprat (April 2000), *How do we study the brain?*, available at: <http://www.ipmc.cnrs.fr/~duprat/neurophysiology/patch.htm> (accessed 23rd November 2009).
- Fertig, N., Blick, R. H. and Behrends, J. C. (2002), "Whole cell patch clamp recording performed on a planar glass chip", *Biophysical Journal*, vol. 82, no. 6, pp. 3056-3062.
- Fertig, N., Tilke, A., Blick, H. and Kotthaus, J. P. "Stable integration of isolated cell membrane patches in a nanomachined aperture", *Applied Physics Letters*, vol. 77, no. 8, pp. 1218-1220.
- Flyion (2007), *Flyion*, available at: www.flyion.com (accessed 12/06).
- Gabriel, C., Gabriel, S. and Courthout, E. (1996), "The dielectric properties of biological tissues", *Phys. Med Biol*, vol. 41, pp. 2231.
- Gimsa, J. and Wachner, D. (1999), "A polarization model overcoming the geometric restrictions of the LaPlace solution for spheroidal cells obtaining new equations for field induced forces and transmembrane potential", *Biophys J*, vol. 77, pp. 2114.
- Glaser, R. (2009), "Energetics and Dynamics of Biological Systems", in *Biophysics*, 2nd ed, Springer, Berlin, pp. 105-233.
- Gleich, H. (2004), *Zusammenhang zwischen Oberflächenenergie und Adhäsionsvermögen von Polymerwerkstoffen am Beispiel von PP und PBT und deren Beeinflussung durch die Niederdruck-Plasma Technologie* (PhD thesis), University of Duisburg-Essen, Faculty of Engineering, Department of Mechanical Engineering, .
- Goddard, J. M. and Hotchkiss, J. H. (2007), "Polymer surface modification for the attachment of bioactive compounds", *Progressive Polymer Science*, vol. 32, pp. 698-725.

- Gomez, N., Chen, S. and Schmidt, C. E. (2004), "Polarization of hippocampal neurons with competitive surface stimuli: contact guidance cues are preferred over chemical ligands", *Journal of Royal Society Interface*, vol. 4, no. 13, pp. 223-233.
- Gottwald, E., Lahni, B., Thiele, D., Giselsbrecht, S., Welle, A. and Weibezahn, K. F. (2008), "Chip-based three-dimensional cell culture in perfused micro-bioreactors", *Journal of visualized experiments*, vol. 15.
- Graham, J. and Gerard, R. W. (1946), "Membrane potentials and excitation of impaled single muscle fibers", *Journal of Cell Computational Physiology*, vol. 28, pp. 99-117.
- Griffith, L. and Naughton, G. (2002), "Tissue engineering - current challenges and expanding opportunities", *Science*, vol. 295 (5557), no. Feb 8, pp. 1009-1014.
- Hamill, O. P., Marty, A., Neher, E., Sakmann, B. and Sigworth, F. J. (1981), "Improved patch clamp techniques for high-resolution current recording from cells and cell-free membrane patches", *Pfluegers Arch*, , no. 391, pp. 85-100.
- Hodgkin, A. L. and Huxley, A. F. (1952), "Currents carried by sodium and potassium through the giant axon of logligo", *Journal of Physiology*, vol. 116, pp. 181-190.
- Kern, W. and Schuegraf, K. K. (1994), "Deposition Technologies and Applications: Introduction and Overview", in *Handbook of Deposition Technologies for Film and Coatings*, 3rd ed, pp. 11-43.
- Kirchner, C., Liedl, T., Kudero, S., Pellegrino, T., Munoz Javier, A., Gaub, H. A., Stoelzle, S., Fertig, N. and Paradi, W. J. (2005), "Cytotoxicity of Colloidal CdSe and CdSe/ZnS Nanoparticles", *Nano Letters*, vol. 5, no. 2, pp. 331-338.
- Knott, T., Single, S. and Stett, A. (2002), "Automatisiertes Patch-Clamping-Loesungen und Herausfoerderungen", *Laborwelt*, , no. 4, pp. 20-22.
- Kutchinsky, J., Friis, S., Asmild, M., Taboryski, R., Pedersen, S., Vestergaard, R. K., Jacobsen, R. B., Krzywkowski, R., Schroeder, R. L., Ljungstrom, T., Sorensen, S. B., Bech, M. and Willumsen, N. J. (2004), "Characterization of Potassium Channel Modulators with Q-Patch Automated Patch-Clamp Technologies: System Characteristics and Performance", *Assay and Drug Development Technologies*, vol. 1, no. 5, pp. 685-693.
- Lampin, M. (1997), "Correlation between substratum roughness and wettability, cell adhesion and cell migration", *Journal of Biomedical Materials research*, vol. 36, no. 1, pp. 99-108.

- Laurens, P. (2000), "Characterization of modifications of polymer surfaces after excimer laser treatments below the ablation threshold", *Applied Surface Science*, vol. 154, no. 211 -216.
- Martinez, M., Luk, C., Py, C., Martinez, D., Comas, T., Monette, R., Denhoff, M., Syed, N. and Mealing, G. A. R. (2011), "Recordings of cultured neurons and synaptic activity using patch-clamp chips", *Journal of Neural Engineering*, vol. 8, pp. 034002-034012.
- Mayer, M., Kriebel, J. K., Tosteson, M. T. and Whitesides, G. M. (2003), "Microfabricated teflon membranes for low noise recording of ion channels in planar lipid bilayers", *Biophysics*, vol. 85, no. 4, pp. 2684-2695.
- Melai, J., Salm, C., Swits, S., Visschers, J. and Schmitz, J. (2009), "The electrical conductive and dielectric strength of SU-8", *Journal of Micromechanics and Microengineering*, vol. 19, pp. 065012.
- Mizradeh, H. and Dadsetan, M. (2003), "Influence of laser surface modifying of polyethylene terephthalate on fibroblast cell adhesion", *Radiation Physics and Chemistry*, vol. 67, pp. 381-385.
- Molecular Devices (2009), *Molecular Devices*, available at: www.moleculardevices.com (accessed 12/06).
- Molleman, A. (2003), *Patch Clamping. An Introductory Guide to Patch Clamp Electrophysiology*, 1st ed, Wiley Interscience.
- Nanion (2010a), available at: www.nanion.de (accessed 02.03.2010).
- Nanion (2010b) (accessed 02.03.2010).
- Neher, E. and Sakmann, B. (1976), "Single-channel currents recorded from membrane of denervated frog muscle fibre", *Nature*, vol. 260, pp. 799-802.
- Neubert, H. (2004), "Patch Clamping moves to chips", *Analytical Chemistry*, , no. Sept., pp. 327-331.
- Pancrazio, J. J., Bey, P. P., Cuttino, D. S., Kusel, J. K., Burkholdt, D. A., Shaffer, K. M., Kovacs, G. T. A. and Stenger, D. A. (1998), "Portable Cell-Based Biosensor System for Toxin Detection", *Sensors and Actuators B, Chemical*, vol. 53, no. 3, pp. 179-185.
- Paynter, R. , *INRS XPS analysis page*, available at: <http://goliath.emt.inrs.ca/commerce/xps-tech.html> (accessed 05/06).
- Pettit, G. H. and Sauerbrey, R. (1993), "Pulsed .;Ultraviolet Laser Ablation", *Applied Physics*, vol. A 56, pp. 51-63.

- Pfleging, W., Bruns, M., Welle, A. and Wilson, S. (2007), "Laser-assisted modification for cell culture application]", *Applied Surface Science*, vol. 253, pp. 9177-9184.
- Py, C., Denhoff, M. W., Martina, M., Monette, R., Comas, T., Ahuja, T., Martinez, D., Wingar, S., Caballero, J., Laframboise, S., Mielke, J., Bogdanov, A., Luk, C., Syed, N. and Mealing, G. (2010), "A novel silicon patch-clamp chip permits high fidelity recording of ion channel activity from functionally defined neurons", *Biotechnology and bioengineering*, vol. 107, no. 4, pp. 593-600.
- Ranella, A., Barberoglou, M., Bakogianni, S., Fotakis, C. and Stratakis, E. (2010), "Tuning cell adhesion by controlling the roughness and wettability of 3D micro/nano silicon structures", *Acta biomaterialia*, vol. in press.
- Regehr, K. J., Domenech, M., Koepsel, J. T., Carver, K. C., Ellison-Zelski, S. G., Murphy, W. L., Schuler, L. A., Alarid, E. T. and Beebe, D. J. (2009), "Biological Implications of PDMS Material Properties", *Lab on Chip*, .
- Roth, E. A., Xu, T., Das, M., Gregory, C., Hickman, J. J. and Boland, T. (2003), "Inkjet printing for high-throughput cell patterning", *Journal of Biomaterials*, vol. 25, no. 17, pp. 3707-3715.
- Sekula, S., Fuchs, J., Weg-Remers, S., Nagel, P., Schuppler, S., Fragala, J., Theilacker, N., Franzreb, M., Wingren, C., Ellmark, P., Borrebaeck, C. A. K., Mirkin, C. A., Fuchs, H. and Lenhert, S. (2008), "Multiplexed Lipid Dip-Pen Nanolithography on Subcellular Scales for the Templating of Functional Proteins and Cell Culture", *Small*, vol. 4, no. 10, pp. 1785-1793.
- Sherman, A. J., Shrier, A. and Cooper, E. (1999), "Series Resistance Compensation for Whole Cell Patch-Clamp Studies Using a Membrane State Estimator", *Biophysics Journal*, vol. 77, pp. 2590-2601.
- Sophion bioscience (2009), available at: www.sophionbioscience.com.
- Stett, A., Burkhardt, C., Weber, U., van Stiphout, P. and Knott, T. (2003), "Cyto-centering: A novel Technique Enabling Automated Cell-by-Cell Patch Clamping with the CYTOPATCH Chip", *Receptors and Channels*, vol. 9, pp. 59-66.
- Thin XXS (2009), available at: www.thinxxs.com.
- Vieweg, R. and Daumiller, G. (1969), "Polystyrol: Herstellung, Eigenschaften, Verarbeitung und Anwendung", in *Kunststoff-Handbuch*, 2nd ed, Carl Hanser Verlag, Munich.

- Voskeican, G., Shire, M. S. and Shawgo, R. S. (2003), "Biocompatibility and biofouling of MEMS drug delivery devices", *Biomaterials*, vol. 24, pp. 1959-1967.
- Welle, A. (2003a), "Competitive plasma protein adsorption on modified polymer surfaces monitored by quartz crystal microbalance technique", *Journal of Biomaterials Science, Polymer Edition*, vol. 15, pp. 357-370.
- Welle, A. (2003b), "Competitive protein adsorption on modified polymer surfaces monitored by Quartz Crystal Microbalance technique", *Journal of Biomaterials Science, Polymer Edition*, vol. 15, pp. 357-370.
- Welle, A. and Gottwald, E. (2002), "UV-based patterning of polymeric substrates for cell culture applications", *Biomedical Microdevices*, vol. 4, pp. 33-41.
- Welle, A., Horn, S., Schimmelpfeng, J. and Kalka, D. (2005), "Photo-chemically patterned polymer surfaces for controlled PC-12 adhesion and outgrowth", *Journal of Neuroscience Methods*, vol. 142, pp. 243-250.
- Wilson, S. (2005), *Materials and Fabrication Design of Micromachined Patch Clamping Devices* (MSc thesis), Cranfield University, Cranfield University.
- Wilson, S., (2009), *Meeting minutes, Meeting with Sophion Bioscience V.P. Development Jonatan Kutchinsky*.
- Xia, Y. and Whitesides, G. M. (1998), "Soft Lithography", *Angewandte Chemie International Edition*, vol. 7, no. 5, pp. 550-575.
- Xu, J., Wang, X., Ensign, B., Li, M., Wu, L., Guia, A. and Xu, J. (2004), "Ion-channel assay technologies: quo vadis?", *Drug Discovery Today*, vol. 6, no. 24, pp. 1278-1287.
- Yamazoe, H., Okuyama, T., Suzuki, H. and Fukada, J. (2010), "Fabrication of patterned cell co-cultures on albumin-based substrate: Applications for microfluidic devices", *Acta Biomaterialia*, vol. 6, no. 2, pp. 526-533.

Appendix A

A.1 Cell handling and protein adsorption protocol

Part 1: Preparing surfaces

Equipment: incubator at 37C with 5% CO₂ supply

Sterile bench with fumehood, pipettes and other typical biology lab supplies

Cell Handling: Use recently passaged cells, 0.5 million cells per 5cm diameter petri dish

Collagen reference petridish preparation

Supplies:

- 3 x 6cm tissue petri dishes (Becton Dickonson Labware, Plymouth, England)
- Rat collagen stock concentration 2mg/mL diluted to 120µL/ 5mL di. water per petridish.
- PBS (phosphate buffered saline) for rinsing

Rinse then aspirate the tissue petri dishes with approx. 4mL PBS then pipette in 5mL of the collagen/ d.i. water mixture into each petridish. Place into the incubator for at least 1 hour. Remove from the incubator and suction out the liquid. Rinse twice with approx. 4 mL PBS. When cells have been trypsinated and counted, add 0.5 million cells in the appropriate cell media to the petri dish and return to the incubator. Culture the cells and exchange media for the same duration and intervals as the other cells in the experimental run.

Patterned (UV mask exposed) reference petri dish preparation

Supplies:

- 6cm bacterial petridishes (Greiner Labortechnik GmbH, Frickenhausen, Germany)
- 3x3cm chrome mask with 20-30 micron features
- Low pressure mercury vapour lamp, NNQ (185nm), 15W (Heraeus Noblelight GmbH, Kleinostheim, Germany)

Procedure

Place the lamp so it will be positioned 10cm above the petri dish for optimum exposure. Place a chrome/quartz mask inside the bottom of each petri dish with the chrome side facing downwards. Two exposed petri dishes are used as references for each cell run. Warm up the lamp for 10-15 minutes, then place the petri dish centred underneath the lamp. Expose the petri dishes for a minimum of one hour or an exposure of at least 1000mJ/cm². Replace the cover on the petri dish, and store until use. The petri dishes can be exposed in advance of cell inoculation (up to 48 h is recommended). The reference exposed petri dishes should be handled exactly the same as those used in the experiment (for example also using the preferential protein adsorption procedure if required), including the same medium exchange intervals and number of cells inoculated.

Preferential protein adsorption procedure

Supplies:

- 6cm bacterial petridishes, either with modified surfaces or with foils attached to petridish bottom (Greiner Labortechnik GmbH, Frickenhausen, Germany)
- 1mg/mL BSA and 1% pluronic F-68 in sterile PBS (no Ca/Mg)
- 5µg/mL laminin and 1% Pluronic F-68 in PBS
- PBS for rinsing

- 1) Take the bacterial petridishes and add to each 4mL of the mixture 1mg/mL BSA, 1% Pluronic in PBS.
- 2) Put the lid on the petridishes and put into the incubator for 1 hour
- 3) Remove from the incubator, suction the liquid out and rinse twice with 2mL PBS
- 4) Add 4mL of the mixture 5µg/mL laminin, 1% Pluronic in PBS, cover and place in the incubator for 3 hours
- 5) Remove from incubator and suction out the liquid. Rinse twice with PBS
- 6) Leave the petridishes in the incubator with 4mL PBS until cell inoculation, suction out PBS before inoculating cells

Part 2: Preparing Cells

Cells in the S1 labs at IBG of the Karlsruhe Institute of Technology are as a rule passaged once per week, and medium is exchanged every second day.

Standard passaging procedures including trypsination are used to split the cells. There are always two 100mL culture bottles filled with approx 20mL medium, one bottle with 4 million cells and the second of 2 million of each cell type.

Passaging PC-12 GFP cells

- Take the 1 million cell culture bottle from the brood cabinet.
- Take a 50mL centrifuge bottle from the main lab, third drawer down „blue top“, and pipette 10mL from the cell culture bottle into it.
- Centrifuge with 10mL counter weight, at 1200 rpm/ 4 minutes

-Siphon off the old medium, then wash once with 5mL PBS (without Ca/Mg) - be sure to warm it first. (37°C water bath for 15 minutes).

-Get an object carrier (2nd drawer behind the fumehoods), place into the fumehood.

-Siphon off the extra PBS from the centrifuged material, then add 5mL PBS (no Ca/Mg) put it into the centrifuge bottle, raising and lowering the medium 2x carefully (to mix medium with cells slightly).

-Add 2mL Trypsine (slowly raise and lower medium in pipette)

-Put the centrifuge bottle into the brooding cabinet for 10 minutes (initially) at 37°C.

(trypsinizing separates cell agglomerates into single cells)

-After 10 minutes, bring the centrifuge bottle out of the brooding cabinet and add 2mL of medium (Diff PC12 GMP-GMP, pink) to it, to stop the trypsinizing.

Take a 1mL pipette and move the solution gently up and down 20-25x.

-Take a drop of it and put it onto the object carrier, check in microscope to see if cells are single.

-Centrifuge the cells/medium at 1200 rpm/ 4 minutes.

-In between, take a coulter counter vial and fill with 9.5mL isotone.

Get a test tube and fill with 4.5 mL medium.

-Remove the cells/medium from the centrifuge and syphon off the trypsin. Add 5mL medium to the cells and move up and down the pipette gently 25x.

-Take 500µL out of the solution and add to the test tube. (1:10 solution), move up and down the pipette. Then take 500µL of this solution and add to the coulter counter vial.

-Operating the coulter counter:

Menu: select set up, program 6 for PC12-GMP (use 'next' button to select programs)

Parameters:

Solution: 2000 x 10E2

Gently rotate the solution to be tested.

We would like 0.5 Mio cells, so for 5 petridishes need 2.5 million cells (0.5 Mio extra for culture bottle)

TML = 4.259 (total in million)

Viability 98.55% (life of cells)

Agg (aggregates) 1.85%, (for PC-12 cells under 2.5 is good)

Wollen/haben $2.5/4.25 = 0.6$

-Remove the coulter bottle and then replace the isotone solution and run the program again..

-For each petridish 3mL of solution is needed, for SU8 on silicon 5mL per dish.

-15mL (per petridish) - 0.6 (cells) = 14.4 mL, volume of medium needed + NGF + Pluronic F64.

-Put 14.4mL medium into a beaker, add pluronic (??), mix with pipette then 0.6mL medium (mix the culture/ cell medium), add 2-3 μ L /mL NGF to beaker (double works better).

-Use a 1mL pipette and mix beaker contents.

-Add 3mL or 5mL (SU8 on Si) per petridish.

-Move the petridishes gently in x and y direction to distribute them over the petridish.

-Put the petridishes in the brood cabinet at 37°C.

Part 3 Staining and fixing cells for laser and lamp adhesion parameter checks

Crystal violet method (for L929 cells in this case):

- Expose petri dishes as control (2x coated with collagen), and foils with masks G5 and H1. Exposure time 1 hour at 10cm distance
- Coat the foils with laminin/albumin/pluronic and then inoculate with 1.0×10^6 L929 cells with additional 1% pluronic
- Incubate at 37C for 48 hours without medium change

- Remove the medium by aspiration and rinse with PBS
- Photograph
- Crystal violet colouring for 30 minutes at 25C
- Rinse with water
- Dry

A.2 XPS results

Table 1: XPS results Norflex© foil UV lamp exposures (lamp intensity 285μW/cm²) – left column exposure time (minutes)

